THE HETEROGENEOUS BINDING OF OXYGEN: THE PREPARATION AND CHARACTERIZATION OF COBALT CYANIDE COMPLEXES INSIDE ZEOLITE Y

BY

ROBERT J. TAYLOR, JR.

A DISSERTATION PRESENTED TO THE GRADUATE SCHOOL
OF THE UNIVERSITY OF FLORIDA IN PARTIAL FULFILLMENT
OF THE REQUIREMENTS FOR THE DEGREE OF
DOCTOR OF PHILOSOPHY

UNIVERSITY OF FLORIDA

1989

TO SHARON, MY WIFE AND BEST FRIEND

ACKNOWLEDGMENTS

I would like to thank the many people who have been a great help to me throughout my career at the University of Florida. First, I would like to thank Dr. Russell Drago for his leadership and encouragement over the years. His excitement about chemistry and unending optimism has been an inspiration. I would also like to thank his wonderful wife, Ruth, for her kindness and hospitality.

Second, I would like to thank the people who have directly contributed to this work. Dr. Iwona Bresinska's initial work was invaluable. Dr. Jim George's comments and discussions as well as his experimental diligence were also much help.

Next, I would like to thank my co-workers in the Drago group for their friendship through the years. Former group members Mark Barnes, Cindy Bailey, Ken Balkus, Rich Riley, Jeff Clark, Andy Griffis, Shannon Davis and Pete Doan always lent a hand when needed. Present group members Larry Chamusco, Ngai Wong, Tom Cundari, Alan Goldstein, Mike Naughton, Don Ferris, Steve Showalter, and Steve Petrosius have been a valuable source of knowledge and advice over the years. I would like to especially thank my true friend

through it all, Jerry Grunewald. From start to finish his friendship and encouragement was always there. I also want to thank the second-in-command of the Drago group, Maribel Lisk, for lending her assistance when needed. Her greatest accomplishment during my years at UF was to keep Doc busy and out of the labs so work could get done. To the newest group members, John Hage and Doug Patton, I would like to offer a word of advice. Take advantage, whenever possible, of the priceless resource available to you while you are at UF, the Drago group.

Most importantly, I would like to thank my wife, Sharon, for her unending love and encouragement through thick and thin. Her caring and understanding have made even the darkest days a little brighter. I would also like to thank my parents, Joel and Becky, for their guidance through my early years and their love and support for a lifetime.

TABLE OF CONTENTS

Abstract of Dissertation Presented to the Graduate School of the University of Florida in Partial Fulfillment of the Requirements for the Degree of Doctor of Philosophy

HETEROGENEOUS BINDING OF OXYGEN:
THE PREPARATION AND CHARACTERIZATION OF
COBALT CYANIDE COMPLEXES INSIDE ZEOLITE Y

By

Robert J. Taylor, Jr.

December 1989

Chairman: Russell S. Drago
Major Department: Chemistry

Cobalt complexes that reversibly bind dioxygen are available in a large variety of ligand systems. The main drawback to the utilization of these materials in catalysis or oxygen enrichment from air arises from the fact that very few complexes bind oxygen in the solid state while in solution dimerization and irreversible oxidation of the complexes occur. Synthesizing these cobalt complexes inside the cage of a zeolite has the potential of eliminating these undesirable properties and several zeolite encapsulated metal complexes that reversibly bind dioxygen have been reported. These compounds all involve neutral ligands and though effective for separating oxygen from air, coordination of water as a sixth ligand or oxidation of the ligand limits their utility.

In this study, these problems have been eliminated by preparing anionic cobalt cyanide complexes that are more stable than the cationic complexes previously reported. The cyanide ligand is very stable to oxidation and the zeolite prevents dimerization to form a μ-peroxo complex. Both $Co(CN)_4^{2-}$ and $Co(CN)_5^{3-}$ have been isolated inside zeolite-Y and shown to reversibly bind oxygen. The former is bound to the zeolite wall through a lattice oxide while the later is formed in the large cavity of the zeolite. Electron paramagnetic resonance spectroscopy, EPR, has been used to characterize both the oxygenated and deoxygenated forms of these two complexes. Quantitative gas uptake measurements have shown the host zeolite materials to exhibit a high selectivity for oxygen over nitrogen or argon. These uptake measurements have been used to determine the equilibrium constant for binding oxygen to both active species and the enthalpy and entropy of O_2 binding have also been determined for the latter. The effect of supporting a transition metal complex inside a zeolite on its oxygen binding properties is discussed.

CHAPTER 1
GENERAL INTRODUCTION

The past two decades have seen a tremedous growth of gas adsorption processes that have made adsorption systems a key separations tool in chemical and petrochemical industries.[1] This growth is a result of significant improvements in both adsorbents and adsorption cycles. The invention of synthetic zeolites[2] and, more recently, carbon molecular sieves[3] has provided new materials which are both versatile and efficient. These materials have, in turn, prompted the development of more efficient processes, such as the pressure swing adsorption (PSA) cycle.

The work presented in this dissertation is concerned with the preparation of a new adsorbent for the separation of oxygen from nitrogen. The goal is to entrap a transition metal complex that reversibly binds oxygen inside a zeolite. Such a material would have a high affinity for oxygen and have certain advantages over the nitrogen selective adsorbents used today in both gas purification and bulk gas separations.

The separation of oxygen from nitrogen or the production of oxygen-enriched air is an important industrial

process,[4] with 37 billion pounds of oxygen being produced in the U.S. in 1988.[5] This large scale production ranks oxygen third among all chemicals produced in the United States. Oxygen and oxygen-rich air find a variety of uses in such processes as steel production, chemical oxidations, waste water treatment, and medical/life support applications.[6] It can be seen that the adsorbents and adsorption processes used for oxygen production are very important to the chemical industry and the search for ways to improve this separation is worthy of further study.

There are several methods for producing pure oxygen and oxygen-rich streams from air, including cryogenic fractional distillation,[7] pressure swing adsorption (PSA),[1] and membrane separation.[8-9] Cryogenic separation--that is, liquefaction followed by distillation--remains the most frequently used process for large scale production of pure oxygen or nitrogen. However, as PSA processes are improved and new adsorbents are discovered, PSAs share of the separations task will increase.[1] In applications where high purity oxygen is not needed, membrane separation is also being used. Recently, these membrane systems are being used in conjunction with the cryogenic air separation processes resulting in hybrid systems which are economically attractive for production of high purity oxygen or nitrogen.[10]

Many of the PSA processes used in the separation of O_2 and N_2 employ adsorbents which preferentially adsorb N_2 over O_2. Figure 1-1 shows a simple flow diagram for a PSA device. In a simple PSA cycle, a bed of adsorbent is charged with air and nitrogen is selectively adsorbed. Oxygen is concentrated in the gas phase and is removed as the product stream. Nitrogen is then removed and collected by lowering the pressure over the adsorbent. This process performs well if the feed air is free of gases which could concentrate and contaminate the oxygen-rich stream. In the case where the oxygen product is to be used in medical or life support applications, contaminants in the air can cause major problems. Nitrogen selective adsorbents in pressure swing process do not, even in principle, allow oxygen to be separated from the contaminants, resulting in a higher contaminant concentration in the oxygen product stream than in the inlet air.

This type of contamination problem could be overcome if a material which preferentially adsorbs O_2 over N_2 and the contaminants were available. In a cycle using this material the oxygen would be adsorbed by the sorbent, leaving the nitrogen and contaminants together in the gas phase. This would allow the contaminants to pass through the system with the N_2, resulting in a pure oxygen stream.

An oxygen selective system would also have other advantages. First, the ability of these new materials to

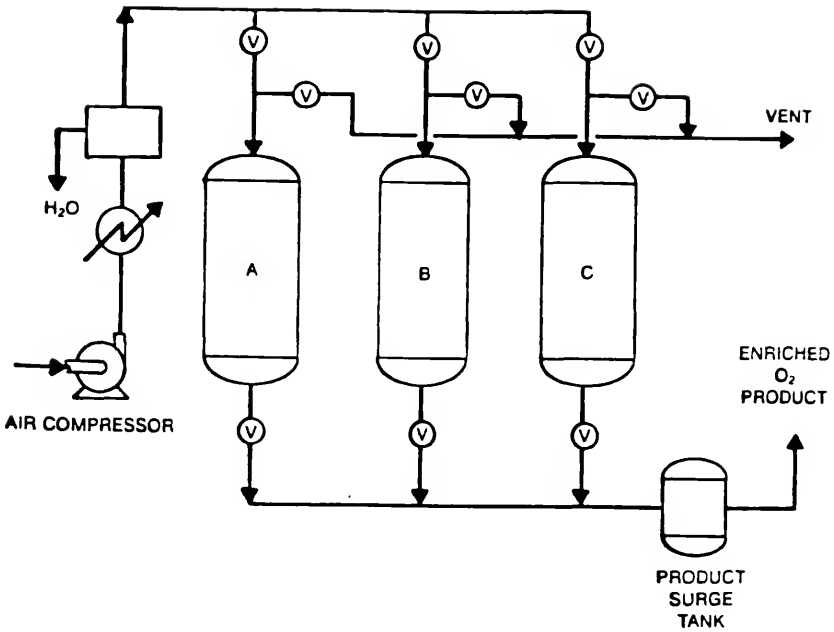

Figure 1-1. Flow diagram for a pressure swing adsorption device.

simply replace molecular sieves in existing pressure swing devices would eliminate to need for construction of new devices. Second, since such an adsorbent would adsorb oxygen (21% in air) instead of nitrogen (78% in air), the adsorbent bed size could be one-fourth the size of a conventional bed. This would result in a saving of weight and space in an era when smaller and more portable oxygen generation systems are desired.

The main impediment to such an oxygen extraction system is the production of an oxygen selective material. Nearly all substances that reversibly bind oxygen decompose upon repeated oxygenation and deoxygenation cycling. The few systems with better stability are extremely moisture sensitive and are deactivated by water. This work reports the preparation of a material that overcomes both of these drawbacks by entrapping a stable, moisture resistant complex that reversibly binds oxygen inside a zeolite cavity. The material has a high affinity for O_2 and is stable to repeated cycling of oxygenation and deoxygenation.

This work is also concerned with the chemistry involved in the preparation and characterization of these zeolite entrapped complexes and on the effect their presence has on the gas uptake characteristics of the zeolite material. Adsorption isotherms of single component gases are measured here. Complex adsorption processes or the use of complex gas mixtures is more of an applied engineering concern. The

primary interest of this work involves formation of the active complexes, their characterization, their influence on the adsoption characteristics of the zeolite in which they are entrapped, and the zeolites influence on their binding constants.

CHAPTER 2
REVIEW OF THE LITERATURE

Introduction

The synthesis and characterization of transition metal complexes inside zeolites have been the subject of much research.[11-17] Zeolites are of interest as a matrix for synthesizing coordinatively unsaturated complexes as reactive intermediates in heterogeneous catalysis and as an interesting medium for carrying out coordination and transition metal chemistry.[14] Zeolites not only function as solid supports for encapsulated complexes, but can also serve as solvents or ligands. In many cases they serve one or more of these functions simultaneously.

The three-dimensional pore structure of zeolites provides the possibility of preparing complexes that are unstable in solution. In the case of zeolites with the faujasite structure, such as zeolite X and Y, this can result by trapping complexes in discrete cavities that would otherwise dimerize in solution.[18] This occurs because zeolite cavities are often larger than the connecting channels, allowing the formation of a "ship-in-a-bottle"

type complex.[19] In addition to the ability to physically isolate complexes, zeolites can also influence the stability of complexes with their unique solvating and ligating properties. This stabilization can result in the formation of complexes with unique coordination numbers[14] or oxidation states[20] that cannot be prepared in solution. Acting as a ligand, zeolites can also stabilize complexes by anchoring them to the lattice through framework oxygens.[21-22]

Zeolites

Before looking at some of the complexes that have been synthesized inside zeolites, a brief introduction to the structure and properties of zeolites is needed.

Zeolites[2] are crystalline aluminosilicates that have a structure based on tetrahedral aluminum and silicon oxygenates. As seen in Figure 2-1, when these Si and Al tetrahedra are linked by mutually sharing oxygens, a three-dimensional framework can result. Figure 2-1(b) and 2-1(c) both represent a sodalite unit, which is the basic building block of zeolites A, X and Y; for simplicity the latter is shown as a line drawing. Using this representation, a tetrahedral atom (Si or Al) is located at each vertex and oxygen atoms are located between the tetrahedral atoms. When these sodalite units are connected together through half of the hexagonal faces, in a tetrahedral arrangement,

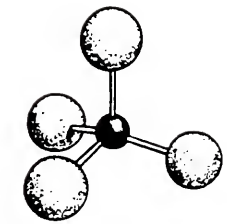

(a)

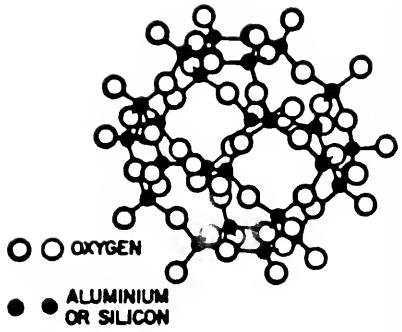

(b)

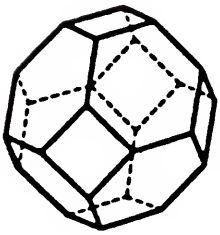

(c)

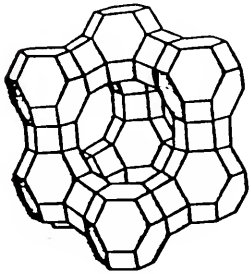

(d)

Figure 2-1. Structural representations of alumino-silicates. (a) Silicon or aluminum tetraheral oxygenates; (b) ball and stick representation of a sodalite unit; (c) line drawing of sodalite unit; (d) line drawing of faujasite structure.

the faujasite structure results, as seen in Figure 2-1(d). This is the structure of both zeolite X and Y.

Much of the work described here focuses on zeolite Y, which was chosen because of its large pore openings, large cavities and three-dimensional pore structure. The only difference between zeolite X and Y is the ratio of Si to Al atoms present in the framework, with zeolite X having the Si/Al ratio of near 1 and zeolite Y between 2 and 3. The higher Si/Al ratio for zeolite Y results in a smaller charge density. Zeolite Y was chosen over zeolite X because the smaller charge density allows the metal cations to be more mobile and more available to coordinate with ligands rather than oxygen atoms of the framework.[12]

Zeolites have a molecular formula based on the number of Si and Al tetrahedra present in the framework. A unit cell of zeolite Y contains 192 $(Si,Al)O_2$ tetrahedra and, with a Si/Al ratio of 2.4, has a molecular formula of $Na_{56}[(AlO_2)_{56}(SiO_2)_{136}]$. Due to the polar nature of the covalent bonds between oxygen and Si or Al and the overall negative charge of the framework, zeolites are very hydrophilic. This results in a typical unit cell of zeolite Y containing 250 water molecules.[2]

Having Al atoms in place of Si atoms gives the zeolite framework an overall negative charge. This negative charge is balanced by the presence of cations located throughout the framework. As shown in Figure 2-2, these cations can be

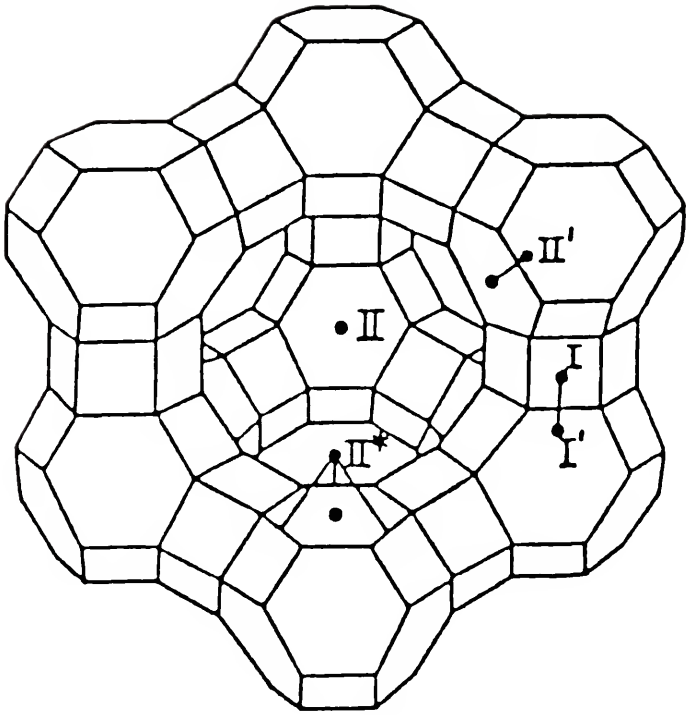

Figure 2-2. Cation sites available in zeolite Y.

located in many different sites. The smallest of these sites is the hexagonal prisms (Site I) located between two connecting sodalite units. The opening to this site is 2.2 Å and the internal diameter is only 2.4 Å; therefore, only unsolvated cations can enter this site. The sodalite cage or beta cage is next in size. It has a pore opening of 2.2 Å and an internal diameter of 6.6 Å and contains two types of cation sites, Site I' and II'. With this size pore opening only small ligands, such as H_2O or NH_3, can enter this site. The large cavities, formed when these sodalite units are linked together, are called alpha cavities or supercages and contain many sites along their internal surface (Site II, III and III'). The opening to the supercage is 8 Å and, therefore, allows much larger ligands to enter. Moreover, these supercages have an internal diameter of 13 Å, which is large enough for a reasonably sized complex to form.

The location of these charge balancing cations in the zeolite is important in understanding their behavior.[17] Since they are only electrostatically bound to the framework, they are able to migrate within the structure and their distribution in the different sites depends on several factors.[2] These factors include (a) the size of the cation, (b) the extent of hydration of the zeolite, (c) the presence of molecules or ions that serve effectively as ligands, and (d) the nature of other cations that may be present. For

example, large cations like rubidium and cesium are unable to enter Site I positions in zeolite Y due to its small 2.2 Å pore opening. Multivalent cations, such as Mg^{2+} and Ca^{2+}, prefer Site I over other sites due to the strong solvation provided by the lattice oxygens in this site. Lunsford proposed[12] that even a cation which might be in an inaccessible site (e.g. Site I) at one moment will be available for complex formation in the large cavity at some later time.

Transition Metal Complexes Inside Zeolites

The ability to exchange transition metal cations into zeolites has allowed the synthesis of many zeolite entrapped transition metal complexes and at least seven review articles have been devoted to this work.[11-17] The characterization of these complexes is made almost entirely with spectroscopic data.[15] X-ray diffraction has not been effective in locating ligands for these samples since they are generally polycrystalline. Therefore, one can see the importance of a complex having an informative spectroscopic handle in order to be studied inside a zeolite.

As mentioned in Chapter 1, this work is concerned with the preparation of a zeolite entrapped transition metal complex that reversibly binds oxygen. This is not a new idea, Lunsford and co-workers have worked in this area for

some time.[18,21,23] His early work focused on preparing cobalt amine complexes inside zeolite Y.[18] Howe and Lunsford were able to prepare and characterize a series of cobalt amine oxygen adducts with the formula $[CoL_5O_2]^{2+}$, where L= NH_3, CH_3NH_2, and n-$CH_3CH_2CH_2NH_2$. Characterization of these 1:1 adducts by EPR spectroscopy yielded similar results to those of analogous adducts in solution. Also similar to the solution adducts was their tendency to dimerize. When the ligand is NH_3 or CH_3NH_2, prolonged exposure to oxygen resulted in the formation of the superoxo dimer, $[L_5CoO_2CoL_5]^{5+}$. The most interesting result of this early work occurred with the n-propylamine complex, where only the monomeric oxygen adduct was formed. This was the first report of using the cavities of a zeolite to sterically inhibit dimerization.

Another interesting complex which came out of this early work[21] was the square planar $Co(en)_2^{2+}$ (en = ethylenediamine), shown in Figure 2-3. In this complex the axial coordination site is occupied by a lattice oxygen. When exposed to molecular oxygen the monomeric oxygen adduct is formed, with no evidence of dimer formation. It is also stable in the presence of oxygen up to 70 °C. This complex is similar to cobalt complexes formed in solution, where the in-plane ligand is a Schiff base or porphyrin and the sixth coordination site is occupied by a coordination base such as pyridine.[24-25] However, these solution analogues dimerize

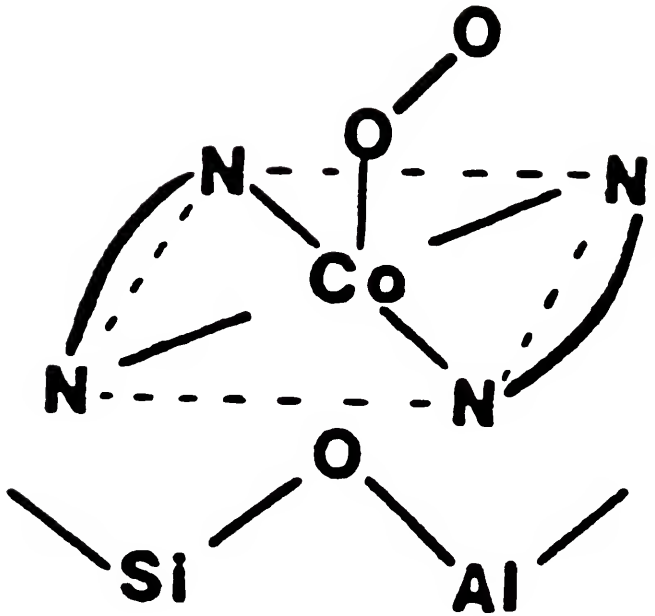

Figure 2-3. Proposed structure[21] of $Co(en)_2^{2+}$ inside zeolite Y.

and decompose under most conditions. The remarkable stability of the supported complex compared with the solution analogues is probably a consequence of its coordination to the zeolite lattice, which inhibits dimer formation. In this case it is not the steric restraints of the cavity that inhibit dimer formation because the ethylenediamine adduct is no larger than the methylamine-cobalt adduct. Instead, this stabilization is most likely due to the immobilization of the complex by anchoring it to the framework.

The most recent zeolite entrapped oxygen carrier reported by Lunsford is $[Co^{II}(bpy)(terpy)]^{2+}$ (bpy = bipyridine and terpy = terpyridine).[23] With this complex, the formation of the oxygen adduct is completely reversible at 25 °C and the complex is thermally stable in the presence of oxygen up to 70 °C. Unlike the previous amine complexes, Lunsford found that the preparation of this complex was not trivial. To get the mixed ligand complex, cobalt exchanged zeolite had to be exposed to both bipyridine and terpyridine vapor simultaneously. This lead to the formation of $[Co(bpy)_3]^{2+}$ and $[Co(terpy)_2]^{2+}$, with the desired complex only being formed in low concentrations, only 5.6×10^{18} spins/g.

This $[Co^{II}(bpy)(terpy)]^{2+}$-Y material was also found to be effective for separating oxygen from air, with a separation factor (O_2/N_2) of 12.3.[26] The major drawback of

this material for use in any practical application is its extreme sensitivity to moisture. Water can occupy the sixth coordination site of the complex and prevent oxygen from binding. This effect is reversed, however, by evacuating the sample to remove the water. In the presence of both water and oxygen, the complex is completely deactivated towards binding oxygen. This effect is irreversible and reported to be caused from oxidation of the ligands by a hydroperoxy radical formed from the reaction of the oxygen adduct with water.[26]

This early work has established the utility of synthesizing cobalt complexes inside a zeolite cavity in order to prevent dimer formation in the presence of oxygen. The steric restrictions of the zeolite cavity allowed both $[Co(n\text{-}C_3H_7NH_2)_5]^{2+}$-Y and $[Co^{II}(bpy)(terpy)]^{2+}$-Y to form stable monomeric oxygen adducts, with no tendency to dimerize. $[Co(en)_2]^{2+}$-Y was also found to form a stable 1:1 oxygen-adduct due to its axial coordination to a lattice oxygen, which anchors it to the framework. Unfortunately, none of these complexes are stable under the conditions needed to be useful in practical applications. Therefore, it appears a new ligand system is needed that is both strong field enough to form a low-spin cobalt(II) configuration and oxidatively stable enough to withstand both oxygen and water. It was for this reason that the work reported here was initiated.

Cobalt Cyanide Complexes

The ligand in this study is the cyanide ion, which is known to form low-spin complexes with cobalt[27] and is very stable to oxidation. Cobalt cyanide complexes were studied in the 1960s as homogeneous hydrogenation catalysis because of their ability to activate molecular hydrogen.[28] This work is, however, concerned with their ability to bind oxygen and serve as oxygen carriers. While in solution they are not useful for this purpose because they irreversibly dimerize,[29] inside a zeolite the monomer may be stablized and become a useful oxygen carrier. Since cyanide is very oxidatively stable, these complexes will also overcome the problem of ligand degradation.

The chemistry of cobalt cyanide complexes in solution is well known.[27] Cobalt(II) cyanide is obtained as a light brownish precipitate from solutions of cobalt(II) and cyanide. When this material dissolves in an aqueous solution of excess cyanide, an olive-green solution containing $Co(CN)_5^{3-}$ is obtained. This complex is stable at low concentration and in the absence of oxygen. At higher concentrations dimerization occurs and ethanol precipitates a violet solid with molecular formula $K_6[Co_2(CN_{10})]$, known as Adamson's salt.[30] This salt can be redissolved in water yielding the pentacyano complex. In the presence of oxygen, however, a μ-peroxo dimer is formed irreversibly.[29]

Formation of either the Co-Co dimer or the oxygen bridged dimer results in complete deactivation of the complex as an oxygen carrier. It can therefore be seen that if cobalt cyanide complexes are to be used as oxygen carriers, one must find a way to inhibit their dimerization.

Both the pentacyanocobalt(II) complex[31-32] and its mono adduct[33] have been isolated from dimethylformamide solutions using bulky tetraalkylammonium counterions. Thus, it is possible to keep dimerization from occurring under the right conditions. Carter et al.[34-35] have reported the formation of several lower coordinate cobalt(II) cyanide complexes in aprotic media by varying the CN:Co ratio. Spectral evidence[31,35] suggests the presence of $Co(CN)_2(solvent)_2$, $Co(CN)_3(solvent)^-$, $Co(CN)_4^{2-}$, and $Co(CN)_5^{3-}$ as the ratio of cyanide to cobalt increases. Only the pentacyano complex forms at ratios greater than six. The tetracyano complex has been isolated and shown to have a square-planar structure with an oxygen atom from a solvent molecule weakly coordinated in the axial position.[34] (See Figure 2-4.)

The solution chemistry of these cobalt(II) cyanide complexes indicates that several complexes with different stoichiometries can be formed inside zeolite cages. The usefulness of the solution complexes as oxygen carries is, however, eliminated because of their facile decomposition in the presence of oxygen. Both in aqueous[36-37] and

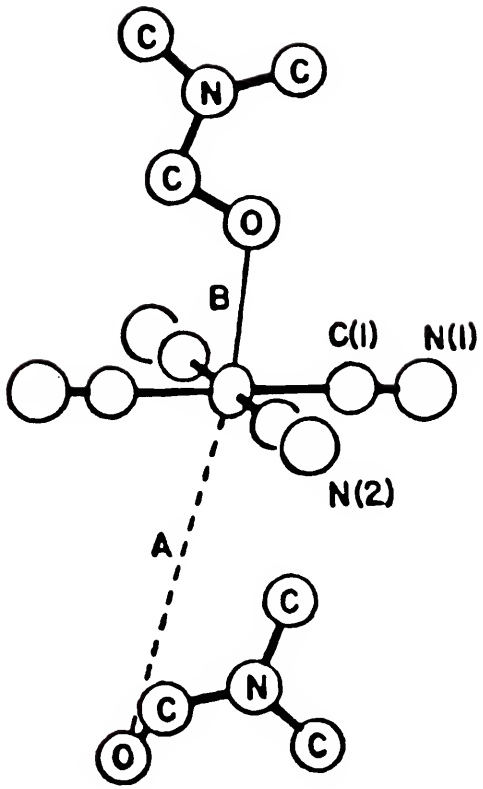

Figure 2-4. Proposed structure[35] of $(PNP)_2Co(CN)_4$.

aprotic[35] solution, decomposition occurs through an intermolecular interaction. If these complexes can, therefore, be prepared inside a zeolite cavity and isolated from one another, they may serve as efficient, stable oxygen carriers.

CHAPTER 3
EXPERIMENTAL

Synthesis

Solvents and Reagents

Methanol used was reagent grade and dried over activated 3A molecular sieves. NaY used was LZY-52 powder obtained from Linde. All chemicals were used as obtained without further purification. $CoCl_2 \cdot 6H_2O$ was an analytical reagent from Mallinckrodt. NaCN was A.C.S. certified from Fischer Scientific. Ethylenediamine-tetraacetic acid, tetrasodium salt 98% (Na_4EDTA) and Cesium Chloride (99.9%) were obtained from Aldrich Chemical Company. Oxygen, argon, nitrogen, and helium were obtained from Liquid Air Corporation. All water used was distilled.

Cobalt Exchanged Zeolites

NaY was first stirred in 0.25M NaCl at room temperature then washed with water until no precipitation was observed when the filtrate was tested with a 0.1 M $AgNO_3$ solution.

The NaY was then dried at 100 °C overnight in a vacuum oven. CoY was then prepared by exchange of Na^+ for Co^{2+} in an aqueous $CoCl_2$ solution at 70 °C for 24 hours. Aqueous $CoCl_2$ solutions were always less than 0.03 M and usually less than 0.01 M. There was very little cobalt remaining in the solution after the reaction. The resulting pink solid was then collected by filtration, washed with water until no Cl^- was present in the filtrate, and dried at 150 °C in the vacuum oven overnight. The resulting solid was deep purple/blue.

Cesium Treatment

Cesium exchanged CoY samples were prepared by stirring CoY in a 0.1 M CsCl or CsOH solution. These exchanges were done at room temperature and allowed to stir a minimum of 16 hours. Often the treatment was repeated to ensure maximum Cs^+ exchange.

General Reaction Conditions

Unless otherwise specified, all reactions were carried out in the presence of atmospheric oxygen and moisture. Flasks were stoppered during stirring but no precaution to exclude air was taken. Reactions done under inert atmosphere were carried out using Schlenk techniques under

purging argon. When water was rigorously excluded, the methanol was freshly distilled from BaO and the argon was passed over activated sieves and NaOH. During reactions where oxygen or water were excluded, the CoY was evacuated at 100 °C and filled with nitrogen at least 3 times prior to use.

Cobalt Cyanide Containing Zeolites

Dry CoY samples were reacted with CN^- in a methanolic NaCN solution (CN:Co 10:1 minimum) at room temperature for 2-4 days. The resulting solids were washed with copious amounts of methanol and dried at 60 °C in the vacuum oven. The resulting solids were gray-blue. The Ni(CN)-Y samples were prepared in the same way, resulting in a yellow solid after drying.

Successive Addition of Cyanide

Some reactions were carried out by adding cyanide to CoY in small portions and filtering between the addition of each portion. This was carried out using a 3-neck flask with a fritted filter as its bottom. The NaCN/methanol solution was added to the CoY in the special flask and the mixture was stirred using an overhead stir motor. The solution was then filtered off and another portion of

NaCN/methanol was added. All these reactions were done under purging argon.

Chelate Treatment

Chelate treatment for removal of free cobalt(II) was carried out by stirring the samples with aqueous 0.1 M Na_4EDTA at 70 °C. The solids were then washed with water and dried at 60 °C in the vacuum oven. The resulting solids were light yellow.

Characterization

Spectral Measurements

All IR spectra were recorded as Nujol mulls using a Nicolet DXB FTIR spectrophotometer. X-band EPR spectra of powder samples were recorded using a Bruker ER200D-SRC spectrometer equipped with a variable temperature unit. For removal or exclusion of oxygen from the EPR samples, tubes were fitted with o-ring connectors and attached to stopcocks, thus allowing connection to a vacuum line. EPR spectral simulations were calculated using the "QPOW" EPR simulation program.[38] Elemental analysis of dissolved samples were conducted using a Perkin-Elmer Plasma II Emission Spectrometer.

Elemental Analysis

Cobalt concentrations were determined by ICP analysis of the dissolved zeolite. A typical sample was dissolved as follows: A 0.1 gram sample of the zeolite was refluxed in 15 ml of 2 M HCl. Next 10 ml of 6 M NaOH and 15 ml of 0.1 M Na_4EDTA were added and the mixture was refluxed again. This treatment completely dissolved the solid. Analysis for nitrogen content was carried out by the Microanalysis Laboratory at the University of Florida. To ensure a constant weight during analysis for Co and N, the samples were allowed to equilibrate over H_2O in a closed chamber for several days prior to analysis. Water contents were calculated from the hydrogen content of the sample and the reported weight percents are corrected back to dry samples. (See Appendix A.)

Quantitative EPR Measurements

When desired, signal intensities for the oxygen adducts were determined by numerical double integration of the first derivative spectrum. Spin concentrations were calculated by comparison with the integrated spectrum of $CuSO_4 \cdot 5H_2O$.[39] Typically a 0.1 gram sample of zeolite was precisely weighted into an EPR tube and the spectrum measured. If

multiple samples were measured in the same experiment, care was taken to be sure the tubes were positioned at the same height in the cavity and the instrument settings were the same. The spectrum for each sample and standard was measured several times to ensure reproducibility.

Spin Concentration versus Oxygen Pressure

The EPR signal intensity of the cobalt-oxygen adduct in Co(CN)-Y was measured at various pressures of oxygen above the sample. A sample of Co(CN)-Y was placed in an epr tube/stopcock assembly. This tube could be attached to the vacuum line. The sample was evacuated until no EPR signal was seen at room temperature. Following this, successive amounts of oxygen were admitted to the sample and the EPR spectrum was measured several times at each interval. Spin concentrations were calculated by comparison to a sample of known concentration.

Titration of CoY with Cyanide

Several samples of Co(CN)Na-Y were prepared using different CN/Co ratios (R) during the synthesis. Potassium bromide pellets were prepared using 0.250 grams KBr (dried at 150 °C) and 7.5 mg of zeolite sample. The IR absorbance of each sample was recorded from 2400 cm^{-1} to 1800 cm^{-1} for

several different orientations of each pellet. Care was taken to ensure the absorbance range was the same in each case. For several of the samples the preparation was repeated and the filtrates were analyzed for Co and CN^-. The test for Co using Na_4EDTA and H_2O_2 in basic solution was negative in each case. A quantitative analysis for CN^- ions was performed using the Vohard method (titration with $AgNO_3$ using Na_2CrO_4 as the indicator).

Adsorption Measurements

The adsorption isotherms were determined using a volumetric technique. (See Figure 3-1.) A sample was placed in a container of known volume and exposed to a known volume of gas at a known pressure and temperature. From this the amount of gas adsorbed by the sample was determined by pressure differences. (See Appendix A.) Pressure measurements were made using a MKS Baratron with a 390A sensor head and 270B signal conditioning unit. Two sensor heads were attached via a MKS Type 274 channel selector to give a readable range of 10^{-5} - 1000 torr. The temperature was monitored during each experiment and did not vary more than ± 1 °C.

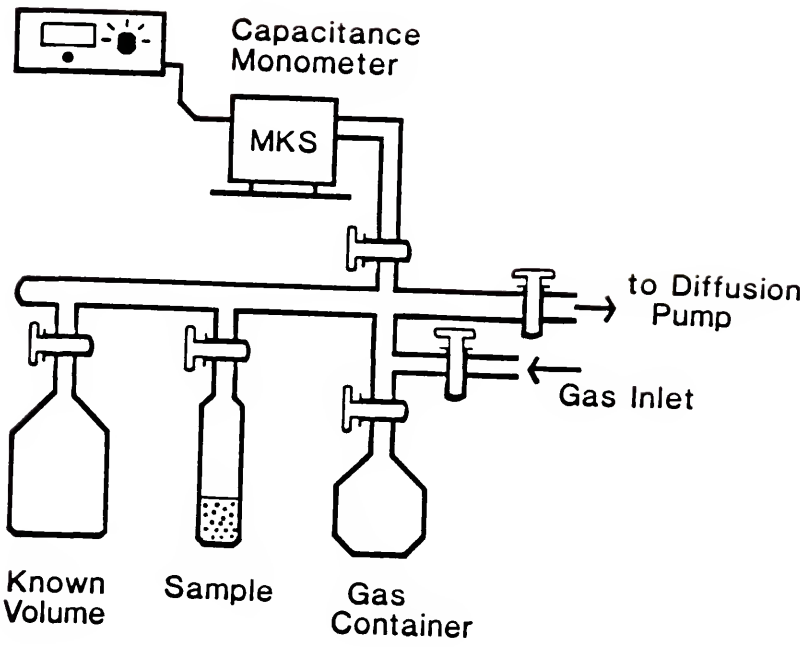

Figure 3-1. Apparatus used for gas adsorption measurements.

CHAPTER 4
RESULTS AND DISCUSSION

$Co(CN)_4^{2-}$ Inside Zeolite Y

Preparation of Co(CN)Na-Y

The reaction of cobalt(II) exchanged into zeolite Y with cyanide solutions produces entrapped cobalt cyanide complexes.[40-41] This reaction is unique because it requires a negatively charged ligand to enter into a negatively charged framework and form an anionic complex. All the previously reported transition metal complexes synthesized inside a zeolite framework have been either cationic or neutral.[11-17] In this case, the driving force to overcome the charge repulsions between the ligand and framework is likely the large formation constant for the cobalt cyanide complexes. Cyanide does not enter the framework when stirred under similar synthesis conditions with zeolites exchanged with Group IA and IIA cations. Furthermore, cobalt cyanide complexes, such as $Co(CN)_5^{3-}$ and $Co(CN)_6^{3-}$ prepared in solution, do not enter into Na-Y under synthesis conditions.

Since charge balance inside the zeolite must be maintained during this reaction, a cation must also be incorporated into the zeolite when a cyanide enters. Elemental analysis of these Co(CN)Na-Y materials shows increased sodium ion content.

Solvent effects are important in the reaction of CoNaY with NaCN. Table 4-1 lists the dielectric constants and Gutman acceptor numbers[42] for several solvents used in this work. When water is the solvent more than 80% of the cobalt is removed from the zeolite to form the cobalt cyanide complexes in solution. When, however, methanol (CH_3OH) is the solvent, very little cobalt is lost from the zeolite during the reaction with cyanide. Formamide ($HCONH_2$) gives similar results to methanol. When dimethyl sulfoxide (DMSO), N,N-Dimethyl formamide (DMF), and N,N-Dimethyl Acetamide (DMA) are used as the reaction media, very little cobalt is lost during the cyanide reaction but very little cyanide is coordinated to the cobalt in the zeolite. The effectiveness of the solvent is dependent on its ability to solvate the cyanide ion and correlates well with the acceptor numbers, AN, listed for each solvent.[42] Water is good at solvating ions but extracts cobalt from the zeolite to form complexes in solution. The best solvent for the formation of cobalt cyanide complexes inside zeolite Y must have a balance between the ability to solvate cyanide and to extract cobalt.

Table 4-1. Dielectric constants and acceptor numbers for various solvents.

Solvent	E	AN[a]
Water	78.5	54.8
MeOH	32.6	41.3
$HCONH_2$	109.6	39.8
DMSO	46.6	19.3
DMF	37.8	16.0
DMA	36.7	13.6

[a]Reference 42.

Characterization of Co(CN)Na-Y

Infrared and EPR characterization of Co(CN)Na-Y

The IR spectrum of Co(CN)Na-Y exhibits a C-N stretching vibration, ν_{CN}, at 2129 cm^{-1}. Table 4-2 lists IR data for complexes prepared here as well as for several known metal cyanide complexes. These results suggest that the major species formed in the zeolite is $Co(CN)_6^{3-}$; however, the zeolite lattice may influence the frequency and other complexes with similar ν_{CN} may be masked by this large peak. The species formed are not cobalt dimers or oxygen bridged dimers, both of which have multiple cyanide stretching frequencies.[48-49]

The EPR spectrum of Co(CN)Na-Y consists of a broad signal near g=2. (See Figure 4-1.) The EPR parameters (Table 4-3) are characteristic of a wide variety of low-spin $Co-O_2$ adducts, including several cationic and neutral adducts which have been synthesized in zeolite Y.[18,19,21,23] Hyperfine splitting resulting from ^{59}Co (S=7/2) is small, as predicted by the spin pairing model for $Co-O_2$ adducts in which the unpaired electron resides predominately on the dioxygen molecule.[21,50-52] The spin pairing model of binding dioxygen to a low-spin cobalt(II), see Figure 4-2, can be viewed as a free radical reaction in which the lone unpaired electron on cobalt(II) combines with one of the π^*electrons

Table 4-2. IR Data for Cobalt Cyanide Complexes

Compound	$\nu_{CN}(cm^{-1})$
Co(CN)Na-Y	2129
$(Et_4N)_3Co(CN)_5$[a]	2080
$(Et_4N)_3Co(CN)_5(O_2)$[a]	2120
$(PNP)_3Co(CN)_5$[b]	2072
$(PNP)_2Co(CN)_4$[b]	2095
$K_3Co(CN)_6$[c]	2129
$K_3Co(^{13}CN)_6$[d]	2082
$Cs_2Li[Co(CN)_6]$[e]	2142
$Cs_2Na[Co(CN)_5(H)]$[f]	2113
$Co_3[Co(CN)_6]_2$[g]	2176
$K_6[(CN)_5Co\text{-}Co(CN)_5]$[h]	2130(m),2100(s),2073(vs)
$K_6[(CN)_5Co\text{-}O_2\text{-}Co(CN)_5]$[i]	2146, 2132, 2125, 2120

[a] Reference 31 [b] Reference 34 [c] Reference 43
[d] Reference 44 [e] Reference 45 [f] Reference 46
[g] Reference 47 [h] Reference 48 [i] Reference 49

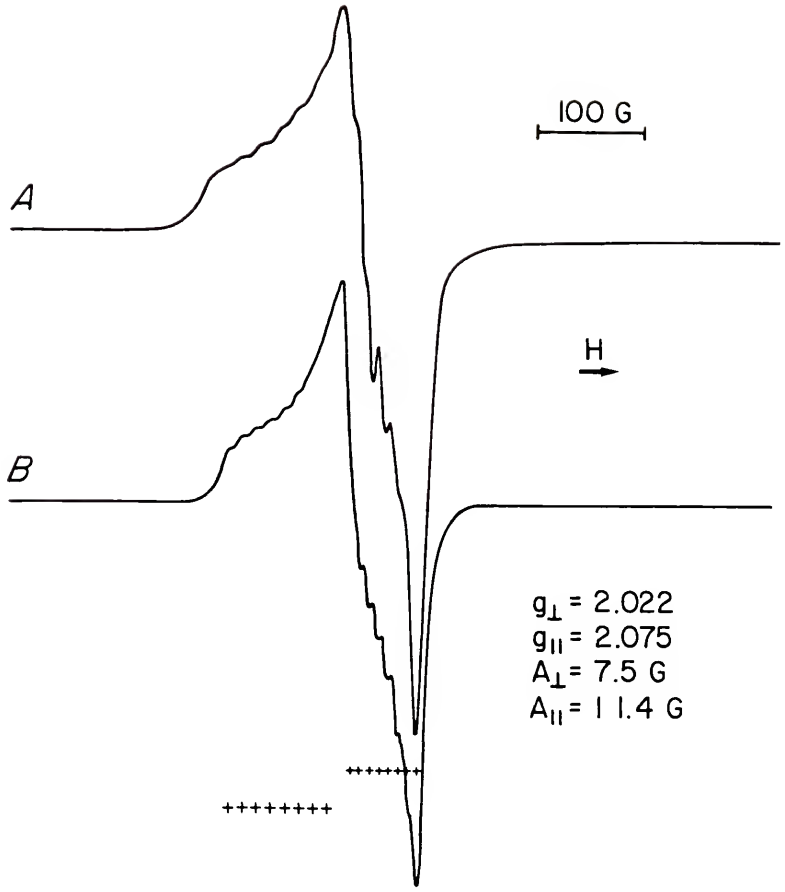

Figure 4-1. X-Band EPR spectrum of $[Co(CN)_4(O_2)^{2-}]$-Y. (A) experimental and (B) simulated.

Table 4-3. EPR parameters for cobalt-oxygen adducts.

$Co-O_2$ ADDUCTS	g_z	g_y	g_x	a_z (G)	a_y (G)	a_x (G)
$Co(CN)_4(O_2)Na$-Y	2.075	2.022		11.4	7.5	
$(Et_4N)_3Co(CN)_5(O_2)$[a] (solid)	2.02-2.03					
$(Et_4N)_3Co(CN)_5(O_2)$[a] (acetone)	2.02			10.5		
$Co(CN)_5(O_2)^{3-}$[b] (water)	2.007			9.8		
$Co(NH_3)_5(O_2)$-Y[c]	2.084	2.010	2.000	17.8	12.0	12.5
$Co(en)_2(O_2)$-Y[d]	2.084	1.998	1.992	20	10	13
$Co(SALEN)(O_2)$-Y[e]	2.078	2.020	2.020	21.0	11.3	11.3
$Co(bpy)(terpy)(O_2)$-Y[f]		2.063	2.007	1.998	15.6	11.0
11.0						

[a] Reference 31 [b] Reference 29 [c] Reference 49 [d] Reference 21
[e] Reference 19 [f] Reference 23

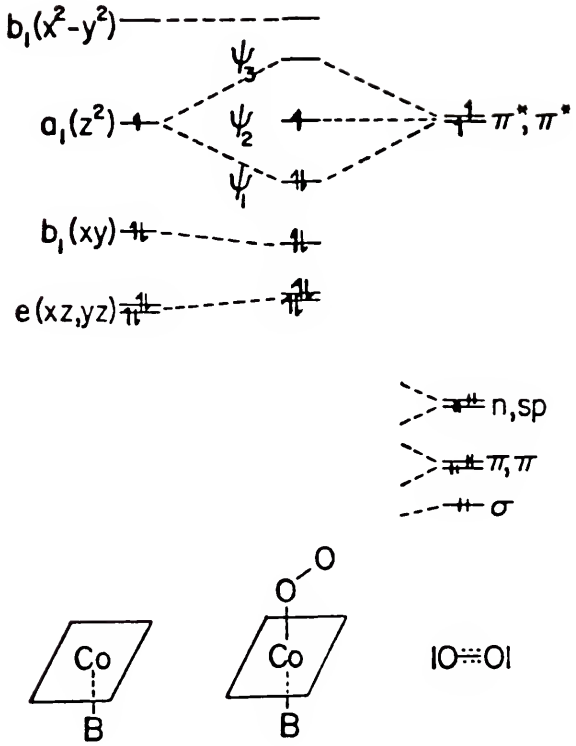

Figure 4-2. Molecular obital diagram for the dioxygen adduct of Co(II).

of the dioxygen molecule to form a σ-bond. The other π^* electron remains unpaired and resides essentially on the oxygen with cobalt hyperfine arising from spin polarization of the cobalt-oxygen σ-bond.[51-52]

This model allows an interpretation of the EPR parameters which produces the cobalt(II) contribution to the σ bonding molecular orbital, α'^2_{Co-O}:

$$\alpha'^2_{Co-O} = \frac{[\ A_{aniso}\ (CoO_2) + 1.0 \times 10^{-4}\ cm^{-1}\ ]}{2.44 \times 10^{-3}\ cm^{-1}} \qquad 4\text{-}1$$

The partial negative charge on the bound O_2 is referred to as the extent of electron transfer from cobalt(II), E.T., and is given by the formula

$$E.T. = 2(1 - \alpha'^2) - 1 \qquad 4\text{-}2$$

Such an analysis produces an electron transfer value of 0.7 e^- for the cyano complex trapped in the zeolite.

The spin concentrations for the $Co\text{-}O_2$ adduct in Co(CN)Na-Y(1) and Co(CN)Na-Y(2) are 4.8×10^{18} and 1.8×10^{18} spins/g respectively. These correspond to 8.0 and 3.0 umoles/g respectively, which is less than 1% of the total cobalt present.

The $Co\text{-}O_2$ adduct can be deoxygenated under vacuum yielding a species with an EPR spectrum which is quite

different from that of the original Co-O_2 adduct. (See Figure 4-3.) The much larger ^{59}Co hyperfine coupling and reversal in magnitude of $g_{\|}$ and $g_{\perp}$ indicates that the unpaired electron density is located mostly in the d_{z^2} orbital of the cobalt(II) ion.[53] (See Table 4-4.) The $g_{\perp}$ values are close to those of the 4-coordinate complex formed in a 3:1 mixture of CN^- to Co^{2+} in acetonitrile solvent.[31] The relatively large anisotropy in the g tensors supports the contention that the complex is not $Co(CN)_5^{3-}$ but rather square-planar $Co(CN)_4^{2-}$ with axial coordination positions occupied by zeolite framework oxygens.

The IR spectrum for square planar $(PNP)_2[Co(CN)_4]$ (PNP = bis(triphenylphosphine) nitrogen(+1) cation) is reported to contain a ν_{CN} at 2096 cm^{-1}, but the oxygen adduct of this square planar complex has not been reported.[34] By assuming the same shift of ν_{CN} upon oxygenation as seen when $Co(CN)_5^{3-}$ (2080 cm^{-1}) forms $Co(CN)_5(O_2)^{3-}$ (2120 cm^{-1}),[31] we can estimate ν_{CN} for $Co(CN)_4(O_2)^{2-}$ to be about 2136 cm^{-1}. The ν_{CN} frequency for metal cyanide complexes is reported to increase as the oxidation state of the metal increases[54] and is consistent with the removal of electron density from cobalt(II) due to the binding of oxygen.[51] Due to the low concentration of the Co-O_2 adduct and the presence of the intense ν_{CN} (2129 cm^{-1}) for $Co(CN)_6^{3-}$ in the sample, the ν_{CN} for the $Co(CN)_4(O_2)^{2-}$ is not observed.

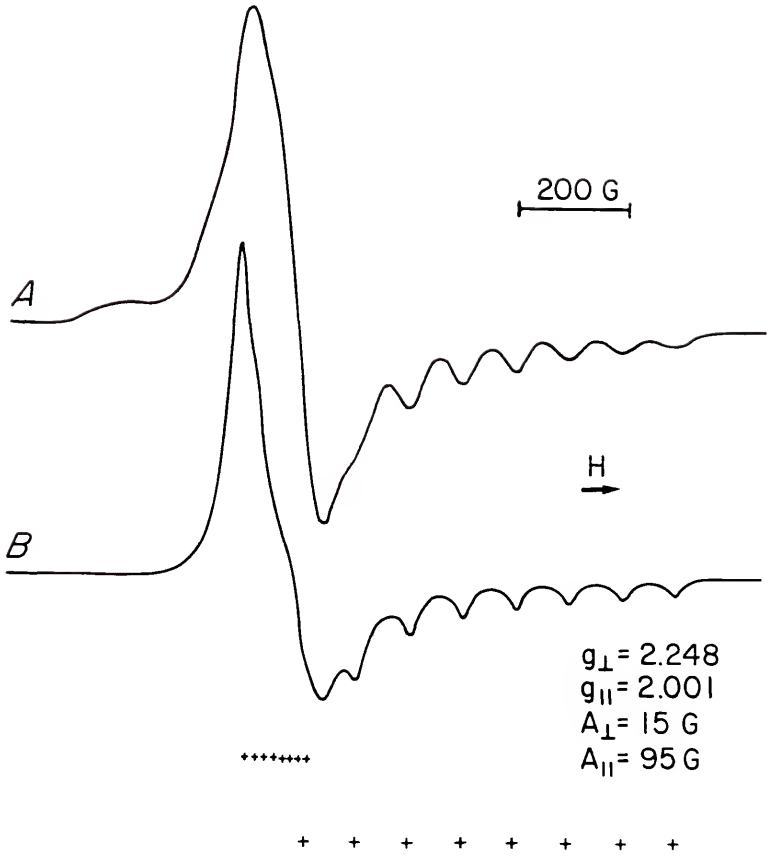

Figure 4-3. X-Band EPR spectrum of $[Co(CN)_4^{2-}]$-Y. (A) experimental and (B) simulated.

Table 4-4. EPR parameters for low-spin cobalt(II) complexes.

NON-ADDUCTS	$g_\perp$	$g_\parallel$	$a_\perp$ (G)	$a_\parallel$ (G)
$Co(CN)_4Na$-Y	2.248	2.001	15	95
$Co(CN)_5^{3-}$ [a]	2.157	1.992	28	87
$Co(CN)_5^{3-}$ [b]	2.20	2.00		
$Co(CN)_5^{3-}$ [c]	2.18	2.00	29	87
$Co(CN)_3(NCCH_3)^-$ [c]	2.28	2.00	14	112
$Co(CNCH_3)_6$-Y[d]	2.087	2.000	72	68
$Co(CNCH_3)_5$-Y[d]	2.163	2.003	32	89
Co(bpy)(terpy)-Y[e]	2.250	2.012	15	101

[a] Reference 53 [b] Reference 29 [c] Reference 31 [d] Reference 22
[e] Reference 23

The active species is stable to repeated cycling experiments in the presence of atmospheric levels of moisture. A sample of Co(CN)Na-Y(1) was alternately oxygenated (atmospheric oxygen) and deoxygenated at room temperature through 510 cycles over a 6-week period without losing its oxygen absorption capacity. Analysis by EPR performed at the end of the experiment indicated that no decomposition had occurred.

It can be concluded from the EPR characterization of this material that a low-spin, d^7 cobalt(II) complex is formed during the reaction of CoNaY with CN^- in methanol. This complex reversibly binds oxygen and is stable during repeated cycling, however, spin concentration measurements show this active complex is only present in low concentrations. It appears from IR data that the major complex formed in this reaction is $Co(CN)_6^{3-}$. This complex is diamagnetic and, therefore, not observed in the EPR spectrum for this material. Its IR spectrum shows a single, strong ν_{CN} at 2129 cm^{-1}. The ν_{CN} for the active complex is not observed due to its low concentration and the presence of the band for the major complex.

Gas adsorption characterization of Co(CN)Na-Y

The gas adsorption properties of these Co(CN)Na-Y materials were studied by volumetric gas uptake measurements to determine if the presence of this active cobalt complex

produces an oxygen selective material. Figure 4-4 shows the equilibrium adsorption isotherms for N_2, O_2, and Ar obtained for Na-Y at 298 K. The enhanced affinity of Na-Y for N_2 over O_2 and Ar is due to the quadropole interaction of the N_2 molecule with the ions present inside the framework.[2] This enhanced affinity for nitrogen is a general property of zeolites and explains why these materials are used in PSA processes to separate O_2 and N_2. As mentioned in Chapter 1, the separation of O_2 and N_2 in the PSA process is based on the difference in the extent of physical adsorption of O_2 and N_2 by the adsorbent. Gases for which these quadropole interactions are minimal, such as O_2 and Ar, show very similar adsorption isotherms resulting in the material having no selectivity for either gas. Consequently, argon is used as the blank when trying to determine any increase in oxygen uptake resulting from the presence of an active, oxygen binding complex.

Figure 4-5 shows the adsorption isotherms for O_2 and Ar on Co(CN)Na-Y(1) and Co(CN)Na-Y(2). From this we see that the presence of the active complex indeed has an influence on the gas uptake properties of this zeolite material. The presence of this active complex results in a material which has a high selectivity for oxygen. At 100 torr, more than twice as much O_2 is adsorbed as Ar on Co(CN)Na-Y(1). A similar increase for O_2 uptake over that of Ar is shown for

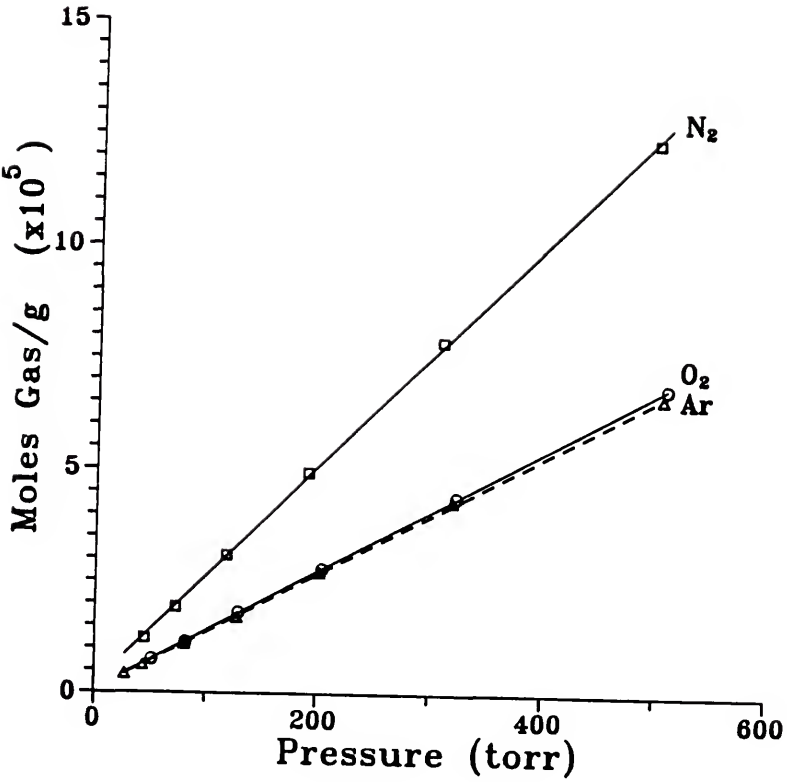

Figure 4-4. Gas adsorption isotherms for Na-Y measured at 298 K.

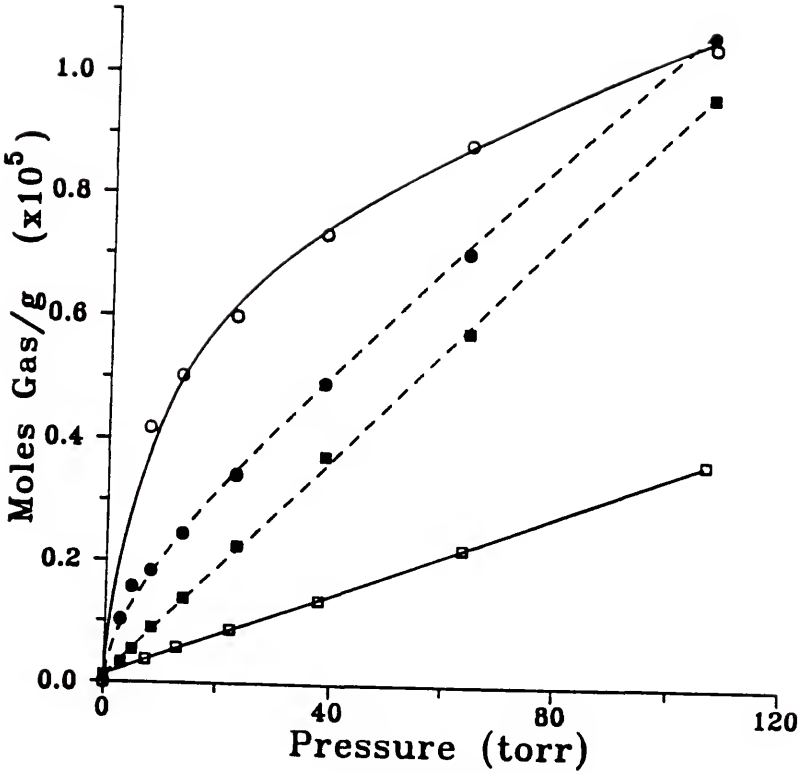

Figure 4-5. Comparison of O_2 and Ar gas adsorption isotherms for Co(CN)Na-Y materials. ——, ○ - Co(CN)Na-Y(1), O_2; ——, □ - Co(CN)Na-Y(1), Ar; - - -, ● - Co(CN)NaY(2), O_2; - - - , ■ - Co(CN)Na-Y(2), Ar.

Co(CN)Na-Y(2), however, it is not as large as in the Co(CN)Na-Y(1) sample due to the lower concentration of active complex in the former. The decreased uptake of Ar for Co(CN)Na-Y(1) and Co(CN)Na-Y(2) compared with NaY is due to the presence of $Co(CN)_6^{3-}$. This species, which occupies space in the zeolite, decreases the pore volume available for gas absorption. (See Appendix A.)

A second approach that demonstrates an increased uptake of O_2 in the Co(CN)Na-Y material involves a comparison of its adsorption isotherm with that of a Ni(CN)-Y material which has the same metal concentration. Square planar nickel cyanide is inert to oxygen. Figure 4-6 shows that the Ni(CN)-Y adsorbs the same amount of O_2 as it does Ar, as expected for a material with no enhanced affinity for either oxygen or nitrogen. Figure 4-7 shows that this material also adsorbs the same amount of Ar as Co(CN)Na-Y(2). When, however, the adsorption isotherm for O_2 in Ni(CN)-Y is compared with that of Co(CN)Na-Y(2), as in Figure 4-8, increased O_2 uptake is clearly established.

Characterization of the active complex in Co(CN)Na-Y

Determination of K_{O2}. The observed equilibrium constant for the binding of O_2 to the active cobalt can be expressed as follows:

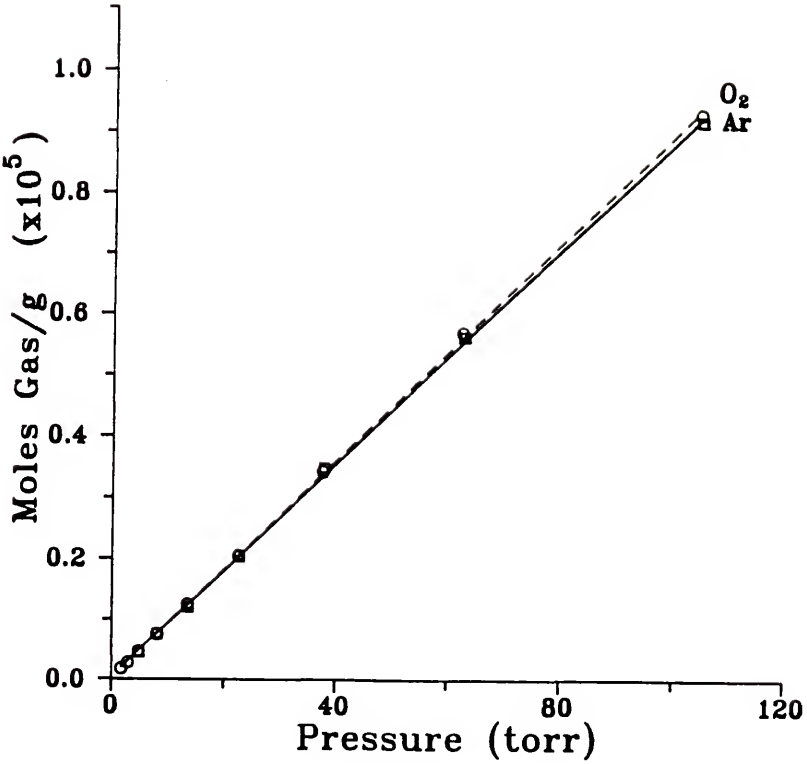

Figure 4-6. Comparison of O_2 and Ar gas adsorption isotherms for Ni(CN)-Y material.

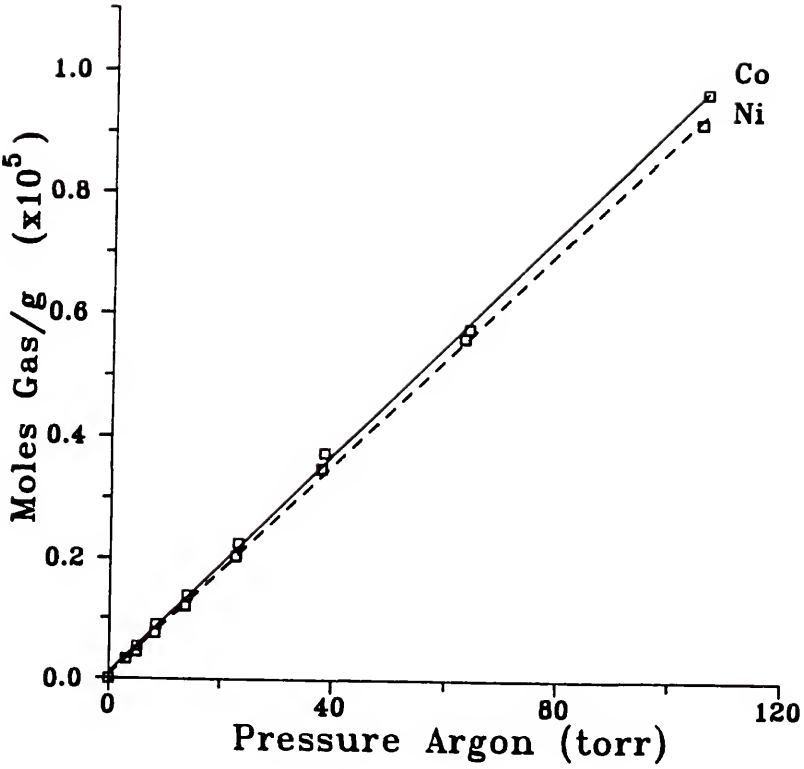

Figure 4-7. Comparison of Co(CN)-Y and Ni(CN)-Y gas adsorption isotherms for argon.

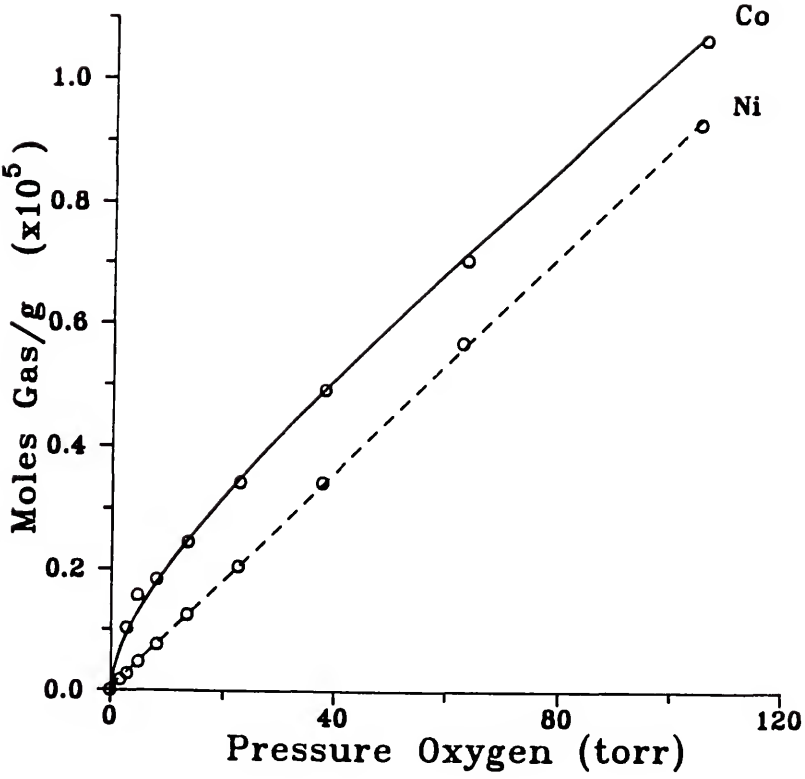

Figure 4-8. Comparison of Co(CN)-Y and Ni(CN)-Y gas adsorption isotherms for oxygen.

$$K_{O2} = \frac{[CoO_2]}{[Co]\ pO_2} \qquad 4\text{-}3$$

where $[CoO_2]$ is the concentration of complexed cobalt, [Co] is the concentration of active cobalt which remains uncomplexed at equilibrium, and pO_2 is the pressure of O_2 above the zeolite. Since the total concentration of active cobalt, $[Co]_T$, is the sum of [Co] and $[CoO_2]$, equation 4-3 can be rearranged to give equation 4-4.

$$[CoO_2] = [Co]_T - K_{O2}^{-1} \frac{[CoO_2]}{pO_2} \qquad 4\text{-}4$$

The volume for each concentration term is the same, therefore a plot of the amount of CoO_2 formed at pO_2 divided by pO_2 versus the amount of CoO_2 yields a straight line, assuming K_{O2} is constant. The equation of this line gives K_{O2} and the total amount of active cobalt present.

The amount of CoO_2 formed at a known pressure above the zeolite can be determined from the data shown in Figure 4-5. The difference between the oxygen and argon adsorption isotherms at the same gas pressure above the zeolite corresponds to the amount of CoO_2 formed at that pressure. The same information can be obtained by determining the amount of CoO_2 formed at a pressure of O_2 above the zeolite using the intensity of its EPR signal.

Figure 4-9 shows a plot of equation 4-4 for Co(CN)Na-Y(1) and Co(CN)Na-Y(2). The slope of these lines are -8.5 ± 0.5 torr and -9 ± 1 torr respectively and indicate the active species in both materials has the same observed equilibrium constant for binding oxygen, K_{O2}, of 0.12 ± 0.01 $torr^{-1}$.

If plots of equation 4-4 are extended to lower pressures, K_{O2} appears to change significantly. This can be explained by the fact that at lower pressures the distribution coefficient, K_d, for gas inside versus

$$[O_2]_{outside} \overset{K_d}{=\!=} [O_2]_{inside} \qquad 4\text{-}5$$

$$K_d = \frac{[O_2]_{in}}{[O_2]_{out}} \qquad 4\text{-}6$$

outside the zeolite increases significantly. This phenomenon is known as the sieving effect. Equation 4-7 can be used to relate K_{O2} to the true K_{eq} and K_d.

$$K_{O2} = K_d\, K_{eq} \qquad 4\text{-}7$$

From equation 4-7 it is seen that when K_d increases, K_{O2} increases and the magnitude of the slope in Figure 4-9 will decrease. This sieving effect has been described as the

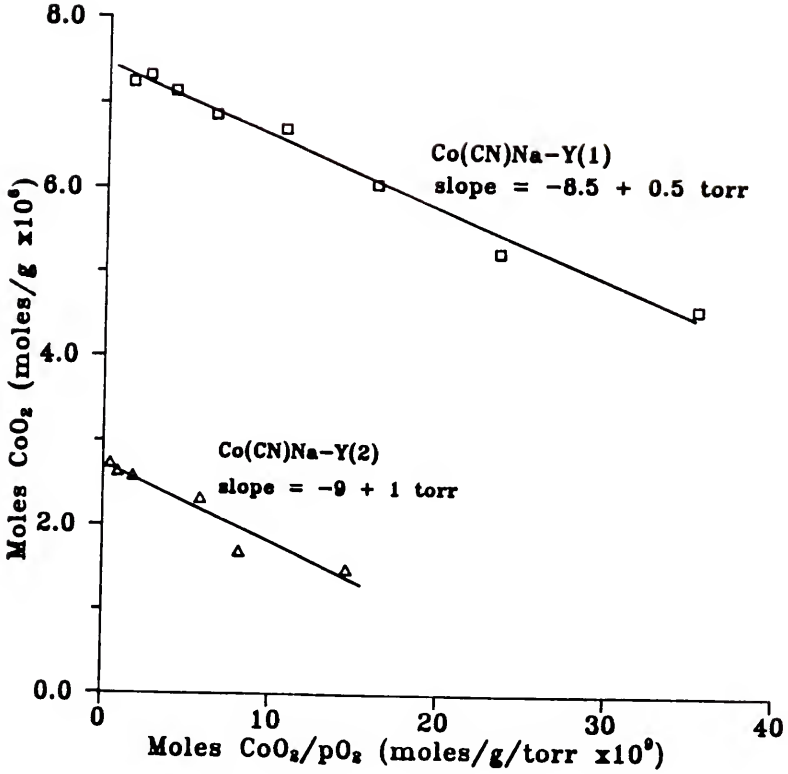

Figure 4-9. A plot of equation 4-4 for Co(CN)Na-Y(1), □ , determined from gas uptake data and Co(CN)Na-Y(2), Δ, determined from EPR data.

ability of the zeolite to "pump" oxygen to the complex and results comparable to ours are reported at these lower pressures.[19] This sieving of oxygen by the zeolite results in a higher effective oxygen pressure inside the pores than the externally applied oxygen pressure would imply, which results in an increased K_d at lower external pressures.

The distribution coefficient for Ar on Co(CN)Na-Y(1) and Co(CN)Na-Y(2) at 25 °C was determined to be 10 ± 1 for pressures of gas above the zeolite greater than 8 torr. The K_d for O_2 and Ar are the same for Na-Y and Ni(CN)-Y and determined to be 8 ± 1 for NaY and 10 ± 1 for Ni(CN)-Y. One would expect the values for NaY and Ni(CN)-Y to be the same. The higher value of K_d for Ni(CN)-Y over Na-Y may result because the pore volume in the former is actually smaller than estimated by the argon ratio technique used here, see Appendix A for details. This would result in a larger concentration of gas being calculated for inside the zeolite and, therefore, result in a larger K_d.

If the concentration of oxygen inside the zeolite, $[O_2]_{in}$, is substituted for pO_2 in equation 4-4, K_{O2} becomes K_{eq} and the influence of K_d on the measured equilibrium constant is corrected. The amount of argon absorbed by Co(CN)Na-Y at a designated pressure can be assumed to be the amount of uncomplexed oxygen present in the zeolite at that pressure during oxygen absorption. A plot of equation 4-4 can be made with $[O_2]_{in}$ replacing pO_2 to produce a K_{eq} of

240 ± 10 M^{-1}. Converting the K_{O2}, in units of $torr^{-1}$, to units of $molarity^{-1}$ gives a value for K_{O2} of 2200 ± 100 M^{-1}. With a value of 10 for K_d and equation 4-7, we see that a value of 220 results for K_{eq}.

It can be seen from this study that the sieving effect of zeolites will make the complete removal of O_2 from the active cobalt more difficult than that expected from the K_{O2} measured at near atmospheric pressures. This is because the increased K_d at lower pressures will increase the "effective" equilibrium constant, causing it to be more difficult to remove the oxygen.

Not only can the zeolite host affect oxygen binding of an active complex by influencing the local oxygen concentration, it can also influence the thermodynamics of oxygen binding. When oxygen binds to cobalt, a partial negative charge on the oxygen results. This negative charge could have an unfavorable interaction with the negatively charged zeolite framework, resulting in lower equilibrium binding constants for complexes inside zeolites. The active complex could also be in a restrictive binding site where steric interactions are important. Recent work[19] has reported this to be the case with $Co(SALEN)^{2+}$ prepared inside zeolite Y. In this work Herron found the $P_{1/2}$ value to be 306 torr for $Co(SALEN)\cdot py^{2+}$ inside Na-Y compared to a value of 10.5 torr in solution. It was reported that inside the zeolite, this lower binding constant is due to a reduced

exothermicity for oxygen binding. This effect is consistent with the oxygen being bound inside the zeolite cavity at a restrictive binding site where sterics and electrostatic interaction of the bound oxygen with the zeolite walls are important.

The $P_{1/2}$ value for a cobalt complex is the pressure of oxygen required to oxygenate half the active complexes. This value can be related to the equilibrium constant for oxygen binding as shown in equation 4-8. Therefore the smaller the $P_{1/2}$ value, the larger the

$$K_{O2} = \frac{1/2[Co]}{1/2[Co]\ P_{1/2}} = \frac{1}{P_{1/2}} \qquad 4\text{-}8$$

equilibrium constant for oxygen binding. Table 4-5 summarizes the $P_{1/2}$ values for several cobalt(II) complexes inside zeolites and in solution. Consistent with the spin pairing model,[51] the $P_{1/2}$ value for the complex reported here is less than that reported for $CoSALEN \cdot py^{2+}$ (SALEN = N,N'-bis(salicylidene)ethylene diamine) prepared in NaY.[19] The cyanide ligands produce a stronger ligand field than SALEN, raising the energy of the d_z2 orbital containing the unpaired electron. (See Figure 4-2.) The higher the energy of d_z2, the more energy gained when the complex forms a $Co\text{-}O_2$ bond and this electron drops down into the σ-bonding orbital. This results in a lower $P_{1/2}$ value.

Table 4-5. $P_{1/2}$ values for Co-O_2 adducts

Complex	$P_{1/2}$ torr
Co(CN)-Y	9 ± 1
CoSALEN·py^{2+} in NaY[a]	306
$CoSALEN^{2+}$ in pyridine[a]	10.5
$CoSALEN^{2+}$ in DMSO[b]	333
$Co(3\text{-}FSALEN)^{2+}$ solid[c]	2
$Co(terpy)(bpy)^{2+}$ in NaY[b]	0.59
$Co(terpy)(bpy)^{2+}$ in LiY[c]	0.34

[a] Reference 19
[b] Reference 23
[c] Reference 26

Comparing the active complex in Co(CN)Na-Y with Co(terpy)(bpy)-Y[23,26] (bpy = bipyridine, terpy = terpyridine) it is seen that the active complex inside the Co(CN)Na-Y material has a larger $P_{1/2}$ value, indicating a weaker overall ligand field. This is consistent with the active cyanide species being a low-spin $Co(CN)_4^{2-}$ ion with the axial position occupied by a lattice oxygen, as suggested by the EPR parameters. In the case of Co(terpy)(bpy)-Y, the axial position is occupied by the stronger nitrogen donor ligand. The weaker axial base in Co(CN)Na-Y results in a lower energy d_{z^2} orbital and a correspondingly larger $P_{1/2}$. This is also consistent with the conclusion that the active species is not $Co(CN)_5^{3-}$, which would give a much smaller $P_{1/2}$ due to the stronger axial ligand. The dramatic influence of the axial ligand on oxygen binding can be seen in comparing $CoSALEN^{2+}$ in solution with pyridine ($P_{1/2}$ = 10.5 torr) and with DMSO ($P_{1/2}$ = 333 torr) as the axial ligands.[19]

Conclusions about the active complex. The EPR parameters and equilibrium constant for oxygen binding suggest that the active complex formed in Co(CN)Na-Y is a square-planar $Co(CN)_4^{2-}$ ion that is coordinated to the zeolite framework through a lattice oxygen. This species is analogous to the bis(ethylenediamine) cobalt(II) complex prepared in zeolite Y by Lunsford.[21] Unlike the Howe and Lunsford complex, this complex is anionic and has much more

oxidatively stable ligands. The proposed structure for this complex is very similar to that of $(PNP)_2Co(CN)_4$ (See Figure 2-4.) prepared by Carter and co-workers.[34] This complex is only formed in low concentration but still has a significant influence on the gas adsorption properties of the zeolite. Attempts to inhibit the oxidation of Co^{2+} during the synthesis and increase the concentration of this active complex are discussed later.

Characterization of the major complex in Co(CN)Na-Y

Elemental analysis. Table 4-6 lists the elemental analyses for the Co(CN)Na-Y materials prepared here. If the major species formed is $Co(CN)_6^{3-}$, as suggested by IR studies, then a N/Co ratio of 6 is expected. Table 4-6 shows that the N/Co values are low even after extended reaction times with cyanide, which suggests that there is still free cobalt(II) present. This is not surprising in Co(CN)Na-Y(1) since each large cavity (8 large cavities per unit cell zeolite Y) contains one $Co(CN)_6^{3-}$ complex, leaving no room for further complex formation.

Chelate treatment. In an attempt to remove this free cobalt(II), the Co(CN)Na-Y samples were treated with a chelating reagent (aqueous Na_4EDTA). When Co-Y samples are treated with this chelate solution, all the cobalt is removed from the zeolite. When, however, a Co(CN)Na-Y

Table 4-6. Elemental analysis for Co(CN)-Y materials

material	Co content wt%	Co content per unit cell	N content wt%	N content per unit cell	N/Co
Co(CN)-Y(1)	5.9	15	4.5	48	3.2
CT-Co(CN)-Y(1)[a]	4.2	11	4.4	48	4.4
Co(CN)-Y(2)	3.1	7.6	3.0	30	4.1
CT-Co(CN)-Y(2)[a]	2.4	5.8	3.0	31	5.2
Co(CN)-Y(3)	5.9	15	3.2	33	2.3
CT-Co(CN)-Y(3)[a]	2.5	6.1	2.9	30	4.9

[a] CT prefix indicates results after chelate treatment

sample is given the same treatment, only part of the cobalt is removed. For Co(CN)Na-Y(1) and Co(CN)Na-Y(2) the N content and IR spectrum for the major complex remain unchanged, suggesting that the major complex present is unaffected. The removal of free cobalt(II) results in an increase in the N/Co ratio approaching, in some cases, a value of 6. The low values of N/Co even after chelate treatment most likely occur due to incomplete removal of free cobalt(II) by EDTA. The presence of the hexacyanide complex in the large cavities may inhibit this process by crowding or blocking the pores.

In the case of Co(CN)Na-Y(3), the chelate treatment removes the species responsible for the ν_{CN} band at 2176 cm^{-1} but leaves the major $Co(CN)_6^{3-}$ species with ν_{CN} at 2129 cm^{-1}. This results in a corresponding decrease in the nitrogen content due to the removal of the surface species.

Reactions with oxidizing agents. As further proof that the major species formed is indeed a Co^{3+} complex, the Co(CN)Na-Y materials were reacted with several oxidizing reagents. (H_2O_2, $Na_2S_2O_8$ and NaOCl). This resulted in no change in color or in the value of ν_{CN} for the material, suggesting the major complex is $Co(CN)_6^{3-}$.

Titration of CoNa-Y with cyanide. Stuhl and co-workers have reported the formation of several cobalt cyanide complexes in solution by varying the CN/Co ratio during preparation.[34-35] Figure 4-10 shows selected IR

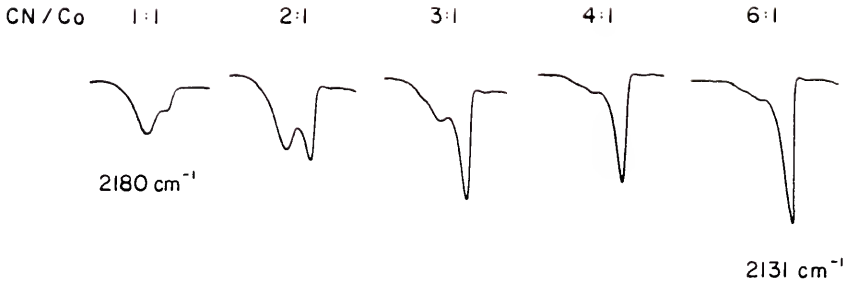

Figure 4-10. IR spectra for Co(CN)Na-Y samples prepared by varying the CN^-/Co ratio during preparation.

spectra of samples prepared here by reacting the same CoNaY material with solutions containing different cyanide concentrations. These spectra show the initial formation of a species with a ν_{CN} at 2180 cm^{-1}. This species is formed in low concentration, is EPR silent, and is believed to be $Co_3[Co(CN)_6]_2$ deposited on the exterior of the zeolite. As the concentration of cyanide increases, this species is washed off the surface. Figure 4-11 shows that the intensity of the ν_{CN} band for $Co(CN)_6^{3-}$ increases steadily as the concentration of cyanide increases until the CN/Co ratio exceeds 6. Above this valve the absorbance remains constant, indicating no more complex formation.

Conclusions about major complex in Co(CN)Na-Y. All the results presented up to this point are consistent with the conclusion that the major complex formed in the reaction of CoNaY with cyanide in methanol is $Co(CN)_6^{3-}$. This is not a surprising result in light of the fact that the reaction is done in the presence of excess cyanide. The availability of excess cyanide is known to have a great effect on E^o for the $Co^{3+}(aq) - Co^{2+}(aq)$ system. An E^o value of -0.8V shown in equation 4-9 suggests that $Co(CN)_6^{3-}$ must be,

$$Co(CN)_6^{3-} + e^- \xrightarrow{E^o = -0.8\ V} Co(CN)_5^{3-} + CN^- \qquad 4\text{-}9$$

thermally as well as kinetically, an extremely stable ion. While the formation constants for $Co(CN)_5^{3-}$ and $Co(CN)_6^{3-}$

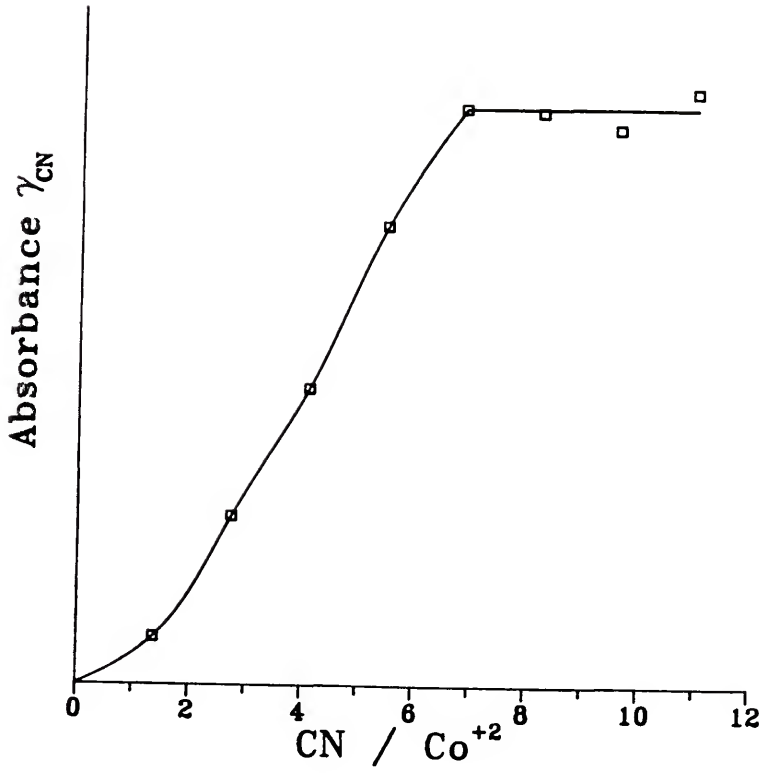

Figure 4-11. Plot of CN/Co ratio used during preparation of Co(CN)Na-Y versus the intensity of the ν_{CN} absorbance at 2131 cm^{-1}.

are not known, the value of β_6 for $Co(CN)_6^{3-}$ has been estimated to be $10^{50.27}$ (β_6 is the equilibrium constant for the reverse of reaction 4-9) From this it can be seen that there is a very large driving force for the oxidation of Co^{2+} to Co^{3+} in the presence of excess cyanide.

This effect is further increased by the slow diffusion of cyanide into the zeolite due to the repulsive forces of the negatively charged ion and framework. Figure 4-12 is a pictorial representation of this effect. It shows that even at low total values of R there is still an excess of cyanide at the surface which results in a large driving force for the oxidation of cobalt.

Synthesis Modification in Preparation of Co(CN)Na-Y

The following outlines many attempts made in trying to inhibit the oxidation of the cobalt during the reaction of CoNaY with cyanide. The results of these attempts also give insight into the mechanism by which this oxidation is occurring. The reaction conditions used in preparing all the previously mentioned samples have been the same. To summarize, the CoNaY is dried at 150 °C prior to use. It is then added to a methanolic solution of NaCN and stirred in a stoppered flask. The methanol is dried over activated 3A sieves prior to use and no special precautions are taken to

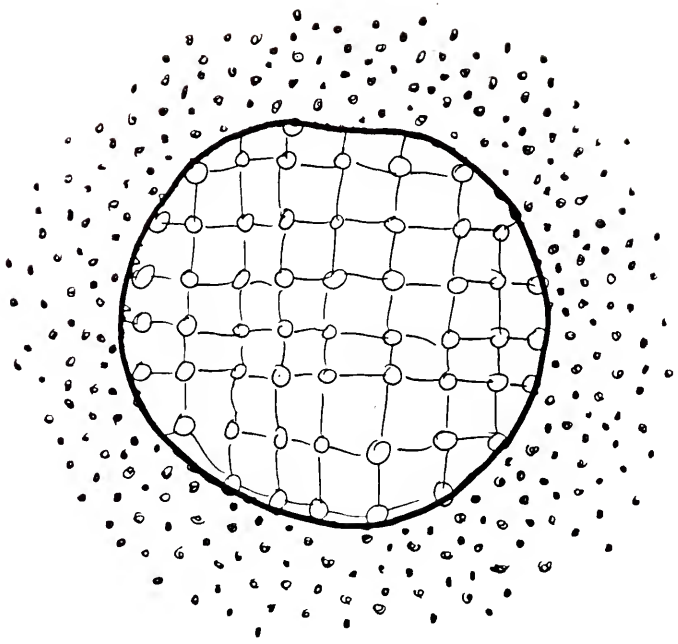

CN / Co = 5

Figure 4-12. A graphical representation of the effect caused by the slow diffusion of cyanide. Each small circle inside the zeolite particle represents a supercage containing 1 cobalt. Each dot outside the particle represents 1 cyanide.

exclude air or atmospheric moisture during the reaction. After stirring for a minimum of 24 hours, the mixture is filtered and the solid washed with dry methanol and dried at 60 °C under vacuum.

Any increase in the concentration of the active complex, $Co(CN)_4^{2-}$, would result in an increase in intensity of the EPR signal for the O_2-adduct and this was the criterion by which the results of these attempts were measured. Samples were also checked for the appearance of new ν_{CN} bands in their IR spectra.

Exclusion of oxygen and water

Many reactions of CoNaY with cyanide were carried out in the absence of oxygen. Solutions were deoxygenated by purging with argon and zeolites were evacuated and filled with nitrogen several times prior to use. Reactions were done under purging argon. No increase in the concentration of the active cobalt resulted as indicated by no increase in the EPR spin internsity or the absence of any new ν_{CN} bands in the IR were observed.

In several reactions extreme care was taken to minimize water as well as oxygen. The complete elimination of water from zeolite Y is very difficult and not only is water present, but hydroxyl groups are also present on the zeolite surface. Under the extreme conditions needed to remove water (550 °C under vacuum) Co^{+2} ions are forced into hidden

sites inside the zeolite, making their reaction with cyanide more difficult.

Solvents were freshly distilled and dried. Argon was dried by passing it over activated sieves and NaOH. Zeolites were dried up to 550 °C under vacuum and all manipulations were carried out using Schlenk procedures in an inert atmosphere glove bag. Again no increase in the amount of active species was observed and oxidation to $Co(CN)_6^{3-}$ still occurred.

Reducing conditions

Attempts were made to prepare the cobalt cyanide complexes in a reducing environment in order to retard the oxidation process. When the cyanide reaction was carried out in the presence of reducing agents such as sodium borohydride or hydrazine in the solution, the major species formed was still $Co(CN)_6^{3-}$. In other attempts NaY was pre-washed with a reducing agent and kept under inert atmosphere during the cobalt exchange and cyanide reaction. Again only the oxidized species was seen in the IR spectrum. Since reactions of $Co(CN)_5^{3-}$, with H_2 are known to form hydride species in solution,[55] the CoNaY/cyanide reaction was carried out under H_2. When CoY was stirred with a NaCN/methanol solution under 50 psig H_2, no significant increase in the concentration of active complex and no new ν_{CN} bands in the IR spectrum were seen.

Slow addition of cyanide

Since the driving force for the oxidation of cobalt results from the high CN/Co ratio, attempts were made to add the cyanide very slowly and allow its concentration to equilibrate throughout all the cobalt before more is added. Even when the cyanide is added dropwise over a 48 hour period leading to a final CN/Co ratio of 5, oxidation of the cobalt is still observed and no increase in the amount of active complex is seen.

Successive addition of cyanide

Another method used in an attempt to limit the CN/Co ratio during the preparation of Co(CN)NaY was to add the cyanide in small, individual portions. (CN/Co = 1 for each portion) After each portion was added and allowed to react and prior to the addition of the next increment, the solution was filtered off. This allowed the total CN/Co ratio not to exceed 1 while giving the cobalt access to a larger amount of cyanide. These reactions were done under argon.

Figure 4-13 shows the IR spectra for the C-N stretching region of samples prepared using this method. After the initial portion of cyanide is added ν_{CN} bands are

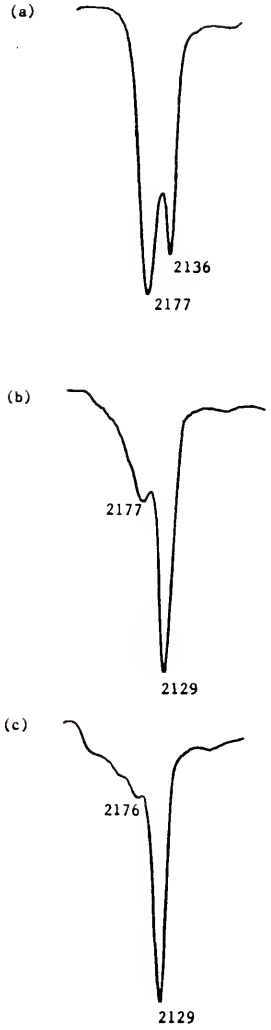

Figure 4-13. IR spectra for samples prepared by the succesive addition technique. (a) after one portion of cyanide, (b) after two portions, (c) after 5 portions.

seen at 2177 cm^{-1} and 2136 cm^{-1} and the sample was epr silent. These results are very similar to those shown in Figure 4-10. The ν_{CN} band at 2177 cm^{-1} is believed to be due to the formation of a complex on the outer portion of the zeolite that is analogous to prussian blue. This complex is reported[47] and can be prepared by the reaction of $Co(CN)_6^{3-}$ with Co^{2+}. The IR spectrum for $Co_3[Co(CN)_6]_2$ prepared in this way and the product of the reaction of CoNaY with $Co(CN)_6^{3-}$ both have a band at 2178 cm^{-1}.

This prussian blue analogue is easily removed with additional cyanide or by reaction with $EDTA^{4-}$ and is believed to be $Co_3[Co(CN)_6]_2$ on the surface. When Co^{2+} reacts, the $Co(CN)_6^{3-}$ goes into solution.

The band at 2129 cm^{-1} is believed to be $Co(CN)_6^{3-}$ formed inside the large cavities of the zeolite. This complex is not removed even after extensive treatments with chelates at elevated temperatures.

Variation of CN/Co ratio

The effect of the CN/Co ratio on the concentration of active complex is shown in Figure 4-14. In this graph the spin concentration, as measured by EPR, is plotted versus the CN/Co ratio used to prepare the sample. It can be seen that the concentration of the active complex steadily increases as the CN/Co ratio increases from 1-10 and then levels off or even decreases as the ratio becomes larger.

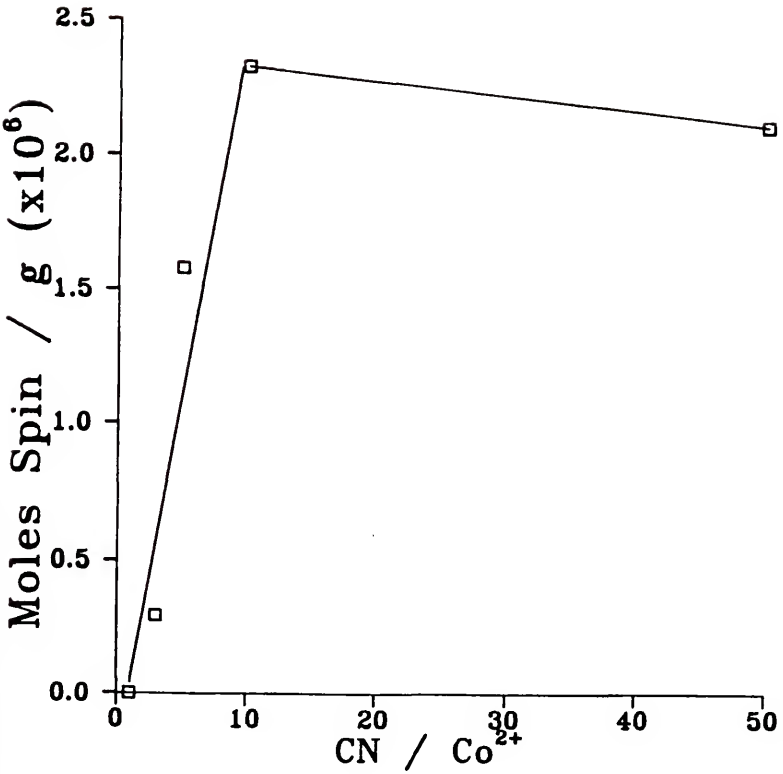

Figure 4-14. Plot of CN/Co ratio used during preparation of Co(CN)Na-Y versus the intensity of the epr signal for $Co(CN)_4(O_2)^{2-}$.

Synthesis with HCN

CoNa-Y was reacted with HCN in an attempt to prepare active cobalt cyanide complexes and inhibit the oxidation of cobalt. The resulting material showed C-N stretching vibrations at 2194 cm^{-1} and 2136 cm^{-1} when the sample was allowed to sit under HCN for 24 hours. After sitting for one week a broad ν_{CN} band at 2185 cm^{-1} with a shoulder at 2145 cm^{-1} was observed. Neither material showed any active cobalt when studied by EPR spectroscopy.

Conclusions About Co(CN)NaY

The major species formed in the reaction of CoY with sodium cyanide is the $Co(CN)_6^{3-}$ ion, which can be characterized by a ν_{CN} at 2129 cm^{-1}. At high cobalt loading a complex can be formed in every large cavity. Oxidation of cobalt occurs even under conditions which exclude oxygen and minimize water. At short reaction times and low CN:Co ratios, a surface species believed to be $Co_3[Co(CN)_6]_2$ also forms.

The oxidation of cobalt(II) to $Co(CN)_6^{3-}$ is driven by the presence of excess cyanide. This problem is magnified by the slow diffusion of cyanide throughout the framework. The mechanism for the oxidation is still unclear. Oxidation does not appear to require the presence of O_2 or large

amounts of water. Dimerization is not observed, most likely due to the size limitations of the cavity, but this does not rule out an intermolecular oxidation mechanism. Cobalt complexes may interact through the connecting channels of the large cavities without forming dimers. Surface species on the interior walls of the zeolite, such as hydroxyl groups, may also aid in the oxidation of cobalt. Whatever the mechanism, it is clear that the majority of the cobalt is readily oxidized under the conditions employed here.

The most interesting species formed in this reaction is a low-spin cobalt(II) complex capable of reversibly binding oxygen. The EPR parameters and equilibrium constant for oxygen binding suggest that this active complex is a square-planar $Co(CN)_4^{2-}$ ion which may be coordinated to the zeolite framework through a lattice oxygen. This species is stable to repeated cycling in air and, even in low concentration, increases the amount of oxygen absorbed by 100% over the amount of argon at 100 torr. The maximum concentration of this active complex is, however, limited. It may be formed in a structural defect site in the zeolite framework or at a very basic lattice oxide site that is only present in low concentration. Unless this site can be identified and increased, the concentration of $Co(CN)_4^{2-}$ inside zeolite Y is fixed at a low value.

$Co(CN)_5^{3-}$ Inside Zeolite Y

Preparation of CsCo(CN)-Y Materials

Due to the limited concentration of $Co(CN)_4^{2-}$ formed in Co(CN)Na-Y and the inability to increase this concentration, it was realized that to produce a material containing a high concentration of active cobalt, the formation of $Co(CN)_6^{3-}$ must be inhibited. This oxidation is driven by excess cyanide present during the synthesis and most likely occurs through intermolecular interaction of the cobalt centers or interaction with surface groups present on the interior walls of the zeolite. In order to inhibit this oxidation the cobalt cyanide complexes need to be shielded from each other and the zeolite walls. This shielding is especially important when excess cyanide is present and their mobility is increased by the presence of the solvent. It was discovered that cesium ion exchanged into the zeolite after cobalt produces this shielding effect. When CoNaY is exchanged with CsOH or CsCl prior to the addition of cyanide, the oxidation of some of the cobalt is inhibited and a new, active cobalt complex is formed inside the zeolite. This new complex reversibly binds oxygen and is present in higher concentration than the previously reported $Co(CN)_4^{2-}$ complex.

Characterization of CsCo(CN)-Y

CsOHCo(CN)-Y

IR characterization. CsOHCo(CN)-Y is prepared by first extensively washing CoNaY with CsOH to form CsOHCo-Y. Elemental analysis shows that very little of the cobalt is removed during this CsOH exchange. After drying, CsOHCo-Y is reacted with a methanolic sodium cyanide solution to form the cobalt cyanide complexes. The IR spectrum for the C-N stretching region of the resulting material is shown in Figure 4-15(a). Assignment of these bands is complicated by the unknown influence of cesium and hydroxide on the ν_{CN} values and the possibility of hydroxide acting as a ligand. Deoxygenation of this material results in no change in the IR spectrum, suggesting these bands are not due to the active complex, but rather from an oxidized species which is inactive. The presence of cesium has been shown[44-45] to shift the C-N stretching band to higher energy. The ν_{CN} for $Cs_2Li[Co(CN)_6]$ is reported at 2142 cm^{-1} and precipitation of a similar complex inside the zeolite may be to source of the band at 2138 cm^{-1}.

EPR characterization. The EPR spectrum of CsOHCo(CN)-Y exhibits a large, broad signal at g=2.0, typical of a cobalt-oxygen adduct. (See Figure 4-16.) A smaller signal at g=2.2 is also present and is attributed to

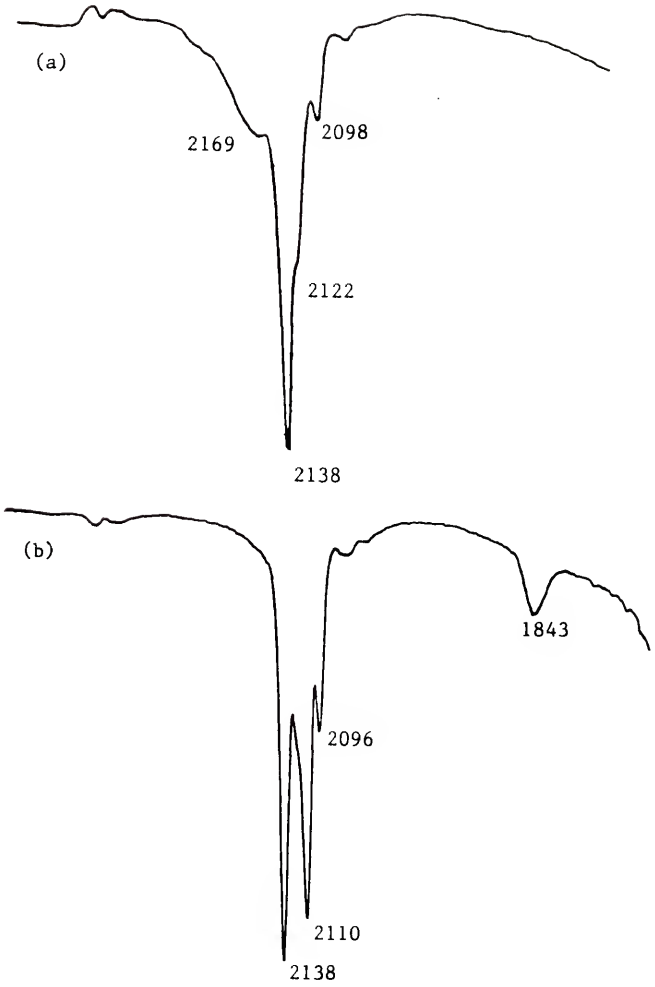

Figure 4-15. IR spectra for CsOHCo(CN)-Y. (a) prepared in air, (b) prepared under argon.

Figure 4-16. EPR spectrum for $Co(CN)_5(O_2)^{3-}$ inside CsOHCo(CN)-Y measured at 98 K.

a small amount of deoxygenated cobalt complex. The presence of this deoxygenated complex is surprising considering that the cyanide reaction was carried out in air and may suggest the interior pores are crowded or blocked due to the presence of Cs^+ or the formation of cobalt oxide.

The $Co\text{-}O_2$ adduct can be deoxygenated under vacuum at elevated temperatures, which removes the signal at g=2.0 and increases the signal at g=2.2. (See Figure 4-17.) The EPR spectrum for the deoxygenated complex is typical of a low-spin cobalt(II) complex and is almost identical to that seen for $Co(CN)_5^{3-}$ in acetonitrile. (See Figure 4-18.) Unlike solution behavior, where exposure to oxygen results in irreversible μ-peroxo dimer formation, $Co(CN)_5^{3-}$ prepared inside the zeolite can be reversibly oxygenated and deoxygenated. This is also in sharp contrast to solid $[NR_4]_3[Co(CN)_5(O_2)]$ where oxygen can only be liberated by pyrolysis, resulting in decomposition of the complex.[31] Therefore, it appears the presence of cesium has stabilized the formation of $Co(CN)_5^{3-}$ inside the zeolite by inhibiting its dimerization and further oxidation to $Co(CN)_6^{3-}$. Once formed, the pentacyano complex is capable of reversibly binding oxygen.

Gas adsorption characterization. Figure 4-19 shows the gas adsorption isotherms for O_2, Ar, and N_2 on CsOHCo(CN)-Y. As seen for Co(CN)Na-Y, this material shows an enhanced O_2 affinity due to the presence of the oxygen

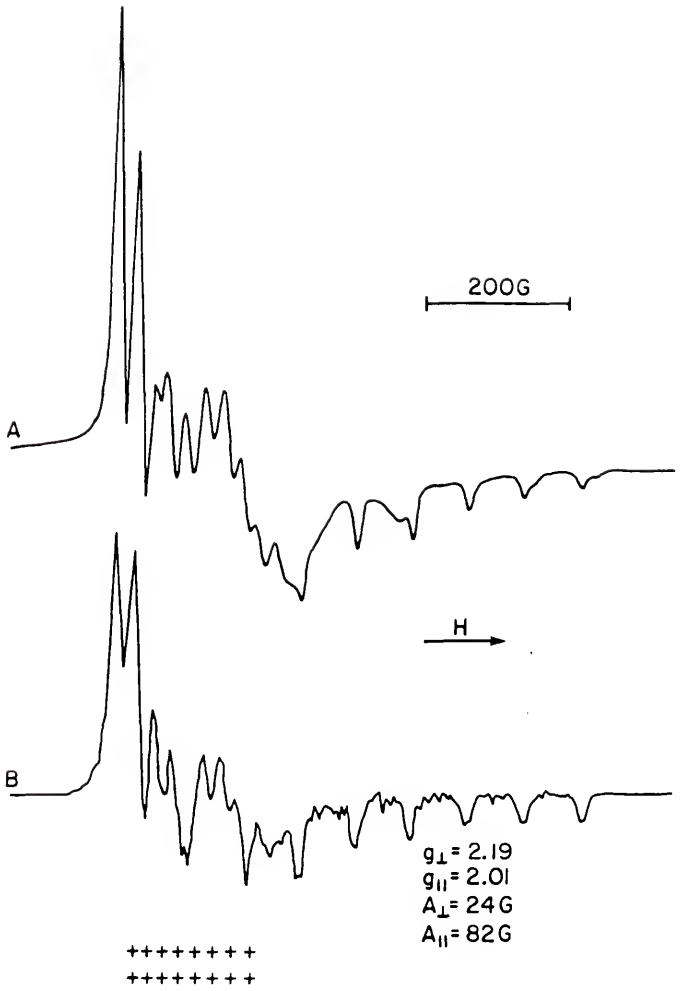

Figure 4-17. EPR spectrum for $Co(CN)_5^{3-}$ inside CsOHCo(CN)-Y measured at 98 K. (a) experimental, (b) simulated.

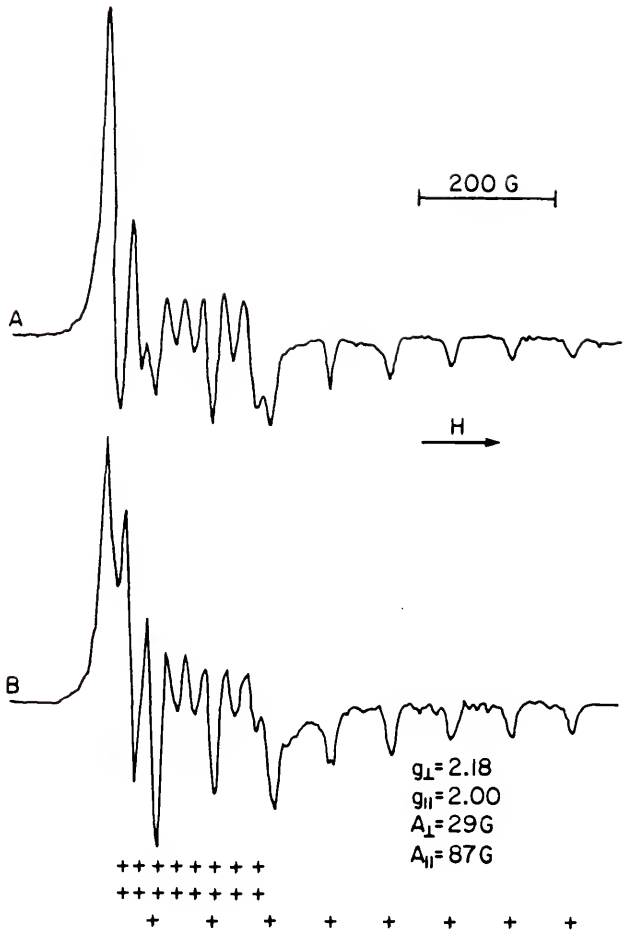

Figure 4-18. EPR spectrum for $Co(CN)_5^{3-}$ in 5:1 CN/Co mixture in acetonitrile.[32] (a) experimental, (b) simulated.

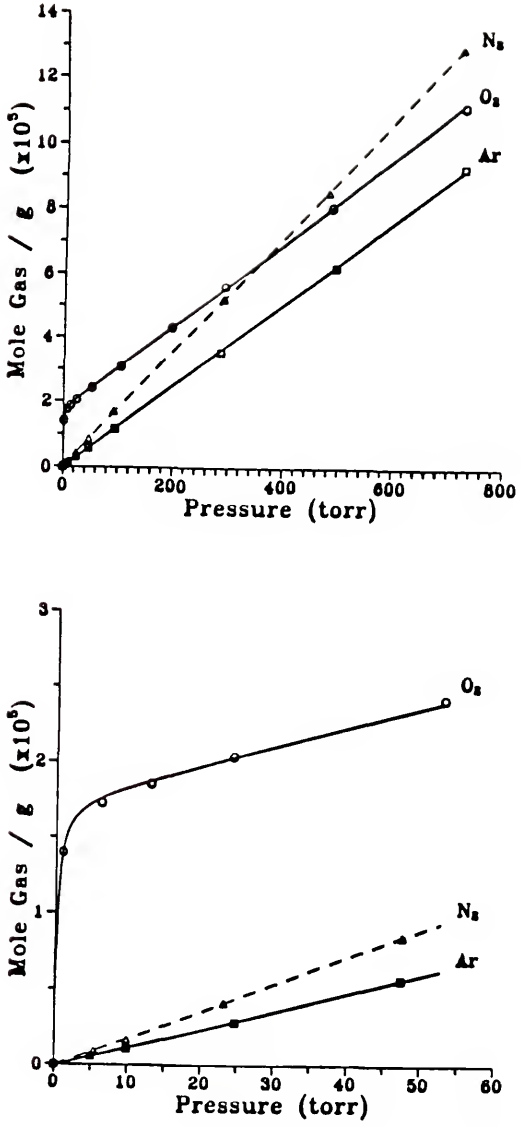

Figure 4-19. Gas adsorption isotherm for CsOHCo(CN)-Y measured at 298 K.

binding complex. From these isotherms, the concentration of $Co(CN)_5^{3-}$ can be calculated to be 18 umoles/g (1.1×10^{19} spins/g). This corresponds to 4% of the total cobalt present and is a greater than a 2 fold increase in the amount of active cobalt over that which is in Co(CN)Na-Y.

To ensure that CsCoY does not exhibit enhanced oxygen affinity, an adsorption isotherm for O_2 and Ar on CsOHCo-Y was measured. The results, shown in Figure 4-20, confirm there is no enhanced O_2 affinity due to the CsOH treatment alone. Only after CsOHCo-Y is reacted with cyanide is oxygen selectivity observed, assuring it is the presence of an active cobalt cyanide complex causing this selectivity.

Determination of K_{O2}. A plot of equation 4-4 for CsOHCo(CN)-Y is shown in Figure 4-21. From this plot the equilibrium binding constant for oxygen to the active complex, K_{O2}, is determined to be 4.2 ± 0.4 $torr^{-1}$. This confirms that the active complex in this material is different from that present in Co(CN)Na-Y, where K_{O2} was determined to be 0.12 ± 0.01 $torr^{-1}$. The much larger K_{O2} value is consistent with the assignment of this active complex as $Co(CN)_5^{3-}$ and results from the presence of cyanide ligand in the axial position. Cyanide is a much stronger axial base than a lattice oxygen, which is present in the $Co(CN)_4^{2-}$ complex, and results in a stronger overall ligand field. As discussed previously, a stronger ligand field around cobalt results in a more stable $Co-O_2$ bond.

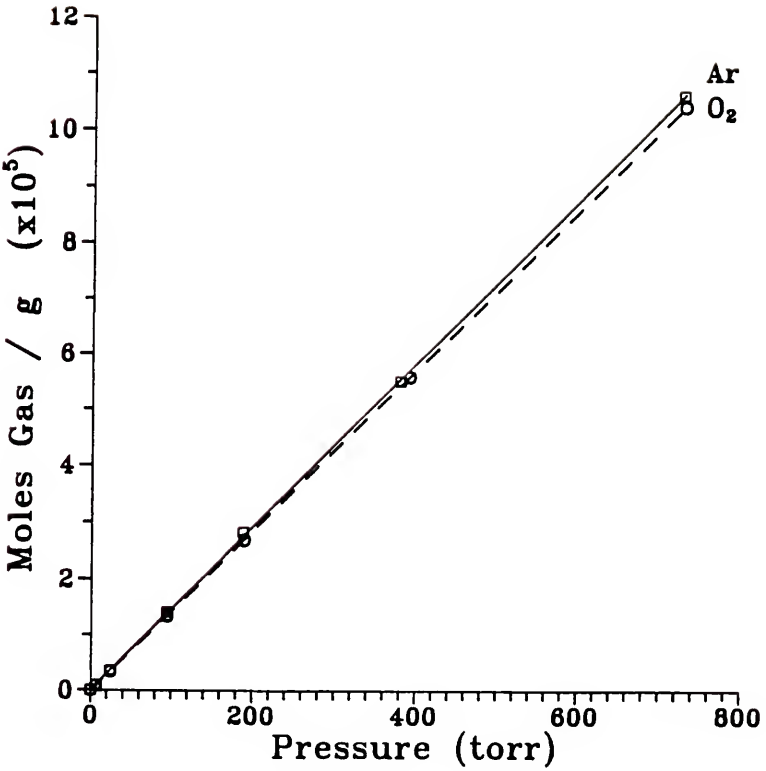

Figure 4-20. Gas adsorption isotherm for CsOHCo-Y measure at 298 K.

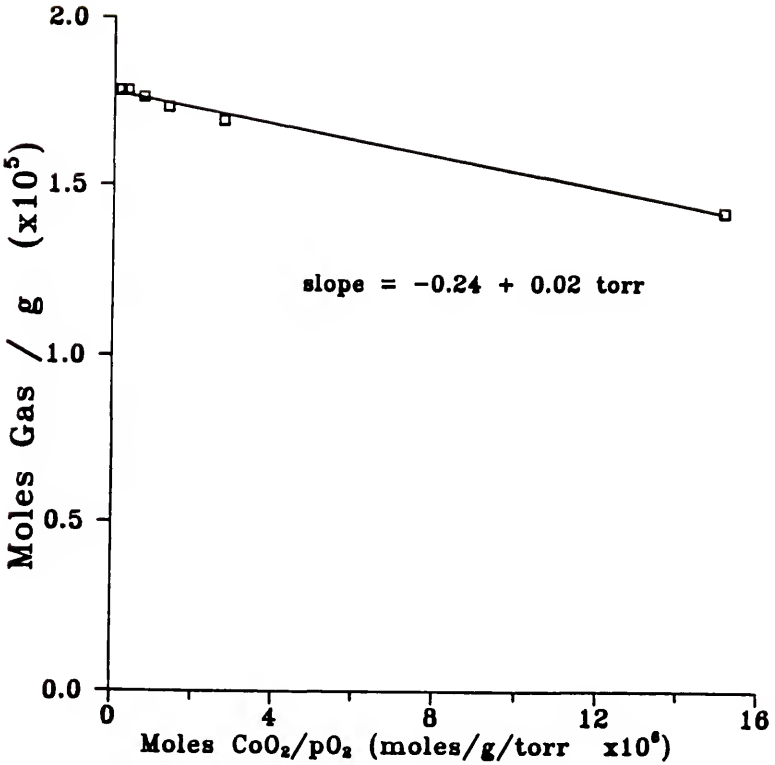

Figure 4-21. Plot of equation 4-4 for CsOHCo(CN)-Y.

Preparation under argon. The preparation of CsOHCo(CN)-Y was repeated under Ar in an attempt to increase the concentration of $Co(CN)_5^{3-}$. The IR spectrum of the resulting material is shown in Figure 5-15(b). The C-N stretching bands seen in the previous sample are all present as well as new bands at 2110 and 1843 cm^{-1}. These new bands match those reported for $Cs_2Na[Co(CN)_5H]$[46] formed from the reaction of an aqueous solution of $Co(CN)_5^{3-}$ with hydrogen and CsCl. No other combination of cations (including Li^+, K^+, Rb^+, NH_4^+, NMe_4^+, NEt_4^+, NBu_4^+, NMe_3Cetyl^+, $MeNH_3^+$, $Me_2NH_2^+$, and NH_3OH^+) resulted in the formation of this salt.[56]

The presence of $Co(CN)_5H^{3-}$ formed in the absence of hydrogen suggests that water plays a role in the oxidation of cobalt. The slow decomposition of $Co(CN)_5^{3-}$ in water has been shown[36-37] to occur through the disproportionation with water. (See equation 4-10)

$$2Co(CN)_5^{3-} + H\text{-}OH \longrightarrow Co(CN)_5H^{3-} + Co(CN)_5^{3-} \quad 4\text{-}10$$

The hydride has been detected by NMR of an aqueous solution of cobalt cyanide.[57] This is the most likely source of $Cs_2Na[Co(CN)_5H]$ seen when the cyanide reaction is done under argon. In air the hydride species would not be expected because it quickly reacts with O_2 to form $Co(CN)_5OOH^{3-}$,[58-59]

which decomposes to the hydroxide. In the presence of free cyanide, the next step in this process is the irreversible formation of the very stable hexacyano species,[37] as shown in equation 4-11.

$$Co(CN)_5OH^{3-} + CN^- \text{ ----> } Co(CN)_6^{3-} + OH^- \qquad 4\text{-}11$$

The rate of these reactions are accelerated as much as 60 times by the presence of alkali metal cations and cesium has been shown[37,60-61] to have the greatest effect. The cause of this increase is unknown but its magnitude does not logically follow the degree of hydration or the electronegativity of the metal ion.[61]

These results suggest that oxidation of cobalt occurs through an intermolecular mechanism involving two cobalt centers. This reaction is accelerated by the large concentration of cations present in the zeolite. Cesium must therefore act to shield the cobalt complexes from each other and slow the oxidation process. In doing so it stabilizes the formation of $Co(CN)_5^{3-}$. Once the reaction is completed and the methanol/CN solution is removed, the mobility of the complex is decreased and it is further stabilized.

The nature of the intermolecular interaction between cobalt centers is still in question. The formation of two $Co(CN)_5^{3-}$ complexes in one large cavity seems unlikely since

this would require a large molecule with a total charge of -6 to be accommodated. The presence of charge balancing cations, beyond those needed to balance the framework charge, would also be needed and further crowd the cavity. The size of the dimer molecules alone would push the limits of the zeolite cage and this crowding would be worsened by the extra cations needed to balance the -6 charge. (See Figure 4-22.) The absence of any experimental evidence for dimer formation in the presence or absence of O_2 also suggests this does not occur. A more reasonable explanation is the interaction of two cobalt centers in separate large cavities through the interconnecting channels. This would allow the oxidation to readily occur in materials where the mobility of $Co(CN)_5^{3-}$ is unrestricted, as is the case in CoNaY. The presence of cesium sterically inhibits a portion of the cobalt centers from interacting and stabilizes $Co(CN)_5^{3-}$.

CsClCo(CN)-Y

IR characterization. CsClCo(CN)-Y is prepared the same way as CsOHCo(CN)-Y except CsCl is used in place of CsOH. Elemental analysis show that 40-50% of the cobalt is removed during the CsCl exchange, which is much more than with CsOH. This suggest that the formation of cobalt hydroxide keeps the cobalt from being washed out in the CsOHCo(CN)-Y preparation.

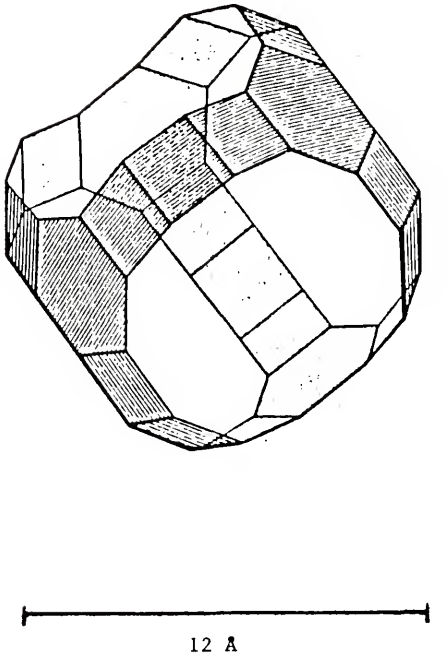

Figure 4-22. Comparison of the size of the large cavity in zeolite Y to the size of the μ-peroxo dimer.

The C-N stretching region in IR spectrum of the CsCl material shows a single, sharp band at 2120 cm^{-1} which shifts to 2127 cm^{-1} upon exposure to moisture. This band appears unaffected by deoxygenation and its intensity is not dependent on the concentration of active cobalt, suggesting it is not due to the active complex. Wilmarth[49] has reported the formation of $Ag_2[Co(CN)_5]$ and its ability to reversibly bind water but its IR spectrum has not been reported.

EPR characterization. The EPR spectrum for CsClCo(CN)-Y, shown in Figure 4-23, is typical of a $Co-O_2$ adduct and very similar to that seen for CsOHCo(CN)-Y. Figure 4-24 shows the EPR spectrum resulting from evacuation of this material for 15 minutes at room temperature. This spectrum shows the presence of both $Co(CN)_5^{3-}$ and $Co(CN)_5(O_2)^{3-}$. Complete deoxygenation of this material results after evacuation for 10 min at 100 °C, yielding a spectrum typical of a low-spin cobalt(II) which is very similar to that seen for deoxygenated CsOHCo(CN)-Y. (See Figure 4-25.)

Low-spin cobalt(II) complexes have a single unpaired electron in the d_z2 orbital which is primarily used in σ-bonding with the axial ligand. Overlap and mixing of these two orbitals places spin density from the unpaired electron directly in the ligand sigma system.[62] If the axial cyanide in $Co(CN)_5^{3-}$ contains a ^{13}C, this spin density

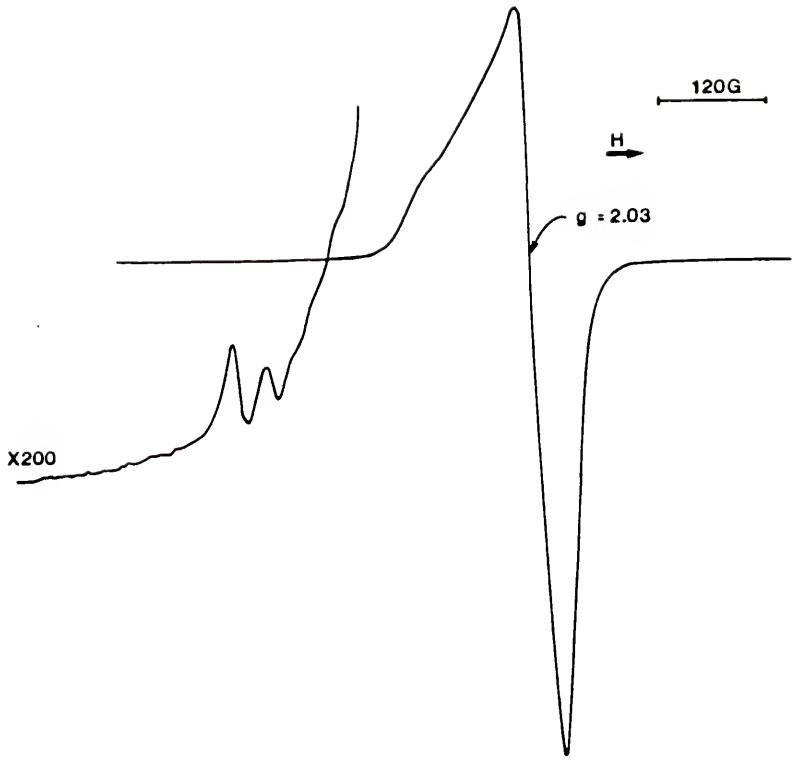

Figure 4-23. EPR spectrum for $Co(CN)_5(O_2)^{3-}$ inside CsClCo(CN)-Y measured at 98 K.

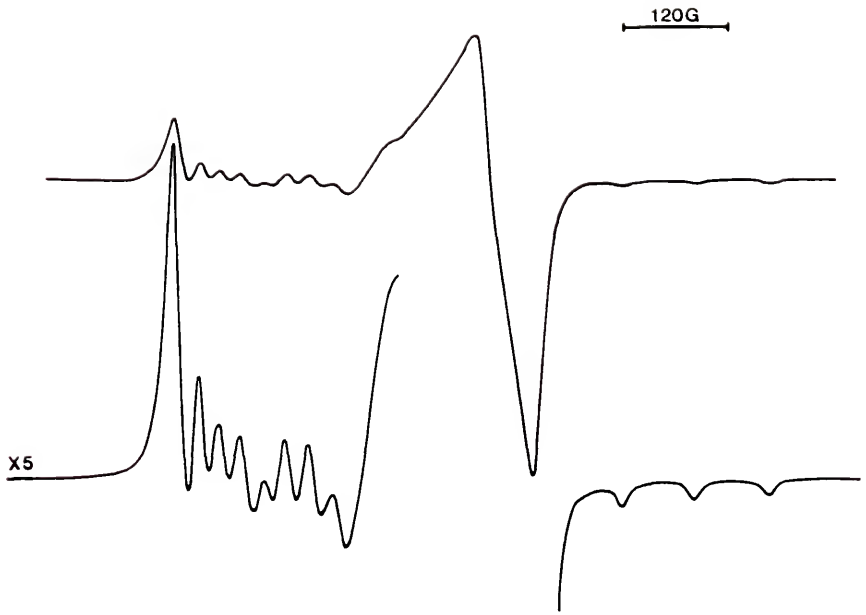

Figure 4-24. EPR spectrum of CsClCo(CN)-Y measured at 98K after evacuation for 15 minutes at 298K.

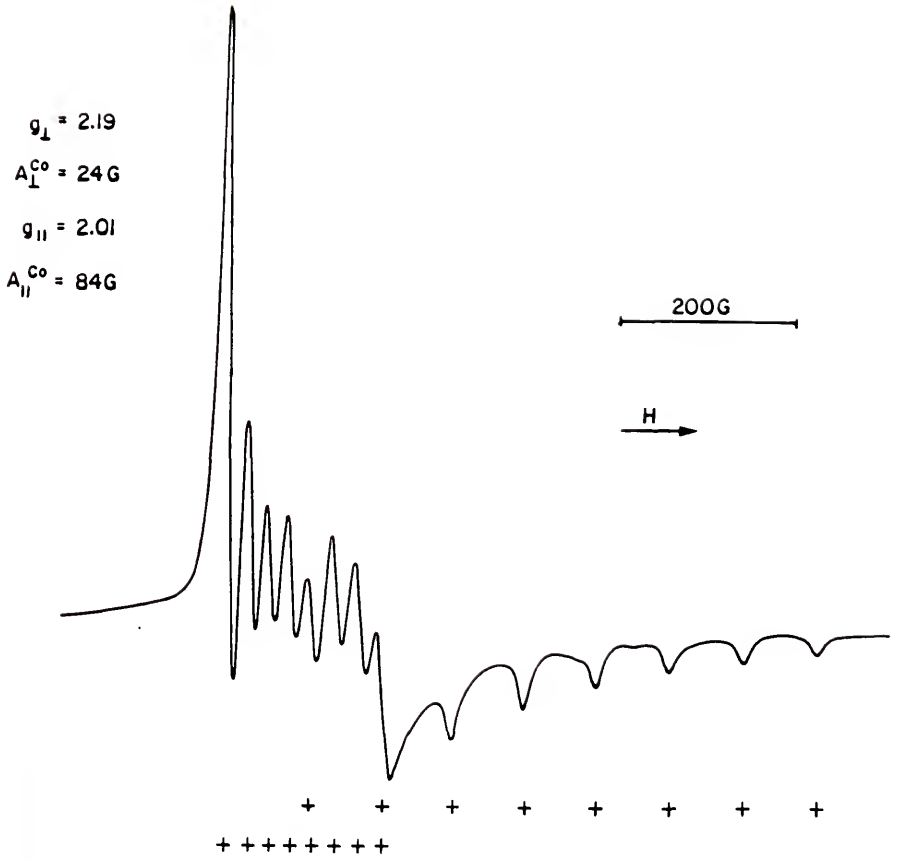

Figure 4-25. EPR spectrum for $Co(CN)_5^{3-}$ inside CsClCo(CN)-Y measured at 98 K.

results in ligand nuclear hyperfine coupling.[63] The synthesis of CsClCo(CN)-Y was repeated with $Na^{13}CN$ and an entrapped $Co(^{13}CN)_6^{3-}$ was prepared. The EPR spectrum for this complex, shown in Figure 4-26, shows that each EPR component is split into two lines by coupling with the axial $^{13}CN^-$. Of the five cyanides, only the axial splitting is resolved. The unresolved equatorial cyanide splitting increases the linewidth.[63]

Carbon-13 hyperfine coupling constants, listed in Table 4-7, provide good experimental estimates for the carbon 3s and 3p spin densities on the axial cyanide. The isotropic ^{13}C coupling constant yields the 3s spin density of 0.033 and the anisotropic coupling yields the 3p spin density of 0.049. The ratio of 3p to 3s spin densities allows the percent s character in the donor orbital to be calculated. For the complex prepared here, the axial σ donor orbital is 40% s character, which corresponds to $sp^{1.5}$ hybridization on the carbon. This is a reasonable value for cyanide.

Color changes. Accompanying the oxygenation and deoxygenation of this material is a drastic color change. The deoxygenated sample is light blue in color, most likely resulting from the presence of free Co^{2+} ions. Upon exposure to oxygen, the color quickly changes to yellow/green. This color change is reversible and is further evidence of the formation of a $Co\text{-}O_2$ adduct.

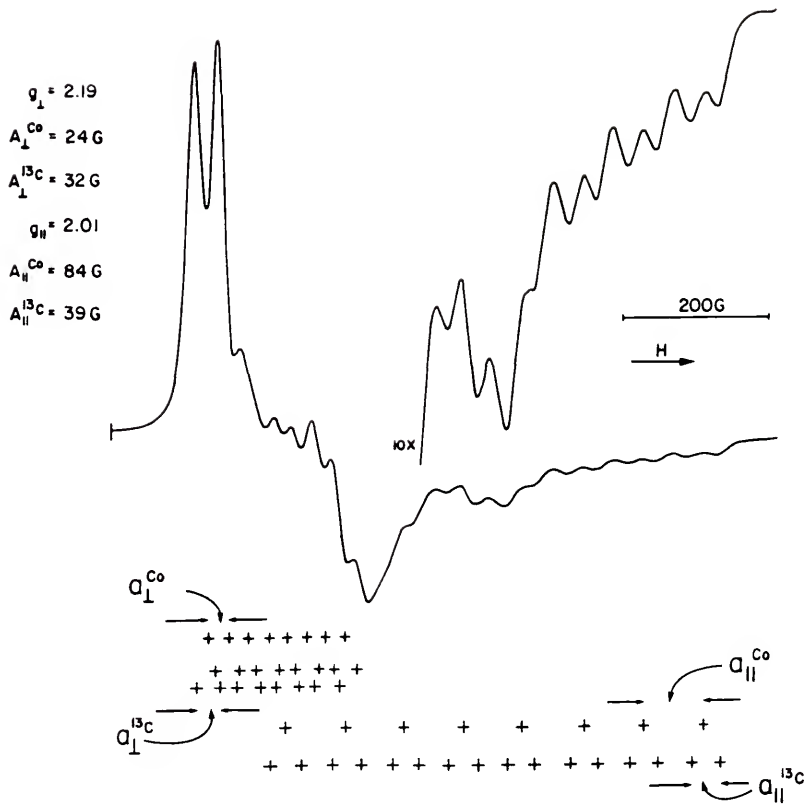

Figure 4-26. EPR spectrum for $Co(^{13}CN)_5^{3-}$ inside CsClCo(CN)-Y measured at 98 K.

Table 4-7 EPR Parameters for $Co(^{13}CN)_6^{3-}$

	$g_{\parallel}$	$g_{\perp}$	^{59}Co $A_{\parallel}$ $x10^4$ cm^{-1}	^{59}Co $A_{\perp}$ $x10^4$ cm^{-1}	^{13}C $A_{\parallel}$ $x10^4$ cm^{-1}	^{13}C $A_{\perp}$ $x10^4$ cm^{-1}
$Co(CN)_5^{3-}$ in CsY[a]	2.01	2.19	79	24		
$Co(^{13}CN)_5^{3-}$ in CsY	2.01	2.19	79	24	37	32
$K_3Co(CN)_5$, powder[b]	2.004	2.175	82	24		
$K_3Co(^{13}CN)_5$, single crystal[b]					38	31
$Co(^{13}CN)_5^{3-}$ in MeOH[c]					39	

[a] from simulation of experimental spectrum [b] Reference 63
[c] Reference 64

Gas adsorption characterization. Figure 4-27 shows the adsorption isotherms for O_2, Ar, and N_2 on CsClCo(CN)-Y. From these isotherms the concentration of active cobalt can be calculated to be 54 umole/g (3.3×10^{19} spins/g), which corresponds to 18% of the total cobalt present and is a 3 fold increase in the amount of active cobalt over that in CsOHCo(CN)-Y. This high concentration of active complex produces a material with a large affinity for oxygen and should result in a high selectivity for O_2 over N_2 in a gas mixture. The separation factor, α, is a measure of this selectivity and is defined in equation 4-12. X_i and Y_i are the equilibrium

$$\alpha_{i/j} = \frac{X_i/Y_i}{X_j/Y_j} \qquad 4\text{-}12$$

mole fraction of component i in the adsorbed and gas phase, respectively. As a first approximation, the pure-gas isotherms can be considered additive which yields the adsorption isotherm from a mixture[1] and allows the separation factor to be calculated. Table 4-8 lists values of $\alpha_{O2/N2}$ for CsClCo(CN)-Y determined from the isotherms shown in Figure 4-27. The details for calculation of this data are given in Appendix A. The first point in the table shows that if a mixture of O_2 and N_2, each at a partial

Table 4-8 Separation Factors for CsClCo(CN)-Y

P_i[a]	P_{fO2}[b]	P_{fN2}[c]	$\alpha_{O2/N2}$
10.2	0.6	9.7	5022
13.4	1.3	12.8	1907
22.6	8.8	21.3	99
38.9	23.9	36.5	24
65.9	45.0	61.5	10
117	96.6	109	5.1
235	206	218	2.6
435	393	304	1.7
797	730	740	1.3

[a] P_i is the initial partial pressure of both O_2 and N_2 in torr.

[b] P_{fO2} is the final partial pressure of O_2 in torr.

[c] P_{fN2} is the final partial pressure of N_2 in torr.

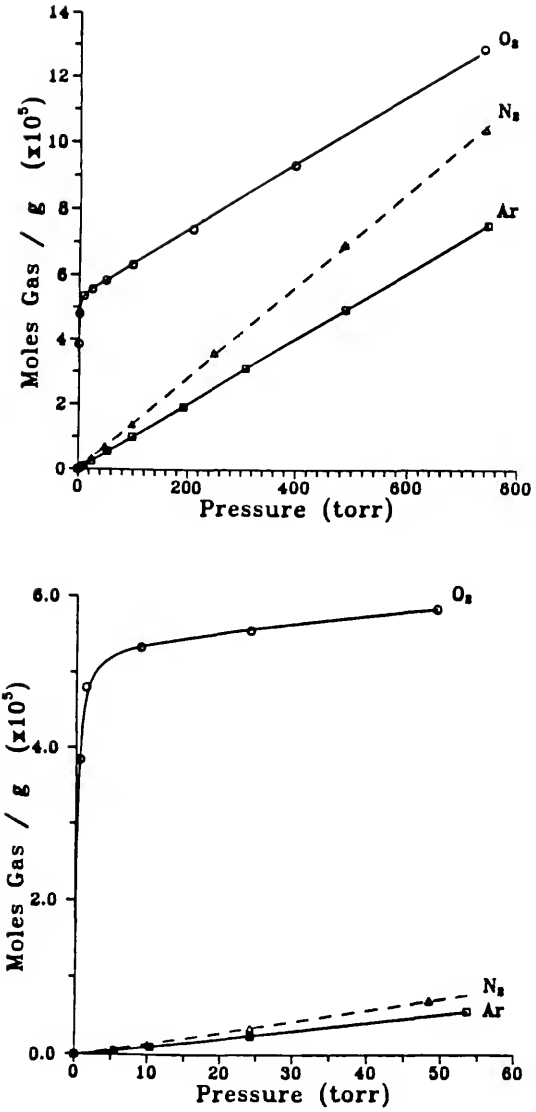

Figure 4-27. Gas adsorption isotherm for CsClCo(CN)-Y measured at 298 K.

pressure of 10 torr, is exposed to 3.1 grams of CsClCo(CN)-Y in a 245 ml apparatus, the final partial pressure of O_2 and N_2 would be 0.57 and 9.7 torr, respectively. This results in an $\alpha_{O2/N2}$ of 5022. It can also be seen from Table 4-8 that as the partial pressure of each gas increases, the separation factor decreases. This occurs because the active complex is quickly saturated, due to its large K_{O2}, and oxygen adsorption is no longer dominated by $Co-O_2$ adduct formation.

Determination of K_{O2} and thermodynamics for oxygen binding. Figure 4-28 shows a plot of equation 4-4 for CsClCo(CN)-Y. The K_{O2} determined from this plot is 4.4 ± 0.4 $torr^{-1}$, the same as that observed for CsOHCo(CN)-Y. This confirms that the active complex in CsClCo(CN)-Y is the same as that in CsOHCo(CN)-Y, as suggested by EPR results.

The value of ΔG for the reaction of O_2 with $Co(CN)_5^{3-}$ can be obtained from K_{O2} by using the relationship below.

$$\Delta G = -RT\ln K_{O2} \qquad 4\text{-}13$$

The value of ΔH is obtained by evaluating the temperature dependence of the equilibrium constant. A plot of $\ln K_{O2}$ against 1/T (termed a van't Hoft plot) gives a straight line with a slope equal to $-\Delta H/R$. Figure 4-29 shows such a plot for CsClCo(CN)-Y and the enthalpy of O_2 binding can be

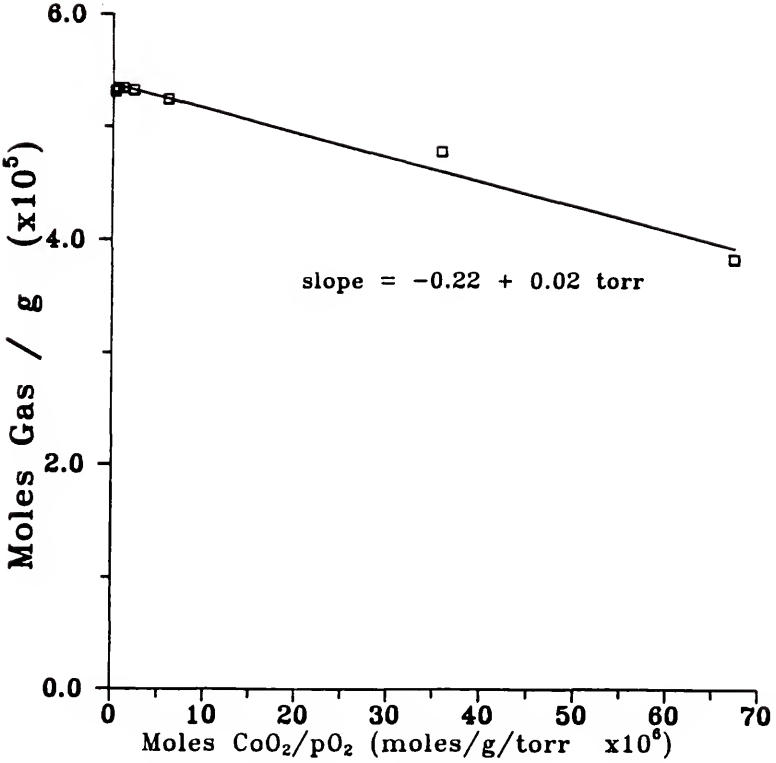

Figure 4-28. Plot of equation 4-4 for CsClCo(CN)-Y.

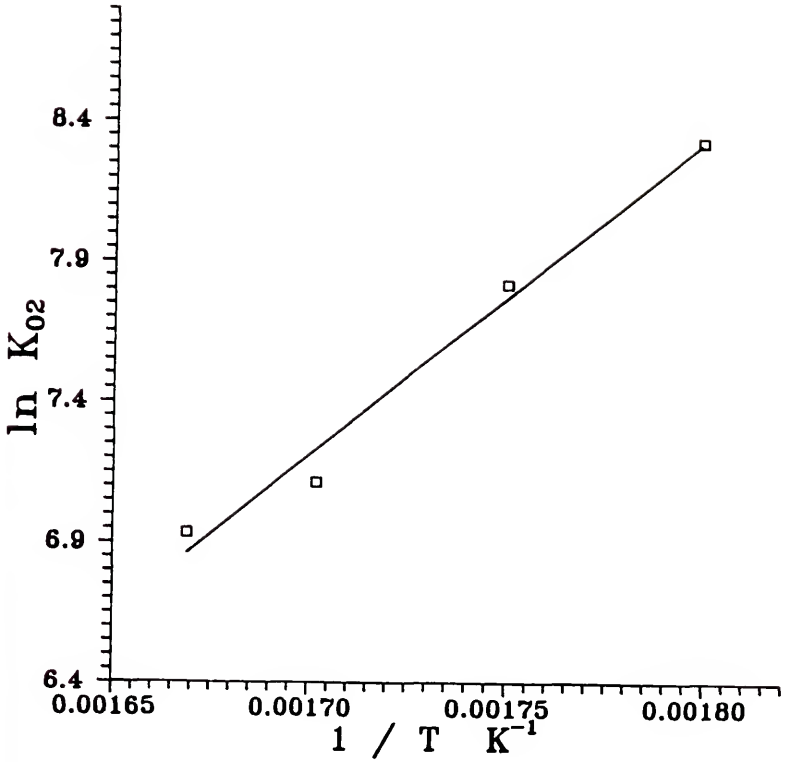

Figure 4-29. Van't Hoff plot for CsClCo(CN)-Y.

calculated to be -23 ± 2 kcal/mol. Once ΔH and ΔG have been determined, ΔS can be calculated from the relationship in equation 4-14.

$$\Delta G = \Delta H - T\Delta S \qquad 4\text{-}14$$

Such a calculation for the data presented here gives the entropy of O_2 binding to be -67 + 5 eu.

The reaction of a complex with O_2 generally involves a large negative entropy change resulting primarily from loss of rotational, vibrational, and translational freedom of the O_2 molecule.[24] This negative entropy change must be offset by a favorable enthalpy change if the free energy of the reaction is to be negative. Enthalpy values vary widely among reported O_2 carriers, as seen in Table 4-9, mainly due to the differences in donor strengths of the attached ligands. Favorable enthalpy is assisted by increasing the strength of the metal-ligand bonds and the large increase in exothermicity seen for $Co(CN)_5^{3-}$ results from the large donor strength of the cyanide ligand. The increased ligand field produced by five cyanides raises the d_{z^2} orbital in energy, resulting in more energy released when the electron in that orbital goes into the $Co\text{-}O_2$ bonding orbital.[51]

The zeolite cage clearly inhibits dimerization of $Co(CN)_5^{3-}$ but the effects of having this complex inside the zeolite on the energetics of O_2 binding is not easily

Table 4-9 Thermodynamic values for binding oxygen to various cobalt complexes.

complex	$-\Delta H$ kcal/mol	$-\Delta S$ eu.
$Co(CN)_5^{3-}$ in CsY	23	67
$CoSALEN \cdot py^{2+}$ in NaY[a]	11.4	51
$CoSALEN^{2+}$ in pyridine[b]	12.4	37
CoACACEN·py in toluene[c]	17.7	72.7
$Co(TPivPP) \cdot Me_2Im^{2+}$ in toluene[d]	11.8	40
Co(p-MeOTPP)·py in toluene[e]	9.3	55
Summary[f]		
in aqueous	9.6-11.3	≈58
in non-aqueous	5-18.5	29-81

[a] Reference 19 [b] Reference 65 [c] Reference 66-67
[d] Reference 68 [e] Reference 69 [f] Reference 24

SALEN = 1,6-bis(2-hydroxyphenyl)-2,5-diaza-1,5-hexadiene
ACACEN = 2,4,8,10 dodecatetraene
TPivPP = meso-α,ß,γ,δ-tetrakis(o-pevalamidophenyl)-porphyrin
p-MeOTPP = p-methoxy meso-tetraphenylporphyrin

deduced. The lack of a solution analogue makes comparison impossible. Solid $[NR_4][Co(CN)_5]$ or $[NR_4][Co(CN)_5(O_2)]$ do not allow a valid comparison since other important factors, such as crystal lattice effects or poor O_2 diffusion in the solids, are not the same.

Synthesis variation. The order of cesium addition is important in stabilizing the pentacyano complex. When NaY is exchanged first with CsCl and then $CoCl_2$, very little $Co(CN)_5^{3-}$ is formed. Figure 4-30 shows the gas adsorption isotherm for O_2 and Ar on Co(CN)CsCl-Y prepared this way. The concentration of active cobalt is much lower than in CsClCo(CN)-Y, only 3.3 umol/g (2×10^{18} spins/g). The EPR spectrum for this material shows the presence of both $Co(CN)_4^{2-}$ and $Co(CN)_5^{3-}$, with the pentacyano complex being present in the highest concentration. This shows that $Co(CN)_4^{2-}$ is also formed in CsCo(CN)-Y but still low concentration.

Preparation of CsClCo(CN)-Y under Ar does not increase the concentration of $Co(CN)_5^{3-}$. Figure 4-31 shows the adsorption isotherm for this material. It can be seen that the amount of active cobalt is actually less than when prepared in air. This suggests that oxygen does not hamper the formation of $Co(CN)_5^{3-}$ but may even aid in its formation. This most likely occurs because oxygen can occupy the sixth coordination site and prevents reaction of the electron in the d_z2 orbital with water. Figure 4-32

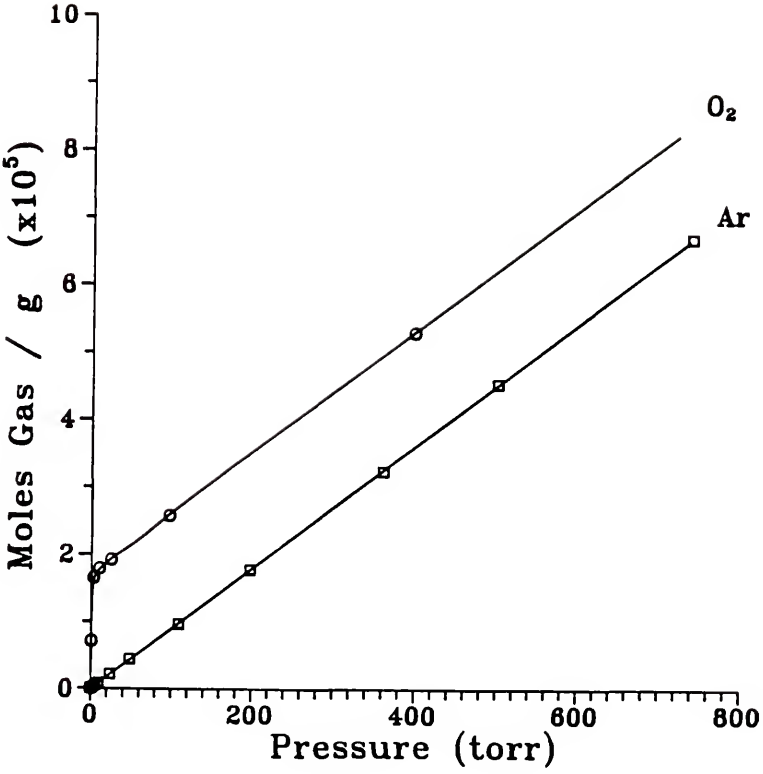

Figure 4-30. Gas adsorption isotherm for Co(CN)CsCl-Y measured at 298 K.

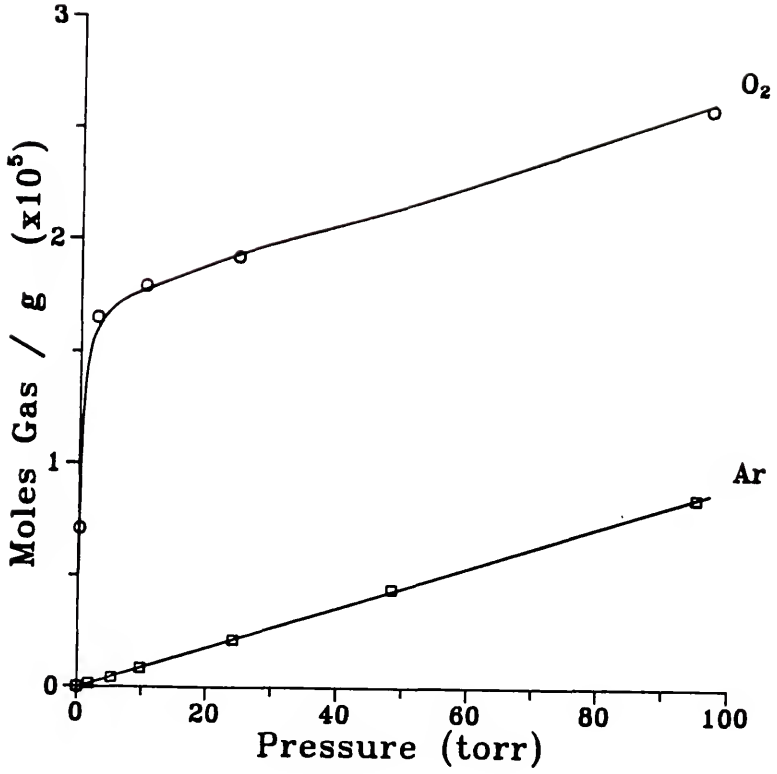

Figure 4-31. Gas adsorption isotherm for CsClCo(CN)-Y prepared under argon measured at 298 K.

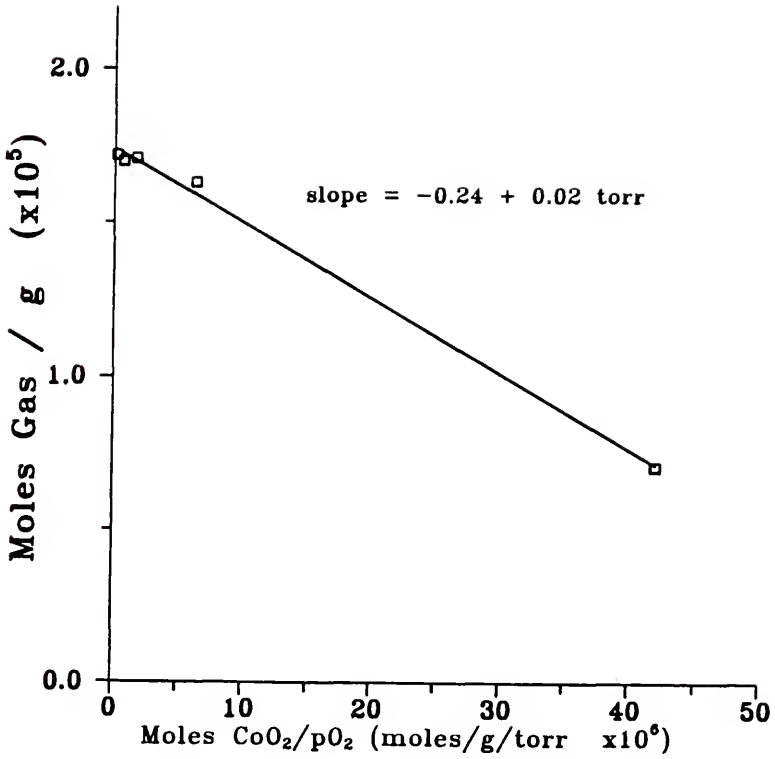

Figure 4-32. Plot of equation 4-4 for CsClCo(CN)-Y prepared under argon.

shows a plot of equation 4-4 for this material and again shows a K_{O2} of 4.2 ± 0.6 $torr^{-1}$ is seen.

Stability of CsCo(CN)-Y

Both CsOHCo(CN)-Y and CsClCo(CN)-Y are stable above 150 °C under vacuum, however, they begin to lose their O_2 affinity when kept at elevated temperatures under oxygen. CsOHCo(CN)-Y was shown to slowly adsorb O_2 irreversibility at 120 °C. After prolonged exposure to 1 atmosphere of O_2 at 120 °C the samples oxygen affinity decreased and its selectivity for O_2 over Ar eliminated. This problem most likely arises from the increased mobility of the $Co(CN)_5^{3-}$ complexes at elevated temperatures.

Conclusions About CsCo(CN)-Y

The presence of cesium in CoY prior to the addition of cyanide stabilizes $Co(CN)_5^{3-}$ inside zeolite Y by inhibiting the oxidation of cobalt(II) to $Co(CN)_6^{3-}$. It was shown in the study of Co(CN)Na-Y that this oxidation is driven by a high CN/Co ratio and most likely occurs through an intermolecular reaction of two $Co(CN)_5^{3-}$ complexes with water. Due to its large size, cesium appears to shield $Co(CN)_5^{3-}$ complexes from each other and inhibits their oxidation. Once formed, $Co(CN)_5^{3-}$ reversibly binds O_2 and thermodynamics show the addition of O_2 to be very

exothermic, $\Delta H = -23 \pm 2$ kcal/mol. The large affinity this complex has for O_2 results in a material which is highly selective for adsorbing O_2. A separation factor above 5000 has been calculated for O_2 adsorption from a mixture of O_2 and N_2.

CHAPTER 5
SUMMARY AND CONCLUSION

Summary

This research has focused on the preparation and characterization of cobalt cyanide complexes inside zeolite Y. It represents the first case in which an anionic complex has been synthesized inside a negatively charged zeolite cavity and opens the possibility of preparing a whole new class of zeolite entrapped compounds. The goal of this work has been to prepare a material which has a high affinity for oxygen by synthesizing a complex inside zeolite Y which reversibly binds oxygen. Such a material will exhibit a high selectivity for O_2 over N_2 adsorption and may find applications in a PSA process.

The reaction of CoNaY with NaCN in methanol results in the formation of entrapped cobalt cyanide complexes. The major species formed in this reaction is $Co(CN)_6^{3-}$, representing about 75% of the total cobalt present. The oxidation of cobalt to $Co(CN)_6^{3-}$ is driven by excess cyanide and appears to occur through the intermolecular interaction of two cobalt centers. Also formed in this reaction is a low-spin cobalt cyanide complex which reversibly binds

oxygen. This complex and its oxygen adduct have been characterized by EPR spectroscopy and shown to be $Co(CN)_4^{2-}$. This square planar complex is anchored to the zeolite wall through an axially bound lattice oxide resulting in a complex which is very stable to repeated O_2 cycling. Spin concentration and quantitative gas uptake measurements have shown this active complex to be present in low concentration, less than 1% of the total cobalt. The presence of this active complex has been shown to have a significant influence on the gas uptake characteristics of the host zeolite, resulting in an increased affinity for oxygen. The observed oxygen binding constant for this complex was determined to be 0.12 ± 0.01 $torr^{-1}$.

By treating the CoNaY with Cs^+ before the addition of cyanide, the formation of $Co(CN)_6^{3-}$ is inhibited resulting in the formation of $Co(CN)_5^{3-}$ inside zeolite Y. This species can be prepared in much larger concentration than $Co(CN)_4^{2-}$, as high as 54 μmoles of active cobalt per gram of material. The EPR spectrum for this material is almost identical to that of $Co(CN)_5^{3-}$ in acetonitrile. However, unlike solution, preparation of this complex inside a zeolite cavity stabilizes it towards dimerization and allows it to reversibly bind oxygen. The oxygen binding constant for $Co(CN)_5^{3-}$ has been determined to be 4.4 ± 0.5 $torr^{-1}$ and is much larger than that of $Co(CN)_4^{2-}$, due to the presence of the much stronger axial cyanide ligand. The high

concentration of this complex results in a very large oxygen affinity for this material. From the O_2 and N_2 adsorption isotherms, a separation factor as high as 5000 can be calculated, suggesting that this material will exhibit a high selectivity for oxygen over nitrogen.

Conclusions

Zeolite entrapped transition metal complexes that reversibly bind oxygen can have a significant influence on the gas uptake characteristics of zeolite materials. By giving the host lattice a large affinity for oxygen, materials that exhibit high selectivity for O_2 over N_2 can be prepared. These materials have the potential for use in PSA processes for O_2 separation from air and for removal of trace amounts of O_2 from gas streams. Only time will tell if this potential can be utilized.

APPENDIX A
PROCEDURES AND CALCULATIONS

Adsorption Isotherms

Using a single container of known volume, an accurate means to measure pressure, and simple manipulations of the gas laws, solid-gas adsorption isotherms can be determined. Two different experimental procedures were used along with Figure 3-1 to measure the gas adsorption isotherms for the zeolite materials studied in this work. These two procedures both produce data which allow the number of moles of gas adsorbed by a material to be calculated. The first is a reversible addition (RA) technique and the second a successive addition (SA) technique. Both require the measurement of pressure differences as a known weight of sample is exposed to a known amount of gas in a container of known volume.

Reversible addition technique

In this procedure the sample is completely degassed after each adsorption point is measured. This requires the

adsorption to be completely reversible and hence, the name reversible addition technique. This procedure was used in measuring the isotherms for Co(CN)Na-Y(1) and Co(CN)Na-Y(2). As shown in Figure 3-1, a capacitance manometer is used to measure the pressure of gas in the apparatus. The known volume container was calibrated by measuring the weight of water required to fill it completely. The temperature was measure using an externally placed thermometer. The exact steps used in this procedure are outlined below.

1) Completely evacuate the entire apparatus and fill the gas container with the desired gas. Close the gas container valve.

2) Evacuate the sample for the desired length of time at the desired temperature. Record P_0 and close the sample valve.

3) Evacuate the known volume and fill it to the desired pressure. Record P_1 and close the known volume valve.

4) With all the valves closed except the one to the manometer, evacuate the apparatus.

5) Close the valve to the vacuum pump and open the valve to the known volume. Wait for equilibrium and record P_2.

6) Open the valve to the sample container and wait for the pressure to equilibrate. Record P_3.

7) Close the valve to the known volume and evacuate the apparatus, including the sample.

8) Close the valve to the sample. The previous P_3 becomes P_1 and the steps are repeated starting with step 5.

This procedure results in a series of pressure readings which can be entered into the VAC4 program listed in Appendix B, and the amount of gas adsorbed by the sample at a pressure of P_3 above the sample is determined.

By carrying out the above procedure with helium, the dead volume of the sample tube can be calculated. The VAC4 program has a routine for doing this calculation. One of the spreadsheets listed in Appendix b can also be used for this calculation. This dead volume of the sample tube can also be determined by using an empty sample tube and any desired gas. When this procedure is used the volume calculated, V_s', must be corrected for the volume the sample itself takes up. This can be done using the density of the sample and its weight and equation 1.

$$V_s = V_s' - \frac{wt_s}{d_s} \qquad (1)$$

Successive addition technique

In this procedure the sample is completely degassed prior to the experiment. It is then subjected to incremental amounts of gas starting at low pressures and as the sample is successively exposed to higher pressures of gas, the amount of gas adsorbed at each increment is calculated. The exact steps used in this procedure are outlined below.

1) Completely evacuate the entire apparatus and fill the gas container with the desired gas. Close the gas container valve.

2) Evacuate the sample for the desired length of time at the desired temperature. Record P_1 and close the sample valve.

3) Evacuate the known volume and fill it to the desired pressure. Record P_a and close the known volume valve.

4) With all the valves closed except the one to the manometer, evacuate the apparatus.

5) Close the valve to the vacuum pump and open the valve to the known volume. Wait for equilibrium and record P_b.

6) Repeat steps 4 and 5 several times to calibrate the delivery volume.

7) Repeat step 2 then add the desired pressure of gas to the delivery volume and record P_2.

8) Open the valve to the sample and wait for it to equilibrate. Record P_3.

9) Close the valve to the sample and add more gas to the delivery volume. Record a new P_2 and the old P_3 becomes the new P_1.

10) Repeat steps 8 and 9 several times at increasing pressures.

In this procedure the dead volume of the vacuum line is calibrated (steps 1-6) and used as the delivery volume in the adsorption measurements (steps 7-10). This procedure results in two series of pressure readings. The first allows the delivery volume to be calibrated and this value is used with the second series to calculate the adsorption isotherm. These calculations were carried out using the spreadsheet listed in Appendix C.

Concentration of Active Complex

The concentration of active complex can be determined in two ways. First, it can be calculated from the gas adsorption isotherms of O_2 and Ar. The amount of $Co\text{-}O_2$ can be determined by subtracting the amount of Ar adsorbed from the amount of O_2 adsorbed at the same gas pressure above the zeolite. At pressures where the active cobalt is saturated this value is the total concentration of active cobalt. This value can also be arrived at by quantitatively measuring the EPR signal for the $Co\text{-}O_2$ adduct as described in Chapter 3.

Equilibrium Constant

The equilibrium constant for oxygen binding to the active complex can be determined experimentally by measuring the amount of O_2 adsorbed at different pressures above the zeolite and the amount of Ar adsorbed over the same pressure range. The Ar adsorption isotherm is linear and the equation for the line can be determined by linear regression. Using this equation, the amount of Ar adsorbed by the material at any pressure can be calculated. The difference between the amount of O_2 and Ar adsorbed at the same pressure can be determined and represents the amount of $Co\text{-}O_2$ formed. By calculating this value at different O_2 pressures, a plot of

equation 4-4 can be constructed with the slope of this line giving $-P_{1/2}$ and the intercept giving the total amount of active cobalt. A spreadsheet for carrying out these calculations is given in Appendix C.

The amount of $Co-O_2$ can also be determined by quantitatively measuring the EPR signal for $Co-O_2$ at different O_2 pressures above the zeolite. This also allows a plot of equation 4-4 and the determination of K_{O2}. This procedure works well when the amount of active complex is low because of the high sensitivity of the EPR instrument for $Co-O_2$.

In the above two procedures, the units for the slope and intercept of the resulting line are $torr^{-1}$ and moles/g, respectively. The equilibrium constant can also be calculated using the concentration of O_2 and $Co-O_2$ inside the zeolite. The concentration of $Co-O_2$, $[Co-O_2]$, can be calculated from the amount of $Co-O_2$ and the pore volume of the zeolite. The amount of free O_2 inside the zeolite can be calculated by assuming the amount of Ar adsorbed at a given pressure is equal to the amount of O_2 inside the zeolite which is not bound to a cobalt at the same pressure of O_2. Using this value and the pore volume, the concentration of oxygen inside the zeolite, $[O_2]$, can be calculated. A plot of equation 4-4 using $[CoO_2]$ and $[O_2]$ gives a slope of $-[O_2]_{1/2}$ in units of molarity. This represents the concentration of O_2 required to oxygenate half the active

complexes and can be converted to a $P_{1/2}$ value using the ideal gas law.

Pore Volume Calculation

The pore volume available for gas adsorption is decreased by the presence of $Co(CN)_6^{3-}$ in samples of Co(CN)Na-Y. This is evident by the decrease in the amount of Ar adsorbed on Co(CN)Na-Y relative to Na-Y. This decrease should be directly related to the decrease in pore volume. Since the pore volume for Na-Y is known, the pore volume of Co(CN)Na-Y can be determined by a ratio of the amount of Ar adsorbed by Co(CN)Na-Y to that adsorbed by NaY.

Distribution Constant

The distribution constant, K_d, gives the concentration of gas inside the zeolite relative to that outside, as shown in equation 4-6. This can be calculated from the argon adsorption isotherms for Co(CN)Na-Y and their pore volumes, as shown below. A_{Ar} is the amount of Ar adsorbed at P_{Ar} above the zeolite.

$$K_d = \frac{A_{Ar} \text{ adsorbed / pore volume}}{P_{Ar} / RT} \qquad (2)$$

Molecular Weight Calculations

The molecular formula for Na-Y is given by Breck[2] and the calculations here were based on LZY-52 having this formula.

Na-Y $Na_{56}[(AlO_2)_{56}(SiO_2)_{136}]$

Mol. Wt. = 12752

Co(CN)Na-Y $Co_x[NaCN]_yNa_{56-2x}[(AlO_2)_{56}(SiO_2)_{136}]$

$$\text{Mol. Wt.} = 59x + 49y + 23*(56-2x) + 11464 \qquad (3)$$

From cobalt and CHN analysis the weight percent of cobalt, $Co_{wt\%}$, and weight percent of nitrogen, $N_{wt\%}$, are determined.

$$Co_{wt\%} = 100 * \frac{59x}{\text{Mol. Wt.}} \qquad (4)$$

$$N_{wt\%} = 100 * \frac{14y}{\text{Mol. Wt.}} \qquad (5)$$

By solving for x and y in equations 4 and 5 and substituting these into equation 3, the molecular weight of Co(CN)Na-Y can be calculated from experimentally determined values using equation 6.

$$\text{Mol. Wt.} = \frac{12752}{[1 - (0.2203*Co_{wt\%} + 3.5*N_{wt\%})*10^{-2}]} \quad (6)$$

The above equation is for a dry sample of zeolite material. Since this is not the case the equations above must be corrected for the water present in Na-Y. As an approximate measure of the amount of water present, the weight percent hydrogen, $H_{wt\%}$, determined from CHN analysis is assumed to be from H_2O. The weight percent water, $H_2O_{wt\%}$, can be calculated using equation 7 and the molecular weight for Na-Y·zH_2O can be determined using equation 9.

$$H_2O_{wt\%} = \frac{H_{wt\%} * 18}{2} \quad (7)$$

$$H_2O_{wt\%} = 100 * \frac{18z}{\text{Mol. Wt.}} \quad (8)$$

$$MW = \frac{12752}{[1-(0.2203*Co_{wt\%}+3.5*N_{wt\%}+1.0*H_2O_{wt\%})*10^{-2}]} \quad (9)$$

Separation Factor

The separation factor, $\alpha_{O2/N2}$, can be calculated using the adsorption isotherm data for O_2 and N_2. A spreadsheet

for doing this calculation is listed in Appendix C. The equation used in this spreadsheet is defined below. Equation 4-12 can be rearranged to give equation 10

$$\alpha_{O2/N2} = \frac{N_{O2}ads * (N_tN_2 - N_{N2}ads)}{N_{N2}ads * (N_tO_2 - N_{O2}ads)} \qquad (10)$$

where $N_{O2}ads$ and $N_{N2}ads$ are the amounts of O_2 and N_2 adsorbed by the solid and N_tO_2 and N_tN_2 are the initial amounts of O_2 and N_2 in the apparatus. In Table 4-8 the initial pressure of O_2 and N_2 are the same and therefore the values of N_tO_2 and N_tN_2 are equal. The initial amount of O_2 can be calculated from the amount remaining in the apparatus plus the amount adsorbed by the sample.

APPENDIX B
COMPUTER PROGRAMS

VAC4 Program

The VAC4 program is written in TURBO BASIC and is used in conjunction with the procedure outlined in Appendix A for doing adsorption measurements using the reversible addition technique. It is specialized for use with zeolite material and assumes these materials have a density of 1.92 g/cc.[2] It also contains a routine which allows a blank sample tube to be calibrated using the RA technique. This program was use with the data for both Co(CN)Na-Y(1) and Co(CN)Na-Y(2).

VAC5 Program

The VAC5 program is an upgrade version of VAC4 which can be used for more general calculations and is also written in TURBO BASIC. It has mainly been used for adsorption measurements with material other than zeolites, due to its general nature.

Double Integration Program

The DOUB_INT program is written in TURBO PASCAL 4.0 and is for use with the quantitative EPR measurements of the cobalt oxygen adduct in Co(CN)Na-Y. The comments include in the source code should be consulted for a complete discription of the program. A small flaw in the program has been disovered which has not been corrected. This flaw causes incorrect results when the baseline of the spectrum has a positive slope. Since all the spectra interpreted in this work had baselines with negative slopes this was not a problem.

```
'   ********************  VAC4 PROGRAM  *************************
'                       UNIVERSITY OF FLORIDA
'              FOR VAC-LINE CALCULATIONS USING ZEOLITES
'       THIS IS A PROGRAM WRITTEN BY R.J. TAYLOR FOR PERSONAL USE

 dim t(50), u(50), v(50,4), p(50,4), m(50,4), dp(50,4),dv(50,4)
 dim dr(50,4), r(50,4), a(50), dm(50), em(50,4), ea(50), edm(50)
' COMMMANDS WHICH USE EGA GRAPHICS HAVE BEEN MADE INTO COMMENTS
'screen 9
'color 15,9,15
sub MENU

      cls

      print
      print "                              Program by RJ Taylor"
      print
      print
      print "                                      MENU"
      print
      print
      print "                          (A)  Enter new data"
      print
      print "                          (B)  Load data from disk"
      print
      print "                          (C)  Do Calibration Calculations"
      print
      print "                          (D)  Do Mole Gas Calculations"
      print
      print "                          (Q)  Quit program"
      print

      for I=1 to 3
'     line (140+I,70+I)-(480-I,250-I),,B
      next I
      print
      print
      input "                       Make a selection (A,B,C,D or Q) : ",x$
           if x$<>"A" then
           if x$<>"B" then
            if x$<>"C" then
              if x$<>"D" then
                if x$<>"Q" then
                   cls
                   sound 500,10
                   call MENU
                end if
             end if
           end if
         end if
       end if
```

```
      if x$="A" then call NEWDAT
      if x$="B" then call LOADAT
      if x$="C" then call DVOL
      if x$="D" then call MOL
      if x$="Q" then goto 5000
end sub

sub NEWDAT
      shared t(),np,nt,t$
      cls
      input "Enter the title of data : ",t$
      input "Enter the number of data points : ",np
      for I=1 to np
        print I;
        input ": Pressure (mmHg) : ",t(I)
      next I
      nt = int((np-1)/2)

100   input "Do you want to store data on disk (Y or N)  :",a$
      if a$="Y" then call STODAT
      if a$<>"Y" then
           if a$<>"N" then
             sound 500,10
             goto 100
           end if
      end if
      cls
      call EXCHANGE



end sub

sub STODAT

      cls
      shared t(),np,nt,t$
      locate 21,1
      input "Enter file name of data to store on disk (name.ext) : ",n$
      cls
      locate 13,35
      print "STORING DATA"
      open n$ for output as #1
      write#1 , t$
      write#1 , np
      for I=1 to np
        write#1, t(I)
      next I
      close 1
      print
      print "DONE STORING"
      call EXCHANGE
```

```
end sub

sub LOADAT

      shared t(),np,nt,t$
      cls
      shell "dir/w"
      locate 21,1
      input "Enter file name to be loaded from disk (name.ext) : ",n$
      cls
      locate 13,35
      print "LOADING DATA"
      open n$ for input as #2
      input#2, t$
      input#2, np
      nt = int((np-1)/2)
        for I=1 to np
        input#2, t(I)
      next I
      close 2
      cls
      locate 13,38
      print "DONE"
      call EXCHANGE


end sub


sub EXCHANGE

      shared t(),np,nt,v(),p(),t$,u(),dp(),u1,u2
'      input "Enter uncertainty for P > 100 mmHg : ",u1
'      input "Enter uncertainty for P < 100 mmHg : ",u2
      u1=.1
      u2=.02
      x=0
     for J=1 to nt

       for I=1 to 3
          p(J,I) = t(J+x)
          if p(J,I) >= 100 then dp(J,I)=u1
          if p(J,I) < 100 then dp(J,I)=u2
          x=x+1
       next I

     x=x-2
     next J
```

```
    call VOL


end sub


sub VOL

      shared t(),v(),p(),m(),np,nt,t$,dp(),ul,u2,w
      w=0
      input "Enter volume of Known container (ml) : ",vk
      for I=1 to nt
       v(I,1)=vk
       v(I,2) = (v(I,1))*((p(I,1)/p(I,2))-1)
       v(I,3) = (v(I,1)+v(I,2))*((p(I,2)/p(I,3))-1)
      next I

    call MENU

end sub

sub MOL

      shared p(),v(),nt,m(),t$, w, dm(), a(), em(), ea(), edm(), fw
      cls
      print
      print
      print
      print "                    MOLE GAS CALCULATION"
      print

      dt=.5
      R=0.08205  'l*atm/(mol*K)
      d=1.92 'g/cc
      input "Weight of zeolite (in g) :",w
      input "Molecular weight of gas: ",fw
      input "Temperature (C) : ", T
      input "Volume of sample tube (ml) : ",vs
      T=T+273.2


        for I=1 to nt
          m(I,1) = (v(I,1)/1000)*(p(I,1)/760)/(R*T)
          m(I,2) = ((v(I,1)+v(I,2))/1000)*(p(I,2)/760)/(R*T)
          m(I,3) = ((v(I,1)+v(I,2)+(vs)-w/d)/1000)*(p(I,3)/760)/(R*T)
          dm(I) = m(I,2)-m(I,3)

          a(I)  = (dm(I)*R*T*1000)*760/p(I,3)
        next I
```

```
      for I=1 to nt

        z=(dv(I,1)/v(I,1))^2
        em(I,1)=m(I,1)*(sqr((dp(I,1)/p(I,1))^2 + z + (dT/T)^2))
        z=(dv(I,1)^2 + dv(I,2)^2)/(v(I,1) + v(I,2))^2
        em(I,2)=m(I,2)*(sqr((dp(I,2)/p(I,2))^2 + z + (dT/T)^2))
        dwd= (w/d)*(sqr((.02/w)^2 + (.02/d)^2))
        z=(dv(I,1)^2 + dv(I,2)^2 + (0.2)^2 + dwd^2)/(vs + v(I,1) + v(I,2))^2
        em(I,3)=m(I,3)*(sqr((dp(I,3)/p(I,3))^2 + z + (dT/T)^2))

        edm(I) = sqr(em(I,2)^2 + em(I,3)^2)
        ea(I)  = a(I)*(sqr((edm(I)/dm(I))^2)+(dT/T)^2+(dp(I,3)/p(I,3))^2)

      next I

     call DISMOL


end sub

sub DISCAL
      shared nt,p(),v(),m(),t$, dv(), dp(), ul,u2,em()

400   input "Do you want a hard copy : ",a$
      if a$="N" then goto 500
      if a$<>"N" then
         if a$<>"Y" then
           sound 500,10
           cls
           goto 400
         end if
      end if

        lprint chr$(15)
        lprint t$
        lprint
        lprint "          Pressure       Volume        Error"
        lprint "            (torr)         (ml)        (torr)"
        lprint "       ---------------------------------------"
      for J=1 to nt
        lprint "Trial "J


        for I=1 to 3
         lprint "          ";
         lprint using "####.##"; p(J,I);
         lprint "        ";
         lprint using "####.#"; v(J,I);
         lprint "      ";
         lprint using "#.###";dv(J,I)
        next I
       next J
```

```
        lprint
        lprint "For P > 100 the uncertainty is ";
        lprint using "#.##";u1
        lprint "For P < 100 the uncertainty is ";
        lprint using "#.##";u2
        lprint chr$(18)


500     print t$
        print
        print "          Pressure       Volume         Error"
        print "            (torr)         (ml)         (torr)"
        print "        ---------------------------------------"
      for J=1 to nt
        print "Trial "J


        for I=1 to 3
         print "          ";
         print using "####.##"; p(J,I);
         print "       ";
         print using "####.#"; v(J,I);
         print "     ";
         print using "#.###";dv(J,I)
        next I
        print
       next J
      print "For P > 100 the uncertainty is ";
      print using "#.##";u1
      print "For P < 100 the uncertainty is ";
      print using "#.##";u2
      input "Hit ENTER to continue",o$

     goto 1000

end sub


sub DVOL

       shared dp(), p(), v(), nt, dv()

       input "Enter error in Known volume (ml) : ",ek
       for I=1 to nt

        dv(I,1)=ek

       next I

       for I=1 to nt
```

```
          r(I,2) = (v(I,1)*p(I,1)/p(I,2))
          dr(I,2) = r(I,2)*sqr((dv(I,1)/v(I,1))^2 + (dp(I,1)/p(I,1))^2 +
(dp(I,2)/p(I,2))^2)
          dv(I,2) = sqr((dr(I,2)^2 + dv(I,1)^2))

          r(I,3) = ((v(I,1) + v(I,2))*p(I,2)/p(I,3))
          x = (dv(I,1)^2 + dv(I,2)^2)/(v(I,1) + v(I,2))^2
          dr(I,3) = r(I,3)*(sqr( x + (dp(I,2)/p(I,2))^2 + (dp(I,3)/p(I,3))^2))
          dv(I,3) = sqr(dr(I,3)^2 + dv(I,1)^2 + dv(I,2)^2)
       next I



    call DISCAL

end sub

sub DISMOL
      shared nt,p(),v(),m(),t$, dv(), dp(), u1,u2,w,a(),em(),ea(),dm(),edm(),
fw

800   input "Do you want a hard copy : ",a$
      if a$="N" then goto 900
      if a$<>"N" then
         if a$<>"Y" then
           sound 500,10
           cls
           goto 800
         end if
      end if

        lprint chr$(15)
        lprint t$
        lprint "  Weight of zeolite (g) : ";
        lprint using "#.##";w
        lprint
        lprint "          Pressure       Volume              Moles of"
        lprint "           (torr)         (ml)                 gas"
        lprint "       ------------------------------------------------"
      for J=1 to nt
        lprint "Trial "J


        for I=1 to 3
         lprint "          ";
         lprint using "####.##"; p(J,I);
         lprint "        ";
         lprint using "####.#"; v(J,I);
         lprint "      ";
         lprint using "#.###^^^^";m(J,I);
         lprint " + ";
         lprint using "#.#^^^^";em(J,I)
```

```
        next I

'       lprint "Moles of gas absorbed : ";
'       lprint using "#.###^^^^";dm(J);
'       lprint " + ";
'       lprint using "#.###^^^^";edm(J)
        lprint "Moles of gas per gram : ";
        lprint using "#.###^^^^";dm(J)/w;
        lprint " + ";
        lprint using "#.###^^^^";edm(J)/w
        lprint "Weight of gas absorbed : ";
        lprint using "#.###^^^^";dm(J)*fw;
        lprint " + ";
        lprint using "#.##^^^^";edm(J)*fw

'       lprint "Volume of gas absorbed (ml) :";
'       lprint using "###.###";a(J);
'       lprint " + ";
'       lprint using "###.###";ea(J)
        lprint "Volume of gas per gram (ml) : ";
        lprint using "##.###";a(J)/w;
        lprint " + ";
        lprint using "##.##";ea(J)/w
        lprint "at a pressure of (torr) :";
        lprint using "###.##";p(J,3)
        lprint

      next J

       lprint chr$(18)



900    print t$
       print "  Weight of zeolite (g) : ";
       print using "#.##";w
       print
       print "          Pressure       Volume         Moles of"
       print "            (torr)         (ml)           gas"
       print "       ---------------------------------------"
     for J=1 to nt
      print "Trial "J



       for I=1 to 3
        print "          ";
        print using "####.##"; p(J,I);
        print "        ";
        print using "####.#"; v(J,I);
        print "      ";
        print using "#.###^^^^";m(J,I);
```

```
         print " + ";
         print using "#.#^^^^";em(J,I)
        next I


'        print "Moles of gas absorbed : ";
'        print using "#.###^^^^";dm(J);
'        print " + ";
'        print using "#.###^^^^";edm(J)
        print "Moles of gas per gram : ";
        print using "#.###^^^^";dm(J)/w;
        print " + ";
        print using "#.###^^^^";edm(J)/w
        print "Weight of gas absorbed : ";
        print using "#.###^^^^";dm(J)*fw;
        print " + ";
        print using "#.##^^^^";edm(J)*fw

'        print "Volume of gas absorbed (ml) :";
'        print using "###.###";a(J);
'        print " + ";
'        print using "###.###";ea(J)
        print "Volume of gas per gram (ml) :";
        print using "##.###";a(J)/w;
        print " + ";
        print using "##.##";ea(J)/w
        print "at a pressure of (torr) :";
        print using "###.##";p(J,3)
        print

      next J

    input "Hit ENTER to continue",o$

    goto 1000

end sub


1000 call MENU


5000 print "end"

end
```

```
'******   VAC5 - PROGRAM FOR VAC-LINE CALCULATIONS   ********

'      THIS IS A PROGRAM WRITTEN BY RJ TAYLOR FOR PERSONAL USE

'      The input needed for this program is a series of pressure
'      values taken during a reversible adsorption experiment.
'      The numbers should be entered from highest to lowest.


 dim t(50), v(50,4), p(50,4), m(50,4), dp(50,4), a(50), dm(50)
call MENU
sub MENU

      cls

      print
      print "                                "
      print "                  VAC5 - Adsorption Calculation Program"
      print
      print
      print "                                        MENU"
      print
      print
      print "                          (A)  Enter new data"
      print
      print "                          (B)  Load data from disk"
      print
      print "                          (C)  Do Mole Gas Calculations"
      print
      print "                          (Q)  Quit program"
      print

      for I=1 to 3
      next I
      print
      print
      input "                      Make a selection (A,B,C or Q) : ",x$
           if x$<>"A" then
           if x$<>"B" then
            if x$<>"C" then

               if x$<>"Q" then
                  cls
                  sound 500,10
                  call MENU
               end if

           end if
         end if
       end if
      if x$="A" then call NEWDAT
```

```
      if x$="B" then call LOADAT
      if x$="C" then goto 700
      if x$="Q" then goto 5000
end sub

sub NEWDAT
      shared t(),np,nt,t$
      cls
      input "Enter the title of data : ",t$
      input "Enter the number of data points : ",np
      for I=1 to np
        print I;
        input ": Pressure (mmHg) : ",t(I)
      next I
      nt = int((np-1)/2)

100   input "Do you want to store data on disk (Y or N)  :",a$
      if a$="Y" then call STODAT
      if a$<>"Y" then
           if a$<>"N" then
             sound 500,10
             goto 100
           end if
      end if
      call MENU

end sub

sub STODAT

      cls
      shared t(),np,nt,t$
      locate 21,1
      input "Enter file name of data to store on disk (name.ext) : ",n$
      cls
      locate 13,35
      print "STORING DATA"
      open n$ for output as #1
      write#1 , t$
      write#1 , np
      for I=1 to np
        write#1, t(I)
      next I
      close 1
      print
      print "DONE STORING"
      call MENU



end sub
```

```
sub LOADAT

      shared t(),np,nt,t$
      cls
      shell "dir/w"
      locate 21,1
      input "Enter file name to be loaded from disk (name.ext) : ",n$
      cls
      locate 13,35
      print "LOADING DATA"
      open n$ for input as #2
      input#2, t$
      input#2, np
      nt = int((np-1)/2)
        for I=1 to np
        input#2, t(I)
      next I
      close 2
      cls
      locate 13,38
      print "DONE"
      call MENU


end sub



700
      cls
      print
      print "          VAC5 - Adsorption Calculation Program"
      print
      print
      print "                    MOLE GAS CALCULATION"
      print


      R=0.08205  'l*atm/(mol*K)
      input "Weight of sample (in g) :",w
      input "Density of sample (in g/ml) :",d
      input "Molecular weight of gas: ",fw
      input "Temperature (C) : ", T
      input "Enter volume of Known container (ml) : ",vk
      input "Volume of sample tube (ml) : ",vs
      T=T+273.2
      x=0
      for J=1 to nt
       for I=1 to 3
          p(J,I) = t(J+x)
          x=x+1
```

```
 next I
 x=x-2
next J



for I=1 to nt
 v(I,1)=vk
 v(I,2) = (v(I,1))*((p(I,1)/p(I,2))-1)
 v(I,3) = (v(I,1)+v(I,2))*((p(I,2)/p(I,3))-1)
next I

  for I=1 to nt
    m(I,1) = (v(I,1)/1000)*(p(I,1)/760)/(R*T)
    m(I,2) = ((v(I,1)+v(I,2))/1000)*(p(I,2)/760)/(R*T)
    m(I,3) = ((v(I,1)+v(I,2)+(vs)-w/d)/1000)*(p(I,3)/760)/(R*T)
    dm(I) = m(I,2)-m(I,3)

    a(I)  = (dm(I)*R*T*1000)*760/p(I,3)
  next I



800   input "Do you want a hard copy : ",a$
      if a$="N" then goto 900
      if a$<>"N" then
         if a$<>"Y" then
           sound 500,10
           cls
           goto 800
         end if
      end if

        lprint chr$(15)
        lprint t$
        lprint "  Weight of sample (g) : ";
        lprint using "#.##";w
        lprint "  Density of sample (g/ml) : ";
        lprint using "#.##";d
        lprint "  Temperature (C) : ";
        lprint using "##.#";T-273.2
        lprint
        lprint "          Pressure       Volume              Moles of"
        lprint "            (torr)        (ml)                 gas"
        lprint "       ------------------------------------------------"
      for J=1 to nt
        lprint "Trial "J


        for I=1 to 3
```

```
        lprint "          ";
        lprint using "####.##"; p(J,I);
        lprint "        ";
        lprint using "####.#"; v(J,I);
        lprint "      ";
        lprint using "#.###^^^^";m(J,I)
      next I

'     lprint "Moles of gas absorbed : ";
'     lprint using "#.###^^^^";dm(J)
      lprint "Moles of gas per gram : ";
      lprint using "#.###^^^^";dm(J)/w;
      lprint using "                #.###^^^^";dm(J)/w
      lprint "Weight of gas absorbed : ";
      lprint using "#.###^^^^";dm(J)*fw

'     lprint "Volume of gas absorbed (ml) :";
'     lprint using "###.###";a(J)
      lprint "Volume of gas per gram (ml) : ";
      lprint using "##.###";a(J)/w
      lprint "at a pressure of (torr) :";
      lprint using "###.##";p(J,3);
      lprint using "                  ###.#";p(J,3)
      lprint

    next J

     lprint chr$(18)


900   print t$
      print "  Weight of sample (g) : ";
      print using "#.##";w
      print "  Density of sample (g/ml) : ";
      print using "#.##";d
      print "  Temperature (C) : ";
      print using "##.#";T-273.2
      print
      print "          Pressure       Volume         Moles of"
      print "            (torr)         (ml)           gas"
      print "       ---------------------------------------"
    for J=1 to nt
      print "Trial "J



      for I=1 to 3
       print "          ";
       print using "####.##"; p(J,I);
       print "        ";
       print using "####.#"; v(J,I);
```

```
          print "      ";
          print using "#.###^^^^";m(J,I);
        next I


'         print "Moles of gas absorbed : ";
'         print using "#.###^^^^";dm(J);
        print "Moles of gas per gram : ";
        print using "#.###^^^^";dm(J)/w;
        print "Weight of gas absorbed : ";
        print using "#.###^^^^";dm(J)*fw;

'         print "Volume of gas absorbed (ml) :";
'         print using "###.###";a(J);
        print "Volume of gas per gram (ml) :";
        print using "##.###";a(J)/w;
        print "at a pressure of (torr) :";
        print using "###.##";p(J,3)
        print

      next J

    input "Hit ENTER to continue",o$

    goto 1000




1000 call MENU


5000 print "end"

end
```

```
PROGRAM DOUB_INT;

{                    DOUBLE INTEGRATION PROGRAM

                              by

                        Robert J. Taylor
                      University of Florida
                        January 1987


  This program does a double integration of area under a curve. It was
  written to find the area under an epr curve. The data points should
  be picked off the experimental spectrum and entered using the manual
  data entry routine provided. The data should be entered in increasing
  x value. The program calculates the baseline using the first and last
  data point. The area is calculated between adjacent points using
  the trapazoid formed between the two points on the curve and the two
  points from the baseline which have the same x value as those on the
  curve.  In the first integration any area above the baseline is
  positive and any below is negative. During this calculation the areas
  are summed after each point and stored in another matrix with the
  corresponding x value. These points describe the absorption curve. The
  area under the absorption curve is then calculated in the same manner.

  In order for this program to run several other files must be present
  in the PATH directory. These routines are HERC.BGI, EGAVGE.BGI, and
  CGA.BGI. These routines let the program determine the proper graphics
  card.

                                                                      }
USES GRAPH, CRT, PRINTER;

VAR
  A_PTS : ARRAY[1..100,1..2] OF REAL; { X and Y values for absorption curve }
  D_PTS : ARRAY[1..100,1..2] OF REAL; { X and Y values for derivative curve }
  NUM_PTS : INTEGER;                  { Number of data points }
  SLOPE_A, INTERCEPT_A : REAL;        { Slope and intercept of baseline }
  SLOPE_D, INTERCEPT_D : REAL;
  SLOPE, INTERCEPT:REAL;
  MESSAGE:STRING;
  NUM_REAL:REAL;
  A_AREA, D_AREA:REAL;                { Total areas under the curves }
  DONE_CALC:BOOLEAN;


PROCEDURE STR_TO_REAL(MESSAGE:STRING;VAR NUM:REAL);

 { This procedure asks a question (MESSAGE) then reads in a string (S).
 It then converts the string to a real number (NUM) and passes it
 back to the calling command }
```

```
VAR I,J:INTEGER;
    CT:REAL;
    X,Y:REAL; {X IS NUMBER, Y IS THE PLACE HOLDER}
    DEC_FLG:BOOLEAN; {TRUE FOR DECIMAL}
    EXP_FLG:BOOLEAN; {TRUE FOR EXPONENTIAL}
    POS_NUM:BOOLEAN; {TRUE IF + FOUND IN FRONT}
    POS_EXP:BOOLEAN; {TRUE FOR POSITIVE EXPONENTIAL}
    NEG_EXP:BOOLEAN; {TRUE FOR NEGATIVE EXPONENTIAL}
    NEG_NUM:BOOLEAN; {TRUE FOR NEGATIVE NUMBER}
    CAS_FLG:BOOLEAN; {TRUE IF VALID CHARACTER}
    FIND_NUM:BOOLEAN; {TRUE IF A NUMBER IS FOUND}
    ERROR:BOOLEAN; {TRUE IF INVALID CHARACTER}
    FLAG1:BOOLEAN; {TRUE AFTER PASS THROUGH EXPONENT}
    FLAG2:BOOLEAN; {TRUE IF A NUMBER IS FOUND BUT CLEARED
                    AFTER EACH CHARACTER IS CHECKED}
    EXP:INTEGER; {HOLDS EXPONENTIAL PLACE}
    S:STRING; {INPUT STRING WHICH IS CONVERTED TO REAL NUMBER}

  PROCEDURE EXPONENT(C:CHAR);
     BEGIN
       IF FLAG1 THEN EXP := EXP*10+ORD(C)-ORD('0')
                ELSE EXP := ORD(C)-ORD('0');
       FLAG1 := TRUE;
     END;

  BEGIN
    REPEAT

      {INITIALIZATION SECTION}
     FLAG1 := FALSE;
     DEC_FLG := FALSE;
     CAS_FLG := FALSE;
     NEG_EXP := FALSE;
     NEG_NUM := FALSE;
     POS_EXP := FALSE;
     POS_NUM := FALSE;
     EXP_FLG := FALSE;
     FIND_NUM := FALSE;
     ERROR :=FALSE;
     X := 0;
     Y := 1;
        {END INITIALIZATION}

    WRITE (MESSAGE);
    READLN(S);
    I := 0;  {THIS IS THE COUNTER FOR THE DIGIT OF THE NUMBER}

    REPEAT
      FLAG2:=FALSE;
      I := I+1;
       IF (S[I] IN ['0'..'9'] ) {IF THE CHARACTER IS A DIGIT}
          THEN
```

```
  IF EXP_FLG THEN EXPONENT (S[I])
    ELSE
     BEGIN
      FLAG2:=TRUE;
      FIND_NUM:=TRUE;
      X:=X*10+ORD(S[I])-ORD('0'); {CONVERT CHARACTER
                                        TO DIGIT}
      IF DEC_FLG THEN Y:=Y*10; {IF DECIMAL POINT HAS BEEN
                                  FOUND}
      END

ELSE {IF CHARACTER IS NOT A DIGIT}
  BEGIN
    IF (S[I]<>'-') AND (S[I]<>'+') THEN
      IF (S[I]<>'E') AND (S[I]<>'.') THEN ERROR:=TRUE;

    CASE S[I] OF

     '.' : BEGIN
             IF DEC_FLG OR EXP_FLG THEN  ERROR:=TRUE;
             CAS_FLG:=TRUE;
             DEC_FLG:=TRUE;
           END;

     'E' : BEGIN
             IF EXP_FLG OR NOT FIND_NUM THEN ERROR:=TRUE;
             CAS_FLG:=TRUE;
             EXP_FLG:=TRUE;
           END;

     '-' : BEGIN
             IF NEG_EXP OR POS_EXP THEN ERROR:=TRUE;
             IF POS_NUM AND NOT EXP_FLG THEN ERROR:=TRUE;
             IF NEG_NUM AND NOT EXP_FLG THEN ERROR:=TRUE;
             IF NOT EXP_FLG AND FIND_NUM THEN ERROR:=TRUE;
             CAS_FLG:=TRUE;
             IF EXP_FLG
                THEN NEG_EXP:=TRUE
                ELSE NEG_NUM:=TRUE;
           END;

     '+' : BEGIN
             IF POS_EXP OR NEG_EXP THEN ERROR:=TRUE;
             IF NEG_NUM AND NOT EXP_FLG THEN ERROR:=TRUE ;
             IF POS_NUM AND NOT EXP_FLG THEN ERROR:=TRUE;
             IF NOT EXP_FLG AND FIND_NUM THEN ERROR:=TRUE;
             CAS_FLG:=TRUE;
             IF EXP_FLG
                    THEN POS_EXP:=TRUE
                    ELSE POS_NUM:=TRUE;
             END;
```

```
          END; {CASE}
        END; {ELSE}

      IF NOT CAS_FLG AND NOT FLAG2 THEN ERROR:=TRUE;
      IF ERROR THEN
         BEGIN
           WRITELN('Invalid number, try again!');
           S:='';
         END;

   UNTIL (I=LENGTH(S)) OR ERROR; {KEEP ON GOING UNTIL THE
                                  NUMBER IS ENTERED OR AN ERROR
                                  IS FOUND}

UNTIL NOT ERROR; {IF AN ERROR WAS FOUND, REPEAT THE WHOLE THING.}

IF EXP_FLG THEN
           BEGIN
               CT:=1;
               FOR J:=1 TO EXP DO
                   CT:=CT*10;
           END;

NUM := (X/Y); {THIS SETS THE DECIMAL POINT}
IF EXP_FLG THEN
  IF NEG_EXP THEN NUM:=NUM/CT
             ELSE NUM:=NUM*CT;

IF NEG_NUM THEN NUM:=0-(NUM);

END; {STR_TO_REAL}

PROCEDURE STORE_DATA;

  VAR
     SPECTRA_DATA:TEXT;
     I:INTEGER;
     FILENAME:STRING;

  BEGIN
    WRITELN;
    WRITE('Enter the file for storing data name ( Do not forget .ext ) : ');
    READLN(FILENAME);
    ASSIGN(SPECTRA_DATA, FILENAME);
    REWRITE(SPECTRA_DATA);
    WRITELN(SPECTRA_DATA,NUM_PTS);
    FOR I:=1 TO NUM_PTS DO
     BEGIN
      WRITELN(SPECTRA_DATA,D_PTS[I,1]);
      WRITELN(SPECTRA_DATA,D_PTS[I,2]);
     END;
    CLOSE(SPECTRA_DATA);
```

```
  END; { STORE_DATA }



PROCEDURE READ_DATA;

 VAR
    SPECTRA_DATA:TEXT;
    I:INTEGER;
    FILENAME:STRING;
    ANSWER:CHAR;
    DISK_ERR, RETURN:BOOLEAN;

 BEGIN
  WRITELN; WRITELN;
  REPEAT
    RETURN:=FALSE;
    DISK_ERR:=FALSE;
    WRITE('Enter the file name for reading data (Do not forget .ext) : ');
    READLN(FILENAME);
    (*$I-*)
    ASSIGN (SPECTRA_DATA,FILENAME);
    RESET(SPECTRA_DATA);
    IF IORESULT<>0 THEN
      BEGIN
        DISK_ERR:=TRUE;
        IF IORESULT=15 THEN
         BEGIN
          WRITE('File not on disk; Do you want to try again : ');
          READLN(ANSWER);
          IF ANSWER='Y' THEN RETURN:=TRUE;
         END
        ELSE WRITELN('Disk error! Check disk.');
       END;
     (*$I+*)
       IF NOT DISK_ERR THEN
         BEGIN
          READLN(SPECTRA_DATA,NUM_PTS);
          FOR I:=1 TO NUM_PTS DO
           BEGIN
            READLN(SPECTRA_DATA,D_PTS[I,1]);
            READLN(SPECTRA_DATA,D_PTS[I,2]);

            WRITELN(D_PTS[I,1]:10:3,D_PTS[I,2]:10:2);
           END;
          END;

   UNTIL NOT RETURN;

  END; {READ_DATA}
```

```
PROCEDURE USER_INPUT;

 VAR
     I, N :INTEGER;
     ER_FLAG:BOOLEAN;
     ANSWER:CHAR;
     MESSAGE, SS:STRING;
     NUM_REAL:REAL;

 BEGIN
  WRITE(CHR(12)); WRITELN;
  WRITELN('Be sure to enter the points in INCREASING X value.');
  WRITELN;
  MESSAGE:='Enter the number of data points to be entered: ';
  STR_TO_REAL(MESSAGE,NUM_REAL);
  NUM_PTS:=ROUND(NUM_REAL);

 FOR I:=1 TO NUM_PTS DO
  BEGIN
   STR(I,SS);
   MESSAGE:=(CONCAT('X[',SS,'] : '));
   STR_TO_REAL(MESSAGE,NUM_REAL);
   D_PTS[I,1]:=NUM_REAL;
   MESSAGE:=(CONCAT('Y[',SS,'] : '));
   STR_TO_REAL(MESSAGE,NUM_REAL);
   D_PTS[I,2]:=NUM_REAL;
  END;

 END; { USER_INPUT }

PROCEDURE CHANGE;

  VAR
      JNEW:INTEGER;
      ERROR:BOOLEAN;
      MESSAGE:STRING;
      NUM_REAL:REAL;

  BEGIN
    REPEAT
      ERROR:=FALSE;
      WRITELN;
      MESSAGE:=('Enter the data point to correct : ');
      STR_TO_REAL(MESSAGE,NUM_REAL);
      JNEW:=ROUND(NUM_REAL);
      IF (JNEW<1) OR (JNEW>NUM_PTS) THEN ERROR:=TRUE;
      IF NOT ERROR THEN
          BEGIN
            MESSAGE:=('New G : ');
            STR_TO_REAL(MESSAGE,NUM_REAL);
            D_PTS[JNEW,1]:=NUM_REAL;
            MESSAGE:=('New A : ');
```

```
            STR_TO_REAL(MESSAGE,NUM_REAL);
            D_PTS[JNEW,2]:=NUM_REAL;
          END
        ELSE
          WRITELN('Data point number out of range! Try again.');

    UNTIL NOT ERROR;
  END;  { CHANGE }


PROCEDURE INSERT;

  VAR
     J, JINSERT : INTEGER;
     X : ARRAY[1..100, 1..2] OF REAL;
     ERROR:BOOLEAN;
     MESSAGE:STRING;
     NUM_REAL:REAL;

  BEGIN
    REPEAT
      ERROR:=FALSE;
      WRITELN;
      MESSAGE:=('Enter the data point to insert : ');
      STR_TO_REAL(MESSAGE, NUM_REAL);
      JINSERT:=ROUND(NUM_REAL);
      IF (JINSERT<1) OR (JINSERT>NUM_PTS+1) THEN ERROR:=TRUE;
      IF NOT ERROR THEN
        BEGIN
          FOR J:=JINSERT TO NUM_PTS DO
            BEGIN
             X[J+1,1]:=D_PTS[J,1];
             X[J+1,2]:=D_PTS[J,2];
            END;
           NUM_PTS:= NUM_PTS + 1;
           FOR J:=JINSERT TO NUM_PTS DO
             BEGIN
               D_PTS[J,1]:=X[J,1];
               D_PTS[J,2]:=X[J,2];
             END;
          MESSAGE:=('G To Insert : ');
          STR_TO_REAL(MESSAGE,NUM_REAL);
          D_PTS[JINSERT,1]:=NUM_REAL;
          MESSAGE:=('A To Insert : ');
          STR_TO_REAL(MESSAGE,NUM_REAL);
          D_PTS[JINSERT,2]:=NUM_REAL;
       END {IF}

     ELSE
         WRITELN('Data point number out of range! Try again.');

  UNTIL NOT ERROR;
```

```
  END; {INSERT}

PROCEDURE DELETE;

  VAR
      J, JDELETE : INTEGER;
      X : ARRAY[1..100,1..2] OF REAL;
      ERROR:BOOLEAN;
      MESSAGE:STRING;
      NUM_REAL:REAL;

  BEGIN
    REPEAT
       ERROR:=FALSE;
       WRITELN;
       MESSAGE:=('Enter the data point number to delete : ');
       STR_TO_REAL(MESSAGE,NUM_REAL);
       JDELETE:=ROUND(NUM_REAL);
       IF (JDELETE<1) OR (JDELETE>NUM_PTS) THEN  ERROR:=TRUE;
       IF NOT ERROR THEN
         BEGIN
            FOR J:=JDELETE TO NUM_PTS DO
              BEGIN
               X[J,1]:=D_PTS[J+1,1];
               X[J,2]:=D_PTS[J+1,2];
              END; {FOR}
            NUM_PTS:=NUM_PTS-1;
            FOR J:=JDELETE TO NUM_PTS DO
             BEGIN
               D_PTS[J,1]:=X[J,1];
               D_PTS[J,2]:=X[J,2];
            END; {FOR}
          END {IF}
        ELSE
          WRITELN('Data point number out of range! Try again.');

     UNTIL NOT ERROR;

  END;  {DELETE}

PROCEDURE CHECK_DATA;

  VAR
     I:INTEGER;
     ER_FLAG:BOOLEAN;
     ANSWER, CORRECT:CHAR;

  BEGIN
    REPEAT
      ClrScr;
      WRITELN;
```

```
      WRITELN('              X           Y');
      WRITELN('          --------------------');
      FOR I:=1 TO NUM_PTS DO
        BEGIN
          WRITELN('Point #',I,D_PTS[I,1]:10:2,D_PTS[I,2]:10:2);
        END; {FOR}

      ER_FLAG:=FALSE;
      WRITELN;
      WRITE('Are all the data points correct ( Y or N ) : ');
      READLN(ANSWER);
      IF ANSWER = 'N' THEN ER_FLAG:=TRUE;
      IF ER_FLAG THEN
           BEGIN
             WRITELN;
             WRITELN('(C)   Correction of a data point');
             WRITELN('(I)   Insertion of a data point');
             WRITELN('(D)   Deletion of a data point');
             WRITELN;
             WRITE('Enter the change needed : ');
             READLN(CORRECT);
             CLRSCR;

             CASE CORRECT OF
                            'C' : CHANGE;
                            'I' : INSERT;
                            'D' : DELETE;

             END;{CASE}
            END; {IF}

    UNTIL NOT ER_FLAG;

  END; {CHECK_DATA}



PROCEDURE FIND_BASELINE(X1, Y1, X2, Y2:REAL; VAR S, I:REAL);

  BEGIN
      S:=0;
      I:=0;
      IF (X2-X1)=0 THEN S:=0
                   ELSE
                        S := (Y2-Y1)/(X2-X1);
                        WRITELN('SLOPE ',S:2);
      I := Y1-S*X1;
      WRITELN('INTERCEPT ',I:2);
  END; { FIND_BASELINE}

PROCEDURE CALC_AREA(TopX_1 ,TopY_1, TopX_2, TopY_2 : REAL ; VAR Area:REAL);
```

```
VAR
    MidY_Top, MidY_Bot : REAL;
    H, W : REAL;
    BotY_1, BotY_2 : REAL;
    N_AREA:BOOLEAN;

  FUNCTION Calc_BotY(X : REAL) : REAL;
    BEGIN

         Calc_BotY := X * Slope + Intercept;
    END;  {function}

BEGIN
     DONE_CALC:=TRUE;
     Area:=0;
     N_AREA:=FALSE;
     BotY_1 := Calc_BotY(TopX_1);
     BotY_2 := Calc_BotY(TopX_2);
     MidY_Top := ((TopY_2 - TopY_1)/2) + TopY_1;
     MidY_Bot := ((BotY_2 - BotY_1)/2) + BotY_1;
     H := ABS( (MidY_Top) - (MidY_Bot));
     W := TopX_2 - TopX_1;
     Area := H * W;
     IF (TopY_1 - BotY_1) < 0 THEN N_AREA:=TRUE;
     IF (TopY_1 - BotY_1) = 0 THEN
       BEGIN
         IF (TopY_2 - BotY_2) < 0 THEN N_AREA:=TRUE;
       END;
     IF N_AREA THEN Area:=-Area;



END;  { CALC_AREA }

PROCEDURE FIRST_INT;

   VAR
       N:INTEGER;
       Area,X, Y, A_TOTAL:REAL;



    BEGIN
          FIND_BASELINE(D_PTS[1,1],D_PTS[1,2],
                  D_PTS[NUM_PTS,1],D_PTS[NUM_PTS,2],
                  Slope, Intercept);
      Slope_D:=Slope;
      Intercept_D:=Intercept;
      A_TOTAL:=0;
      Area:=0;
```

```
      FOR N:=1 TO NUM_PTS DO
        BEGIN
          A_PTS[N,1]:=0;
          A_PTS[N,2]:=0;
        END;


      FOR N:=1 TO NUM_PTS DO
        BEGIN
          IF N=1 THEN
            BEGIN
              X:=D_PTS[1,1];
              Y:=D_PTS[1,2];
              A_PTS[1,1]:=((D_PTS[2,1]-D_PTS[1,1])/2+D_PTS[1,1]);
              A_PTS[1,2]:=0

            END
          ELSE
            BEGIN

              CALC_AREA(X,Y,D_PTS[N,1],D_PTS[N,2],Area);
              A_TOTAL:=A_TOTAL + Area;
              X:=D_PTS[N,1];
              Y:=D_PTS[N,2];
              IF N<NUM_PTS THEN
              BEGIN
                A_PTS[N,1]:=(D_PTS[N+1,1]-D_PTS[N,1])/2+D_PTS[N,1];
                A_PTS[N,2]:=A_TOTAL;

                WRITELN(A_PTS[N,1]:10:2,A_PTS[N,2]:20:2);
              END {IF}

            END {ELSE}
          END; {FOR}
        D_AREA:=A_TOTAL;

        WRITELN('DERIVATIVE AREA = ',D_AREA:10:2);
        END; {FIRST_INT}


PROCEDURE SECOND_INT;

   VAR
       N:INTEGER;
       Area,X, Y , A_TOTAL:REAL;



    BEGIN
      SLOPE:=0;
      INTERCEPT:=0;
```

```
        FIND_BASELINE(A_PTS[1,1],A_PTS[1,2],
                A_PTS[NUM_PTS-1,1],A_PTS[NUM_PTS-1,2],
                Slope, Intercept);
    Slope_A:=Slope;
    Intercept_A:=Intercept;
    A_TOTAL:=0;
    Area:=0;


    FOR N:=1 TO NUM_PTS DO
      BEGIN
        IF N=1 THEN
          BEGIN
            X:=A_PTS[1,1];
            Y:=A_PTS[1,2]
          END
        ELSE
          BEGIN
            CALC_AREA(X,Y,A_PTS[N,1],A_PTS[N,2],Area);
            A_TOTAL:=A_TOTAL + Area;
            X:=A_PTS[N,1];
            Y:=A_PTS[N,2]

          END {ELSE}
        END; {FOR}
      A_AREA:=A_TOTAL;
      WRITELN(' ');WRITELN('ABSORBANCE AREA = ',A_AREA:10:3);

       END; {SECOND_INT}




 PROCEDURE OUTPUT;

VAR
   I:INTEGER;
   TITLE, SS, S1, S2, S3, S4,S5, S6,S7:STRING;

BEGIN
  IF NOT DONE_CALC THEN
                    BEGIN
                        FIRST_INT;
                        SECOND_INT
                    END;
  WRITE(LST,CHR(15));
  WRITE('Enter the title for the hard copy : ');
  READLN(TITLE);
  WRITELN(LST,TITLE);
  WRITELN(LST,' ');
```

```
  WRITELN(LST,'              Double Integration of ESR Spectra');
  WRITELN(LST,' ');
  WRITELN(LST,'                          Derivative          Absorbance');
 WRITELN(LST,'-------------------------------------------------------------');
  FOR I:=1 TO NUM_PTS DO
  BEGIN
     STR(I,S3);
       SS:=CONCAT('Point #',S3,'   ');
       S2:='  |  ';
       IF I<=9 THEN S5:='  '
             ELSE S5:=' ' ;
     WRITELN(LST,SS,S5,S2,D_PTS[I,1]:10:1,D_PTS[I,2]:10:1,S2,
                         A_PTS[I,1]:5:1,A_PTS[I,2]:10:1);
  END;
  WRITELN(LST,'-------------------------------------------------------------');
  WRITELN(LST,' ');


  STR(Slope_D:5:3,S1);
  STR(Intercept_D:5:3,S2);
  WRITELN(LST,' ');
  WRITELN(LST,'Derivative');
  STR(ROUND(D_AREA),S4);
  WRITELN(LST,'     Area:    ',S4);
  WRITELN(LST,'     Baseline:   Slope ',S1,' Intercept ',S2);
  WRITELN(LST,' ');
  STR(Slope_A:5:3,S1);
  STR(Intercept_A:5:3,S2);
  WRITELN(LST,'Absorbance');
  STR(ROUND(A_AREA),S4);
  WRITELN(LST,'     Area:    ',S4);
  WRITELN(LST,'     Baseline:   Slope ',S1,' Intercept ',S2);
  WRITE(LST,CHR(12));



END;


PROCEDURE GRAPH_D;

CONST
VP1 : ViewPortType = (X1:10; Y1:10; X2:310; Y2:210; Clip : ClipOn);
VP2 : ViewPortType = (X1:320; Y1:10; X2:620; Y2:210; Clip : ClipOn);
VP3 : VIEWPORTTYPE = (X1:10; Y1:240; X2:620; Y2:340; CLIP : CLIPON);
Vp1Pts : array[1..4] of PointType =
( ( x:10;y:10),
  ( x:10;y:210),
  ( x:310;y:210),
  ( x:310;y:10));

Vp2Pts : array[1..4] of PointType =
```

```
( (x:320;y:10),
  (x:320;y:210),
  (x:620;y:210),
  (x:620;y:10));

Vp3Pts : array[1..4] of PointType =
( ( x:10;y:240),
  ( x:10;y:340),
  ( x:620;y:340),
  ( x:340;y:240));

  VP1_COLOR = BLACK;
  VP2_COLOR = BLACK;
  VP3_COLOR = BLACK;
  L_COLOR = WHITE;
  BL_COLOR = WHITE;



VAR
C, GraphDriver, GraphMode, I : INTEGER;
SSS,SS :STRING;
MAXY,R,Y:REAL;



BEGIN
IF NOT DONE_CALC THEN
                      BEGIN
                         FIRST_INT;
                         SECOND_INT
                      END;
  GraphDriver := Detect;
  InitGraph(GraphDriver,GraphMode,'');
  if GraphResult<> grOK then
     BEGIN

              CLRSCR;
              WRITELN;
              WRITELN;
       WRITELN('     There is a GRAPHICS ERROR: ',GRAPHERRORMSG(GRAPHDRIVER));
       WRITELN('     You will not be able to graph your data.');
       WRITELN;
       WRITELN('      Hit any key to continue.......');
       READLN
     END

   ELSE
         BEGIN

  with vp1 do
```

```
begin
    SetFillStyle(solidFill,VP1_COLOR);
    SetColor(L_COLOR);
    Rectangle(Succ(x1),Succ(y1), Pred(x2), Pred(y2));
    FillPoly(4,VplPts);

SetViewPort(x1, y1, x2, y2, ClipOn);
SetTextJustify(centertext,centertext);
OutTextXY(220,10,'First Derivative');

MOVETO(0,100);
LINETO(300,100);
FOR I:=1 TO 30 DO
BEGIN

 MOVETO(I*20,100);
 LINETO(I*20,100+2);
 LINETO(I*20,100-2);
 MOVETO(I*20,100);



END;

 MAXY:=0;
 FOR I:=2 TO NUM_PTS-1 DO
   BEGIN
     IF (ROUND(ABS(D_PTS[I+1,2])) > ROUND(ABS(D_PTS[I,2]))) THEN
             MAXY:=ABS(D_PTS[I+1,2]);
   END;
 R:=90/MAXY;

STR(ROUND(MAXY),SS);
OUTTEXTXY(12,7,SS)    ;



 Y:=0;
FOR I:=1 TO NUM_PTS DO
  BEGIN

    SETCOLOR(BL_COLOR);
    Y:=Slope_D*D_PTS[I,1]+Intercept_D;
    IF I=1 THEN MOVETO(2*ROUND(D_PTS[1,1]),100-ROUND(Y*R));
    IF I=(NUM_PTS) THEN LINETO(2*ROUND(D_PTS[I,1]),100-ROUND(Y*R));
    SETCOLOR(L_COLOR);
 END;


FOR I:=1 TO NUM_PTS DO

 BEGIN
```

```
 SETCOLOR(L_COLOR);
 IF I=1 THEN MOVETO((2*ROUND(D_PTS[1,1])),100-(ROUND(D_PTS[1,2]*R)));
 LINETO(2*ROUND(D_PTS[I,1]),100-(ROUND(D_PTS[I,2]*R)));
 END;
end;

SetViewPort (0,0,GETMAXX, GETMAXY, ClipON);



with vp2 do

begin

Rectangle(Succ(x1), Succ(y1), Pred(x2), Pred(y2));
SetFillStyle(solidFill, VP2_COLOR);
FillPoly(4,Vp2Pts);
SetViewPort(x1, y1, x2, y2, ClipOn);


 MAXY:=0;
 FOR I:=2 TO NUM_PTS-1 DO
   BEGIN
     IF (ROUND(A_PTS[I+1,2]) > ROUND(A_PTS[I,2])) THEN MAXY:=A_PTS[I+1,2];
   END;

STR(ROUND(MAXY),SS);
OUTTEXTXY(12,7,SS)   ;

FOR I:=1 TO NUM_PTS-1 DO

 BEGIN

 SETCOLOR(L_COLOR);


 R:=(90/MAXY);
 IF I=1 THEN MOVETO((2*ROUND(A_PTS[1,1])),100-(ROUND(A_PTS[1,2]*R)));

 LINETO(2*ROUND(A_PTS[I,1]),100-(ROUND(A_PTS[I,2]*R)));

 END;


Y:=0;
 FOR I:=1 TO NUM_PTS-1 DO
  BEGIN

    SETCOLOR(BL_COLOR);


    Y:=Slope_A*A_PTS[I,1]+Intercept_A;
```

```
      IF I=1 THEN MOVETO(2*ROUND(A_PTS[1,1]),100-ROUND(Y*R));
      IF I=(NUM_PTS-1) THEN LINETO(2*ROUND(A_PTS[I,1]),100-ROUND(Y*R));
      SETCOLOR(L_COLOR);
    END;

   MOVETO(0,100);
   LINETO(300,100);
   FOR I:=1 TO 30 DO
   BEGIN
    MOVETO(I*20,100);
    LINETO(I*20,100+2);
    LINETO(I*20,100-2);
    MOVETO(I*20,100);

   END;




   OutTextXY(220,10,'Absorbance');
   end;

  with vp3 do

   begin
       SetFillStyle(solidFill,VP3_COLOR);
       SetColor(L_COLOR);
       Rectangle(Succ(x1),Succ(y1), Pred(x2), Pred(y2));
       FillPoly(4,Vp3Pts);

   SetViewPort(x1, y1, x2, y2, ClipOn);

   OUTTEXTXY(320,25,'Hit any key to continue......');

  end;

   readln;
   CloseGraph
   end { GRAPH_D }
  END;



PROCEDURE MENU1;

  VAR
     CHOICE:CHAR;
     ERFL:BOOLEAN;
```

```
  BEGIN
    REPEAT
      ERFL:=TRUE;
      ClrScr;
      WRITELN('               DOUBLE INTEGRATION PROGRAM');
      WRITELN('                        by');
      WRITELN('                    Robert J. Taylor');
      WRITELN;
      WRITELN;
      WRITELN('                     DATA INPUT MENU');
      WRITELN;
      WRITELN('              (M)   Manual keyboard input');
      WRITELN('              (D)   Disk file input');
      WRITELN;
      WRITE('Enter input device : ');
      READLN(CHOICE);
        CASE CHOICE OF
         'M' : BEGIN
                 ERFL:=FALSE;
                 USER_INPUT;
                 CHECK_DATA;
               END;
         'D' : BEGIN
                 ERFL:=FALSE;
                 READ_DATA;

               END;
        END; {CASE}

      ClrScr;
      IF ERFL THEN WRITELN('That is not a choice! Try again.');

    UNTIL NOT ERFL;

  END; {MENU1}

PROCEDURE MENU2;

  VAR
     CHOICE:CHAR;
     ERFL, QUIT:BOOLEAN;

  BEGIN
    REPEAT
      CLRSCR;
      ERFL:=TRUE;
      QUIT:=FALSE;
      WRITELN('               DOUBLE INTEGRATION PROGRAM');
      WRITELN('                        by');
      WRITELN('                    Robert J. Taylor');
      WRITELN;
      WRITELN;
```

```
 WRITELN('                    MAIN MENU');
 WRITELN; WRITELN;
 WRITELN('          (S)       Store data on disk');
 WRITELN('          (C)       Calculate data');
 WRITELN('          (D)       Enter more data');
 WRITELN('          (G)       Graph data');

 WRITELN('          (E)       Edit Data');
 WRITELN('          (O)       Hard Copy Output');
 WRITELN('          (Q)       Quit');
 WRITELN;
 WRITE('Enter choice : ');
 READLN(CHOICE);
 ClrScr;

CASE CHOICE OF
  'S' : BEGIN
          ERFL:=FALSE;
          STORE_DATA;
        END;

  'C': BEGIN
         ERFL:=FALSE;
         FIRST_INT;
         SECOND_INT;
       END;

  'D':  BEGIN
         ERFL:=FALSE;
         MENU1;
        END;
  'G':  BEGIN
         ERFL:=FALSE;
         GRAPH_D;
        END;

  'E' : BEGIN
         ERFL:=FALSE;
         CHECK_DATA;
        END;

  'O' : BEGIN
         ERFL:=FALSE;
         OUTPUT;
        END;

  'Q' : BEGIN
         ERFL:=FALSE;
         QUIT:=TRUE;
        END;

END; {CASE}
```

```
    IF ERFL THEN WRITELN('Not a choice! Try again.');

   UNTIL QUIT;

 END; {MENU2}

BEGIN


    DONE_CALC:=FALSE;
    MENU1;
    MENU2;

END.
```

APPENDIX C
QUATTRO SPREADSHEETS

This appendix contains three spreadsheets used to interpret the gas adsorption data taken using the successive addition technique discribed in Appendix A. Following each spreadsheet is a listing of the formulas found in each cell of the spreadsheet. The first spreadsheet is one page and allows the dead volume of the sample tube to be determined. The second spreadsheet is much longer and contains data and calculation for argon, nitrogen and oxygen isotherms as well as a plot of equation 4-4 to determine K_{O2}. These two spreadsheets were used in determing the isotherms and equilibrium constants for CsOHCo(CN)-Y and CsClCo(CN)-Y. The final spreadsheet calculates the $\alpha_{O2/N2}$ from the data in second spreadsheet. Consult the listings of the cell contents for details of the calculations. All the equations used in these spreadsheets were determined by manipulating the gas laws.

Absorption Isotherms -- measured using SAT method

RJT4- 220A helium calibration of 3.14g CsClCoCN-Y in sealed tube

Vd Calibration		758.8	488.1	235.7	
		488.1	314.3	235.0	
		314.3	202.3	235.3	
	Vd=	235.3	0.3		
	P1	P2	P3	Vs	
1	0.30	17.69	16.95	10.46	
2	16.95	51.45	49.98	10.47	
3	49.98	129.50	126.10	10.51	
4	126.10	376.10	365.40	10.52	
				10.49	0.03

```
A1: [W9] ^Absorption Isotherms --  measured using SAT method
A3: [W9] ^RJT4-
B3: [W9] '220A
C3: [W9] ^helium calibration of 3.14g CsClCoCN-Y in sealed bulb
A5: [W9] "   Vd Calibration
C5: (F1) [W9] 758.8
D5: (F1) [W9] 488.1
E5: (F1) [W9] (C5/D5-1)*425
C6: (F1) [W9] +D5
D6: (F1) [W9] 314.3
E6: (F1) [W9] (C6/D6-1)*425
C7: (F1) [W9] +D6
D7: (F1) [W9] 202.3
E7: (F1) [W9] (C7/D7-1)*425
B8: [W9] "Vd=
C8: (F1) [W9] @AVG(E5..E7)
D8: (F1) [W9] @STD(E5..E7)
B9: [W9] ^P1
C9: [W9] ^P2
D9: [W9] ^P3
E9: [W9] ^Vs
A10: [W9] 1
B10: (F2) [W9] 0.3
C10: (F2) [W9] 17.69
D10: (F2) [W9] 16.95
E10: (F2) [W9] ((D10-C10)/(B10-D10))*$C$8
F10: [W9] ^
A11: [W9] 2
B11: (F2) [W9] +D10
C11: (F2) [W9] 51.45
D11: (F2) [W9] 49.98
E11: (F2) [W9] ((D11-C11)/(B11-D11))*$C$8
A12: [W9] 3
B12: (F2) [W9] +D11
C12: (F2) [W9] 129.5
D12: (F2) [W9] 126.1
E12: (F2) [W9] ((D12-C12)/(B12-D12))*$C$8
A13: [W9] 4
B13: (F2) [W9] +D12
C13: (F2) [W9] 376.1
D13: (F2) [W9] 365.4
E13: (F2) [W9] ((D13-C13)/(B13-D13))*$C$8
A14: [W9] ^
E14: (F2) [W9] @AVG(E10..E13)
F14: (F2) [W9] @STD(E10..E13)
```

Absorption Isotherm -- measured using SAT method

RJT4-220B ARGON Absorption on CsClCoCN-Y in sealed bulb
wt sample 3.14 g

Vd= 235.2 ml Vs= 10.49 ml
756.7 486.9 235.5
486.9 313.6 234.9

	P1	P2	P3	Na	Na/g	calc. Na/g
			0		0	3.33E-08
1	0.30	5.81	5.46	1.52E-06	4.83E-07	5.87E-07
2	5.46	10.72	10.38	3.04E-06	9.68E-07	1.09E-06
3	10.38	25.19	24.22	7.50E-06	2.39E-06	2.49E-06
4	24.22	55.59	53.49	1.75E-05	5.59E-06	5.46E-06
6	53.49	100.84	97.75	3.17E-05	1.01E-05	9.95E-06
7	97.75	198.1	191.6	6.09E-05	1.94E-05	1.95E-05
8	191.60	315.5	307.4	9.81E-05	3.12E-05	3.12E-05
9	307.40	500.5	487.9	1.56E-04	4.95E-05	4.95E-05
10	487.90	760.4	742.7	2.36E-04	7.51E-05	7.54E-05

Regression Output: for P3 vs Na/g

Constant	3.33E-08
Std Err of Y Est	1.24E-07
R Squared	0.999979
No. of Observations	10
Degrees of Freedom	8
X Coefficient(s)	1.01E-07
Std Err of Coef.	1.65E-10

RJT4-224G NITROGEN Absorption on CsClCoCN-Y in sealed bulb
wt sample 3.14 g

Vd= 234.7 ml Vs= 10.49 ml
752.4 484.8 234.6
484.8 312.3 234.8

	P1	P2	P3	N2 Na	N2 Na/g	calc. NAr/g	N2-Ar	calc AN2
			0		0	3.33E-08		4.95E-08
1	0.28	5.68	5.30	1.97E-06	6.29E-07	5.71E-07	5.78E-08	8.04E-07
2	5.30	10.40	10.02	4.12E-06	1.31E-06	1.05E-06	2.62E-07	1.48E-06
3	10.02	25.29	24.14	1.07E-05	3.41E-06	2.48E-06	9.25E-07	3.49E-06
4	24.14	50.27	48.31	2.19E-05	6.96E-06	4.93E-06	2.03E-06	6.93E-06
6	48.31	100.99	97.13	4.31E-05	1.37E-05	9.89E-06	3.85E-06	1.39E-05
7	97.13	260	247.8	1.12E-04	3.58E-05	2.52E-05	1.06E-05	3.53E-05
8	247.80	503.5	484.6	2.18E-04	6.94E-05	4.92E-05	2.02E-05	6.9E-05
9	484.60	756.5	736.6	3.27E-04	1.04E-04	7.47E-05	2.95E-05	0.000105

Regression Output: for P3 vs Na/g

Constant	4.95E-08
Std Err of Y Est	3.4E-07
R Squared	0.999927
No. of Observations	9
Degrees of Freedom	7
X Coefficient(s)	1.42E-07
Std Err of Coef.	4.59E-10

Evacuated 13 hr at 66 C
RJT4-221E OXYGEN Absorption on CsClCoCN-Y in sealed bulb
wt sample 3.14 g
0.29

Vd= 234.9 ml Vs= 10.49 ml

753.6 484.8 235.6
484.8 312.3 234.8
312.3 201.3 234.4

	P1	P2	P3	O2 Na	O2 Na/g	calc. NAr/g	O2-Ar	AO2/PO2
			0		0	3.33E-08		
1	0.30	10.10	0.57	1.20E-04	3.83E-05	9.12E-08	3.82E-05	6.71E-05
2	0.57	3.76	1.34	1.51E-04	4.79E-05	1.69E-07	4.78E-05	3.57E-05
3	1.34	10.50	8.83	1.67E-04	5.33E-05	9.29E-07	5.24E-05	5.93E-06
4	8.83	25.18	23.95	1.74E-04	5.56E-05	2.46E-06	5.31E-05	2.22E-06
5	23.95	50.98	49.16	1.83E-04	5.84E-05	5.02E-06	5.33E-05	1.09E-06
6	49.16	100.3	96.96	1.99E-04	6.32E-05	9.87E-06	5.34E-05	5.5E-07
7	96.96	214.8	207.2	2.32E-04	7.40E-05	2.10E-05	5.30E-05	2.56E-07
8	207.20	407.7	394.6	2.92E-04	9.31E-05	4.01E-05	5.31E-05	1.35E-07
9	394.60	757.8	733.7	4.06E-04	1.29E-04	7.45E-05	5.48E-05	7.47E-08

Regression Output: for P3 vs Na/g
P>9 torr

Constant	5.3E-05
Std Err of Y Est	4.75E-07
R Squared	0.999774
No. of Observations	6
Degrees of Freedom	4
X Coefficient(s)	1.04E-07
Std Err of Coef.	7.79E-10

CsClCoCN-Y Summation of data and Keq calculation

PO2	AO2	calc AAr	calc AN2	calc AO2	AO2-AAr	ACoO2/PO2	calc ACoO2
0	0	3.33E-08	4.95E-08				
0.57	3.83E-05	9.12E-08	1.31E-07		3.82E-05	6.71E-05	3.92E-05
1.34	4.79E-05	1.69E-07	2.4E-07		4.78E-05	3.57E-05	4.61E-05
8.83	5.33E-05	9.29E-07	1.31E-06	5.39E-05	5.24E-05	5.93E-06	5.25E-05
23.95	5.56E-05	2.46E-06	3.46E-06	5.55E-05	5.31E-05	2.22E-06	5.33E-05
49.16	5.84E-05	5.02E-06	7.05E-06	5.81E-05	5.33E-05	1.09E-06	5.36E-05
96.96	6.32E-05	9.87E-06	1.39E-05	6.31E-05	5.34E-05	5.5E-07	5.37E-05
207.2	7.4E-05	2.1E-05	2.96E-05	7.45E-05	5.3E-05	2.56E-07	5.38E-05
394.6	9.31E-05	4.01E-05	5.62E-05	9.39E-05	5.31E-05	1.35E-07	5.38E-05
733.7	0.000129	7.45E-05	0.000105	0.000129	5.48E-05	7.47E-08	5.38E-05

Regression Output: for ACoO2/PO2 vs ACoO2

Constant	5.38E-05	
Std Err of Y Est	9.6E-07	
R Squared	0.970117	
No. of Observations	9	
Degrees of Freedom	7	
	P1/2	
X Coefficient(s)	-0.21804	4.586419 torr

```
                          Std Err of Coef.  0.014464 0.304248 torr
 A1: [W5] ^Absorption Isotherm -- measured using SAT method
 A3: [W5] "RJT4-
 B3: [W8] '220B
 C3: [W9] ^ARGON Absorption on CsClCoCN-Y in sealed bulb
 C4: [W9] ^wt sample=
 D4: (F2) [W9] 3.14
 E4: [W9] 'g
 A5: [W5] ^
 B5: [W8] ^
 B6: [W8] ^
 C6: [W9] "Vd=
 D6: (F1) [W9] @AVG(F7..F8)
 E6: [W9] 'ml
 F6: [W9] "Vs=
 G6: [W9] 10.49
 H6: [W9] 'ml
 D7: [W9] 756.7
 E7: [W9] 486.9
 F7: (F1) [W9] (((D7-$B$5)/(E7-$B$5))-1)*425
 D8: [W9] +E7
 E8: [W9] 313.6
 F8: (F1) [W9] (((D8-$B$5)/(E8-$B$5))-1)*425
 D9: [W9] ^
 E9: [W9] ^
 F9: (F1) [W9] ^
 G9: [W9] ^calc.
B10: [W8] ^P1
C10: [W9] ^P2
D10: [W9] ^P3
E10: [W9] ^Na
F10: [W9] ^Na/g
G10: [W9] ^Na/g
D11: [W9] 0
F11: [W9] 0
G11: [W9] +D11*$F$28+$G$22
A12: [W5] 1
B12: (F2) [W8] 0.3
C12: (F2) [W9] 5.81
D12: (F2) [W9] 5.46
E12: (S3) [W9] ((B12-D12)*$G$6+(C12-D12)*$D$6)/(62396*298)
F12: (S3) [W9] +E12/$D$4
G12: (S3) [W9] +D12*$F$28+$G$22
A13: [W5] 2
B13: (F2) [W8] +D12
C13: (F2) [W9] 10.72
D13: (F2) [W9] 10.38
E13: (S3) [W9] ((B13-D13)*$G$6+(C13-D13)*$D$6)/(62396*298)+E12
F13: (S3) [W9] +E13/$D$4
G13: (S3) [W9] +D13*$F$28+$G$22
A14: [W5] 3
B14: (F2) [W8] +D13
```

```
C14: (F2) [W9] 25.19
D14: (F2) [W9] 24.22
E14: (S3) [W9] ((B14-D14)*$G$6+(C14-D14)*$D$6)/(62396*298)+E13
F14: (S3) [W9] +E14/$D$4
G14: (S3) [W9] +D14*$F$28+$G$22
A15: [W5] 4
B15: (F2) [W8] +D14
C15: [W9] 55.59
D15: [W9] 53.49
E15: (S3) [W9] ((B15-D15)*$G$6+(C15-D15)*$D$6)/(62396*298)+E14
F15: (S3) [W9] +E15/$D$4
G15: (S3) [W9] +D15*$F$28+$G$22
A16: [W5] 6
B16: (F2) [W8] +D15
C16: [W9] 100.84
D16: [W9] 97.75
E16: (S3) [W9] ((B16-D16)*$G$6+(C16-D16)*$D$6)/(62396*298)+E15
F16: (S3) [W9] +E16/$D$4
G16: (S3) [W9] +D16*$F$28+$G$22
A17: [W5] 7
B17: (F2) [W8] +D16
C17: [W9] 198.1
D17: [W9] 191.6
E17: (S3) [W9] ((B17-D17)*$G$6+(C17-D17)*$D$6)/(62396*298)+E16
F17: (S3) [W9] +E17/$D$4
G17: (S3) [W9] +D17*$F$28+$G$22
A18: [W5] 8
B18: (F2) [W8] +D17
C18: [W9] 315.5
D18: [W9] 307.4
E18: (S3) [W9] ((B18-D18)*$G$6+(C18-D18)*$D$6)/(62396*298)+E17
F18: (S3) [W9] +E18/$D$4
G18: (S3) [W9] +D18*$F$28+$G$22
A19: [W5] 9
B19: (F2) [W8] +D18
C19: [W9] 500.5
D19: [W9] 487.9
E19: (S3) [W9] ((B19-D19)*$G$6+(C19-D19)*$D$6)/(62396*298)+E18
F19: (S3) [W9] +E19/$D$4
G19: (S3) [W9] +D19*$F$28+$G$22
A20: [W5] 10
B20: (F2) [W8] +D19
C20: [W9] 760.4
D20: [W9] 742.7
E20: (S3) [W9] ((B20-D20)*$G$6+(C20-D20)*$D$6)/(62396*298)+E19
F20: (S3) [W9] +E20/$D$4
G20: (S3) [W9] +D20*$F$28+$G$22
E21: [W9] ^Regression Output:
D22: [W9] ^Constant
G22: [W9] 3.333788867957E-08
D23: [W9] ^Std Err of Y Est
G23: [W9] 1.239361890214E-07
```

```
D24: [W9] ^R Squared
G24: [W9] 0.9999788609205
D25: [W9] ^No. of Observations
G25: [W9] 10
D26: [W9] ^Degrees of Freedom
G26: [W9] 8
D28: [W9] ^X Coefficient(s)
F28: (S3) [W9] 1.014302591879E-07
D29: [W9] ^Std Err of Coef.
F29: [W9] 1.648808311813E-10
A31: [W5] ^
C32: [W9] ^
A33: [W5] "RJT4-
B33: [W8] '224G
C33: [W9] ^NITROGEN Absorption on CsClCoCN-Y in sealed bulb
C34: [W9] ^wt sample=
D34: (F2) [W9] 3.14
E34: [W9] 'g
A35: [W5] ^
B35: [W8] ^
B36: [W8] ^
C36: [W9] "Vd=
D36: (F1) [W9] @AVG(F37..F38)
E36: [W9] 'ml
F36: [W9] "Vs=
G36: [W9] 10.49
H36: [W9] 'ml
D37: [W9] 752.4
E37: [W9] 484.8
F37: (F1) [W9] (((D37-$B$5)/(E37-$B$5))-1)*425
D38: [W9] +E37
E38: [W9] 312.3
F38: (F1) [W9] (((D38-$B$5)/(E38-$B$5))-1)*425
D39: [W9] ^
E39: [W9] ^
F39: (F1) [W9] ^
D40: [W9] ^
E40: [W9] ^N2
F40: (F1) [W9] ^N2
G40: [W9] ^calc.
I40: [W9] ^calc
B41: [W8] ^P1
C41: [W9] ^P2
D41: [W9] ^P3
E41: [W9] ^Na
F41: [W9] ^Na/g
G41: [W9] ^NAr/g
H41: [W9] ^N2-Ar
I41: [W9] ^AN2
D42: [W9] 0
F42: [W9] 0
G42: [W9] +D42*$F$28+$G$22
```

```
H42: (S3) [W9] ^
I42: [W9] +D42*$G$58+$H$52
A43: [W5] 1
B43: (F2) [W8] 0.28
C43: (F2) [W9] 5.68
D43: (F2) [W9] 5.3
E43: (S3) [W9] ((B43-D43)*$G$36+(C43-D43)*$D$6)/(62396*298)
F43: (S3) [W9] +E43/$D$4
G43: (S3) [W9] +D43*$F$28+$G$22
H43: (S3) [W9] +F43-G43
I43: [W9] +D43*$G$58+$H$52
A44: [W5] 2
B44: (F2) [W8] +D43
C44: (F2) [W9] 10.4
D44: (F2) [W9] 10.02
E44: (S3) [W9] ((B44-D44)*$G$36+(C44-D44)*$D$6)/(62396*298)+E43
F44: (S3) [W9] +E44/$D$4
G44: (S3) [W9] +D44*$F$28+$G$22
H44: (S3) [W9] +F44-G44
I44: [W9] +D44*$G$58+$H$52
A45: [W5] 3
B45: (F2) [W8] +D44
C45: (F2) [W9] 25.29
D45: (F2) [W9] 24.14
E45: (S3) [W9] ((B45-D45)*$G$36+(C45-D45)*$D$6)/(62396*298)+E44
F45: (S3) [W9] +E45/$D$4
G45: (S3) [W9] +D45*$F$28+$G$22
H45: (S3) [W9] +F45-G45
I45: [W9] +D45*$G$58+$H$52
A46: [W5] 4
B46: (F2) [W8] +D45
C46: [W9] 50.27
D46: [W9] 48.31
E46: (S3) [W9] ((B46-D46)*$G$36+(C46-D46)*$D$6)/(62396*298)+E45
F46: (S3) [W9] +E46/$D$4
G46: (S3) [W9] +D46*$F$28+$G$22
H46: (S3) [W9] +F46-G46
I46: [W9] +D46*$G$58+$H$52
A47: [W5] 6
B47: (F2) [W8] +D46
C47: [W9] 100.99
D47: [W9] 97.13
E47: (S3) [W9] ((B47-D47)*$G$36+(C47-D47)*$D$6)/(62396*298)+E46
F47: (S3) [W9] +E47/$D$4
G47: (S3) [W9] +D47*$F$28+$G$22
H47: (S3) [W9] +F47-G47
I47: [W9] +D47*$G$58+$H$52
A48: [W5] 7
B48: (F2) [W8] +D47
C48: [W9] 260
D48: [W9] 247.8
E48: (S3) [W9] ((B48-D48)*$G$36+(C48-D48)*$D$6)/(62396*298)+E47
```

```
F48: (S3) [W9] +E48/$D$4
G48: (S3) [W9] +D48*$F$28+$G$22
H48: (S3) [W9] +F48-G48
I48: [W9] +D48*$G$58+$H$52
A49: [W5] 8
B49: (F2) [W8] +D48
C49: [W9] 503.5
D49: [W9] 484.6
E49: (S3) [W9] ((B49-D49)*$G$36+(C49-D49)*$D$6)/(62396*298)+E48
F49: (S3) [W9] +E49/$D$4
G49: (S3) [W9] +D49*$F$28+$G$22
H49: (S3) [W9] +F49-G49
I49: [W9] +D49*$G$58+$H$52
A50: [W5] 9
B50: (F2) [W8] +D49
C50: [W9] 756.5
D50: [W9] 736.6
E50: (S3) [W9] ((B50-D50)*$G$36+(C50-D50)*$D$6)/(62396*298)+E49
F50: (S3) [W9] +E50/$D$4
G50: (S3) [W9] +D50*$F$28+$G$22
H50: (S3) [W9] +F50-G50
I50: [W9] +D50*$G$58+$H$52
F51: [W9] ^Regression Output:
H51: [W9] ^
E52: [W9] ^Constant
H52: [W9] 4.951349856248E-08
E53: [W9] ^Std Err of Y Est
H53: [W9] 3.398538962539E-07
E54: [W9] ^R Squared
H54: [W9] 0.999927140717
E55: [W9] ^No. of Observations
H55: [W9] 9
E56: [W9] ^Degrees of Freedom
H56: [W9] 7
E58: [W9] ^X Coefficient(s)
G58: [W9] 1.423779808512E-07
C59: [W9] ^
D59: [W9] ^
E59: [W9] ^Std Err of Coef.
G59: [W9] 4.593588393587E-10
C60: [W9] ^
D60: [W9] ^
C61: [W9] ^
D61: [W9] ^
C62: [W9] ^Evacuated 13 hr at 66 C
A63: [W5] "RJT4-
B63: [W8] '221E
C63: [W9] ^OXYGEN Absorption on CsClCoCN-Y in sealed bulb
C64: [W9] ^wt sample=
D64: (F2) [W9] 3.14
E64: [W9] 'g
A65: [W5] ^
```

```
B65: [W8] 0.29
B66: [W8] ^
C66: [W9] "Vd=
D66: (F1) [W9] @AVG(F67..F69)
E66: [W9] 'ml
F66: [W9] "Vs=
G66: [W9] 10.49
H66: [W9] 'ml
D67: [W9] 753.6
E67: [W9] 484.8
F67: (F1) [W9] (((D67-$B$5)/(E67-$B$5))-1)*425
D68: [W9] +E67
E68: [W9] 312.3
F68: (F1) [W9] (((D68-$B$5)/(E68-$B$5))-1)*425
D69: [W9] +E68
E69: [W9] 201.3
F69: (F1) [W9] (((D69-$B$5)/(E69-$B$5))-1)*425
D70: [W9] ^
E70: [W9] ^O2
F70: (F1) [W9] ^O2
G70: [W9] ^calc.
B71: [W8] ^P1
C71: [W9] ^P2
D71: [W9] ^P3
E71: [W9] ^Na
F71: [W9] ^Na/g
G71: [W9] ^NAr/g
H71: [W9] ^O2-Ar
D72: [W9] 0
F72: [W9] 0
G72: [W9] +D72*$F$28+$G$22
H72: (S3) [W9] ^
I72: [W9] ^AO2/PO2
A73: [W5] 1
B73: (F2) [W8] 0.3
C73: (F2) [W9] 10.1
D73: (F2) [W9] 0.57
E73: (S3) [W9] ((B73-D73)*$G$6+(C73-D73)*$D$6)/(62396*298)
F73: (S3) [W9] +E73/$D$4
G73: (S3) [W9] +D73*$F$28+$G$22
H73: (S3) [W9] +F73-G73
I73: [W9] +H73/D73
A74: [W5] 2
B74: (F2) [W8] +D73
C74: (F2) [W9] 3.76
D74: (F2) [W9] 1.34
E74: (S3) [W9] ((B74-D74)*$G$6+(C74-D74)*$D$6)/(62396*298)+E73
F74: (S3) [W9] +E74/$D$4
G74: (S3) [W9] +D74*$F$28+$G$22
H74: (S3) [W9] +F74-G74
I74: [W9] +H74/D74
A75: [W5] 3
```

```
B75: (F2) [W8] +D74
C75: (F2) [W9] 10.5
D75: (F2) [W9] 8.83
E75: (S3) [W9] ((B75-D75)*$G$6+(C75-D75)*$D$6)/(62396*298)+E74
F75: (S3) [W9] +E75/$D$4
G75: (S3) [W9] +D75*$F$28+$G$22
H75: (S3) [W9] +F75-G75
I75: [W9] +H75/D75
A76: [W5] 4
B76: (F2) [W8] +D75
C76: [W9] 25.18
D76: [W9] 23.95
E76: (S3) [W9] ((B76-D76)*$G$6+(C76-D76)*$D$6)/(62396*298)+E75
F76: (S3) [W9] +E76/$D$4
G76: (S3) [W9] +D76*$F$28+$G$22
H76: (S3) [W9] +F76-G76
I76: [W9] +H76/D76
A77: [W5] 5
B77: (F2) [W8] +D76
C77: [W9] 50.98
D77: [W9] 49.16
E77: (S3) [W9] ((B77-D77)*$G$6+(C77-D77)*$D$6)/(62396*298)+E76
F77: (S3) [W9] +E77/$D$4
G77: (S3) [W9] +D77*$F$28+$G$22
H77: (S3) [W9] +F77-G77
I77: [W9] +H77/D77
A78: [W5] 6
B78: (F2) [W8] +D77
C78: [W9] 100.3
D78: [W9] 96.96
E78: (S3) [W9] ((B78-D78)*$G$6+(C78-D78)*$D$6)/(62396*298)+E77
F78: (S3) [W9] +E78/$D$4
G78: (S3) [W9] +D78*$F$28+$G$22
H78: (S3) [W9] +F78-G78
I78: [W9] +H78/D78
A79: [W5] 7
B79: (F2) [W8] +D78
C79: [W9] 214.8
D79: [W9] 207.2
E79: (S3) [W9] ((B79-D79)*$G$6+(C79-D79)*$D$6)/(62396*298)+E78
F79: (S3) [W9] +E79/$D$4
G79: (S3) [W9] +D79*$F$28+$G$22
H79: (S3) [W9] +F79-G79
I79: [W9] +H79/D79
A80: [W5] 8
B80: (F2) [W8] +D79
C80: [W9] 407.7
D80: [W9] 394.6
E80: (S3) [W9] ((B80-D80)*$G$6+(C80-D80)*$D$6)/(62396*298)+E79
F80: (S3) [W9] +E80/$D$4
G80: (S3) [W9] +D80*$F$28+$G$22
H80: (S3) [W9] +F80-G80
```

```
I80: [W9] +H80/D80
A81: [W5] 9
B81: (F2) [W8] +D80
C81: [W9] 757.8
D81: [W9] 733.7
E81: (S3) [W9] ((B81-D81)*$G$6+(C81-D81)*$D$6)/(62396*298)+E80
F81: (S3) [W9] +E81/$D$4
G81: (S3) [W9] +D81*$F$28+$G$22
H81: (S3) [W9] +F81-G81
I81: [W9] +H81/D81
C82: [W9] ^
D82: [W9] ^
F82: [W9] ^Regression Output:
H82: [W9] ^P>9 torr
E83: [W9] ^Constant
H83: [W9] 5.30239352694E-05
E84: [W9] ^Std Err of Y Est
H84: [W9] 4.745683111406E-07
E85: [W9] ^R Squared
H85: [W9] 0.9997744175345
E86: [W9] ^No. of Observations
H86: [W9] 6
E87: [W9] ^Degrees of Freedom
H87: [W9] 4
E89: [W9] ^X Coefficient(s)
G89: [W9] 1.036606010652E-07
E90: [W9] ^Std Err of Coef.
G90: [W9] 7.785479880493E-10
C91: [W9] ^
D91: [W9] ^
A93: [W5] ^CsClCoCN-Y
D94: [W9] ^calc
E94: [W9] ^calc
F94: [W9] ^calc
I94: [W9] ^calc
B95: [W8] ^PO2
C95: [W9] ^AO2
D95: [W9] ^AAr
E95: [W9] ^AN2
F95: [W9] ^AO2
G95: [W9] ^AO2-AAr
H95: [W9] ^ACoO2/PO2
I95: [W9] ^ACoO2
B96: [W8] +D72
C96: [W9] +F72
D96: [W9] +B96*$F$28+$G$22
E96: [W9] +B96*$G$58+$H$52
B97: [W8] +D73
C97: [W9] +F73
D97: [W9] +B97*$F$28+$G$22
E97: [W9] +B97*$G$58+$H$52
G97: [W9] +C97-D97
```

```
H97: [W9] +G97/B97
I97: [W9] +H97*$F$113+$G$107
B98: [W8] +D74
C98: [W9] +F74
D98: [W9] +B98*$F$28+$G$22
E98: [W9] +B98*$G$58+$H$52
G98: [W9] +C98-D98
H98: [W9] +G98/B98
I98: [W9] +H98*$F$113+$G$107
B99: [W8] +D75
C99: [W9] +F75
D99: [W9] +B99*$F$28+$G$22
E99: [W9] +B99*$G$58+$H$52
F99: [W9] +B99*$G$89+$H$83
G99: [W9] +C99-D99
H99: [W9] +G99/B99
I99: [W9] +H99*$F$113+$G$107
B100: [W8] +D76
C100: [W9] +F76
D100: [W9] +B100*$F$28+$G$22
E100: [W9] +B100*$G$58+$H$52
F100: [W9] +B100*$G$89+$H$83
G100: [W9] +C100-D100
H100: [W9] +G100/B100
I100: [W9] +H100*$F$113+$G$107
B101: [W8] +D77
C101: [W9] +F77
D101: [W9] +B101*$F$28+$G$22
E101: [W9] +B101*$G$58+$H$52
F101: [W9] +B101*$G$89+$H$83
G101: [W9] +C101-D101
H101: [W9] +G101/B101
I101: [W9] +H101*$F$113+$G$107
B102: [W8] +D78
C102: [W9] +F78
D102: [W9] +B102*$F$28+$G$22
E102: [W9] +B102*$G$58+$H$52
F102: [W9] +B102*$G$89+$H$83
G102: [W9] +C102-D102
H102: [W9] +G102/B102
I102: [W9] +H102*$F$113+$G$107
B103: [W8] +D79
C103: [W9] +F79
D103: [W9] +B103*$F$28+$G$22
E103: [W9] +B103*$G$58+$H$52
F103: [W9] +B103*$G$89+$H$83
G103: [W9] +C103-D103
H103: [W9] +G103/B103
I103: [W9] +H103*$F$113+$G$107
B104: [W8] +D80
C104: [W9] +F80
D104: [W9] +B104*$F$28+$G$22
```

```
E104: [W9] +B104*$G$ 3+$H$52
F104: [W9] +B104*$G$89+$H$83
G104: [W9] +C104-D104
H104: [W9] +G104/B104
I104: [W9] +H104*$F$113+$G$107
B105: [W8] +D81
C105: [W9] +F81
D105: [W9] +B105*$F$28+$G$22
E105: [W9] +B105*$G$58+$H$52
F105: [W9] +B105*$G$89+$H$83
G105: [W9] +C105-D105
H105: [W9] +G105/B105
I105: [W9] +H105*$F$113+$G$107
B106: [W8] ^
E106: [W9] ^Regression Output:
B107: [W8] ^
D107: [W9] ^Constant
G107: [W9] 5.383300719008E-05
D108: [W9] ^Std Err of Y Est
G108: [W9] 9.597840796309E-07
D109: [W9] ^R Squared
G109: [W9] 0.970116543939
D110: [W9] ^No. of Observations
G110: [W9] 9
D111: [W9] ^Degrees of Freedom
G111: [W9] 7
G112: [W9] ^P1/2
D113: [W9] ^X Coefficient(s)
F113: [W9] -0.2180350422158
G113: [W9] @ABS(1/F113)
H113: [W9] 'torr
D114: [W9] ^Std Err of Coef.
F114: [W9] 0.0144637442585
G114: [W9] @ABS(F114/F113*G113)
H114: [W9] 'torr
```

P1	ntO2	sep. fact	P2O2	P2N2
10.2	0.000128	5022.135	0.567683	9.74905
13.4	0.000168	1907.681	1.334553	12.80133
22.6	0.000283	98.65695	8.794106	21.32833
38.9	0.000488	24.4792	23.85264	36.46968
65.9	0.000826	10.36709	48.96016	61.49194
116.9	0.001467	5.127912	96.56585	108.8287
234.6	0.002943	2.638045	206.3577	217.9007
434.7	0.005454	1.695941	392.9959	403.4898
797.3	0.010004	1.249117	730.7175	739.6959

```
A86: [W9] ^P1
B86: [W9] ^ntO2
C86: [W9] ^sep. fact.
D86: [W9] ^P2O2
E86: [W9] ^P2N2
A87: (F1) [W9] +B87*0.08215*300/0.235*760
B87: [W9] +B74/760*0.245/(0.08215*300)+C74*3.14
C87: [W9] (C74*3.14*(B87-E74*3.14))/(E74*3.14*(B87-C74*3.14))
D87: [W9] (B87-C74*3.14)*0.08215*300/0.246*760
E87: [W9] (B87-E74*3.14)*0.08215*300/0.245*760
A88: (F1) [W9] +B88*0.08215*300/0.235*760
B88: [W9] +B75/760*0.245/(0.08215*300)+C75*3.14
C88: [W9] (C75*3.14*(B88-E75*3.14))/(E75*3.14*(B88-C75*3.14))
D88: [W9] (B88-C75*3.14)*0.08215*300/0.246*760
E88: [W9] (B88-E75*3.14)*0.08215*300/0.245*760
A89: (F1) [W9] +B89*0.08215*300/0.235*760
B89: [W9] +B76/760*0.245/(0.08215*300)+C76*3.14
C89: [W9] (C76*3.14*(B89-E76*3.14))/(E76*3.14*(B89-C76*3.14))
D89: [W9] (B89-C76*3.14)*0.08215*300/0.246*760
E89: [W9] (B89-E76*3.14)*0.08215*300/0.245*760
A90: (F1) [W9] +B90*0.08215*300/0.235*760
B90: [W9] +B77/760*0.245/(0.08215*300)+C77*3.14
C90: [W9] (C77*3.14*(B90-E77*3.14))/(E77*3.14*(B90-C77*3.14))
D90: [W9] (B90-C77*3.14)*0.08215*300/0.246*760
E90: [W9] (B90-E77*3.14)*0.08215*300/0.245*760
A91: (F1) [W9] +B91*0.08215*300/0.235*760
B91: [W9] +B78/760*0.245/(0.08215*300)+C78*3.14
C91: [W9] (C78*3.14*(B91-E78*3.14))/(E78*3.14*(B91-C78*3.14))
D91: [W9] (B91-C78*3.14)*0.08215*300/0.246*760
E91: [W9] (B91-E78*3.14)*0.08215*300/0.245*760
A92: (F1) [W9] +B92*0.08215*300/0.235*760
B92: [W9] +B79/760*0.245/(0.08215*300)+C79*3.14
C92: [W9] (C79*3.14*(B92-E79*3.14))/(E79*3.14*(B92-C79*3.14))
D92: [W9] (B92-C79*3.14)*0.08215*300/0.246*760
E92: [W9] (B92-E79*3.14)*0.08215*300/0.245*760
A93: (F1) [W9] +B93*0.08215*300/0.235*760
B93: [W9] +B80/760*0.245/(0.08215*300)+C80*3.14
C93: [W9] (C80*3.14*(B93-E80*3.14))/(E80*3.14*(B93-C80*3.14))
D93: [W9] (B93-C80*3.14)*0.08215*300/0.246*760
E93: [W9] (B93-E80*3.14)*0.08215*300/0.245*760
A94: (F1) [W9] +B94*0.08215*300/0.235*760
B94: [W9] +B81/760*0.245/(0.08215*300)+C81*3.14
C94: [W9] (C81*3.14*(B94-E81*3.14))/(E81*3.14*(B94-C81*3.14))
D94: [W9] (B94-C81*3.14)*0.08215*300/0.246*760
E94: [W9] (B94-E81*3.14)*0.08215*300/0.245*760
A95: (F1) [W9] +B95*0.08215*300/0.235*760
B95: [W9] +B82/760*0.245/(0.08215*300)+C82*3.14
C95: [W9] (C82*3.14*(B95-E82*3.14))/(E82*3.14*(B95-C82*3.14))
D95: [W9] (B95-C82*3.14)*0.08215*300/0.246*760
E95: [W9] (B95-E82*3.14)*0.08215*300/0.245*760
```

REFERENCES

1. Yang, R. T. Gas Separations by Adsorption Processes, Buterworths; Boston, 1988.

2. Breck, D. W. Zeolite Molecular Sieves, John Wiley; New York, 1974.

3. Konnert, J.; D'Antonio, P. Carbon 1983, 21, 193.

4. Keller, G. E. In Industrial Gas Separations, Whyte, Jr., T. E.; Yon, C. M.; Wagner, E. H., Eds.; ACS Symposium Series 223, American Chemical Society; Washington, DC. 1983; p 145.

5. Heylin, M., Ed. Chem. Eng. News 1984, 67, 39.

6. Grayson, M., Ed. Kirk-Othmer Encyclopedia of Chemical Technology, 3rd ed., Wiley; New York, 1977, Vol. 16, p. 653.

7. Hands, B. A. Cryogenic Engineering, Academic; London, 1986.

8. Mears, P. Membrane Separation Processes, Elsevier Scientific; Amsterdam, 1976.

9. Whyte, Jr., T. E.; Yon, C. M.; Wagner, E. H., Eds. Industrial Gas Separations, ACS Symposium Series 223; American Chemical Society; Washington DC, 1983.

10. Kawaski, T. Sep. Sci. Tech. 1988, 24, 451.

11. Lunsford, J. H. In Molecular Sieves - II, Katzer, J. R., Ed.; ACS Symposium Series 40, American Chemical Society; Washington DC, 1977, p 473.

12. Lunsford, J. H. Rev. Inorg. Chem. 1987, 9, 1.

13. Klier, K. Langmuir 1988, 4, 136.

14. Seff, J. Acc. Chem. Res. 1976, 9, 121.

15. Lunsford, J. H. Cat. Rev. 1975, 12, 137.

16. Kellerman, R.; Klier, K. In Surface and Defect Properties of Solids, Blow, J., Ed., Burlington House; London, Vol. 4, p 1.

17. Mikheikin, I. D.; Zhidomirov, G. M.; Kazanski, V. B. Russ. Chem. Rev. 1972, 41, 468.

18. Howe, R. F.; Lunsford, J. H. J. Am. Chem. Soc. 1975, 97, 5156.

19. Herron, N. Inorg. Chem. 1986, 25, 4714.

20. Michalik, J.; Narayana, M.; Kevan, L. J. Phys. Chem. 1984, 88, 5236.

21. Howe, R. F.; Lunsford, J. H. J. Phys. Chem. 1975, 79, 1836.

22. Vansant, E. F.; Lunsford, J. H. J. Chem. Soc., Faraday Trans 1973, 69, 1028.

23. Mizumo, K.; Imamura, S.; Lunsford, J. H. Inorg. Chem. 1984, 23, 3510.

24. Niederhoffer, E. C.; Timmons, J. H.; Martell, A. E. Chem. Rev. 1984, 84, 137.

25. Jones, R. D.; Summerville, D. A.; Basolo, F. Chem. Rev. 1979, 79, 139.

26. Imamura, S.; Lunsford, J. H. Langmuir 1985, 1, 326.

27. Sharpe, A. G. The Chemistry of Cyano Complexes of the Transition Metals 1976, Academic; London, Chap. 8, and references therein.

28. Kwiatek, K. Catal. Rev. 1967, 1, 37.

29. Bayston, J. H.; Looney, F. D.; Winfield, M. E.; Aust. J. Chem. 1963, 16, 557.

30. Adamson, A. W. J. Am. Chem. Soc. 1951, 73, 5710.

31. White, D. A.; Solodar, A. J.; Balzer, M. M. Inorg. Chem. 1972, 11.

32. Brown, L. D.; Raymond, K. N. Inorg. Chem. 1975, 14, 2590.

33. Brown, L. D.; Raymond, K. N. Inorg. Chem. 1975, 14, 2595.

34. Carter, S. J.; Foxman, B. M.; Stuhl, L. S. J. Am. Chem. Soc. 1984, 106, 4265.

35. Carter, S. J.; Foxman, B. M.; Stuhl, L. S. Inorg. Chem. 1986, 25, 2888.

36. DeVries, B. J. Cat. 1962, 1, 489.

37. King, N. K.; Winfield, M. E. J. Amer. Chem. Soc. 1961, 83, 3363.

38. Belford, R. L.; Nilges, M. J. Computer Simulation of Powder Spectra, EPR Symposium, 21st Rocky Mountain Conference, Denver, Colorado, 1979.

39. Wertz, J. E.; Bolton, J. R. Electron Resonance Spectroscopy 1972, McGraw-Hill; New York.

40. Drago, R. S.; Bresinska, I.; George, J. E.; Balkus, Jr., K. J.; Taylor, R. J. J. Am. Chem. Soc. 1988, 110, 304.

41. Taylor, R. J.; Drago, R. S.; George, J. E. J. Am. Chem. Soc. 1989, 111, 6610.

42. Gutman, V. The Donor Acceptor Approach to Molecular Interactions 1978, Plenum Press; New York.

43. Jones, J. H. J. Chem. Phys. 1962, 36, 1204.

44. Jones, J. H.; Memering, M. N.; Swanson, B. I. J. Chem. Phys. 1971, 54, 4666.

45. Swanson, B. I.; Jones, J. H. J. Chem. Phys. 1970, 53, 3761.

46. Banks, R. G. S.; Pratt, J. M. Chem. Comm. 1967, 776.

47. Shriver, D. F.; Brown, D. B. Inorg. Chem. 1969, 8, 42.

48. Simon, G. L.; Adamson, A. W.; Dohl, L.F. J. Am. Chem. Soc. 1972, 94, 7654.

49. Haim, A.; Wilmarth, W. K. J. Am. Chem. Soc. 1961, 83, 509.

50. Vansant, E. F.; Lunsford, J. H. Adv. Chem. Ser. 1973, 121, 441.

51. Drago, R. S.; Corden, B. B. Acc. Chem. Res. 1980, 13, 353.

52. Torrog, D. S.; Kitho D. S.; Drago, R. S. J. Am. Chem. Soc. 1976, 98, 5144.

53. Alexander, J. J.; Gray, H. B. J. Am. Chem. Soc. 1967, 89, 3356.

54. Nakamoto, K., Infrared Spectra of Inorganic and Coordination Compounds, 2nd ed., 1970, John Wiley; New York, p. 178.

55. Halpern, J.; Pribanic, M. Inorg. Chem. 1970, 9, 2616.

56. Banks, R. G. S.; Pratt, J. M. J. Chem. Soc. (A) 1968, 854.

57. Griffith, W. P.; Wilkinson, G. J. Chem. Soc. 1959, 2757.

58. Roberts, H. L.; Symes, W. R. J. Chem. Soc. (A) 1968, 1450.

59. Bayston, J. H.; Winfield, M. E. J. Cat. 1964, 3, 123.

60. Pratt, J. M.; Williams, R. J. P. J. Chem. Soc. (A) 1967, 1291.

61. King, N. K.; Winfield, M. E. J. Amer. Chem. Soc. 1958, 80, 2060.

62. Wayland, B. B.; Adb-Elmageed, M. E. J. Amer. Chem. Soc. 1974, 96, 4809.

63. Booth, R. J.; Lin, W. C. J. Chem. Phys. 1974, 61, 1226.

64. Cockle, J. A. Chem. Comm. 1973, 905.

65. Ochiai, E. I. J. Inorg. Nucl. Chem. 1973, 35, 1727.

66. Tauzher, G.; Amiconi, G.; Antonini, E.; Brunori, M.; Costa, G. Nature (London) 1973, 241, 222.

67. Tauzher, G.; Amiconi, G.; Antonini, E.; Brunori, M.; Costa, G. Nature (London) 1970, 228, 549.

68. Collman, J. P.; Brauman, J. I.; Doxdee, K. M.; Halbert, T. R.; Suslick, K. J. Proc. Natl. Acad. Sci. U.S.A. 1978, 75, 564.

69. Walker, F. A. J. Am. Chem. Soc. 1973, 95, 1154.

BIOGRAPHICAL SKETCH

Robert Joel Taylor, Jr., was born in Panama City, Florida, on November 12, 1963. He attended Rutherford High School where he was active in football and baseball before he graduated in June 1981. In the fall of that year he enrolled at Gulf Coast Community College, also in Panama City, where he studied for two years. While at GCCC he worked as a co-op student at the Naval Coastal Systems Center as an engineering aid and gas analysis technician, where he conducted research with Al Purer and was co-author on two publications. In 1983 he was honored as the Co-op Student of the Year for his work at the NCSC. In the fall of 1983 he transferred to the University of West Florida in Pensacola, Florida, to study chemistry. While at UWF he worked as an NMR technician for the Chemistry Department and spent summers working as a lab technician for the Arizona Chemical Company. In May 1985 he graduated magna cum laude and was awarded the Monsanto Award in Chemistry and the Outstanding Student Award at UWF.

In August 1985, he continued his study of chemistry at the University of Florida under the leadership of Professor Russell Drago. While at UF, he has presented papers at the

Florida Catalysis Conference, the Florida Advanced Materials Conference, and regional and nation ACS meetings. Upon receiving the degree of Doctor of Philosophy, he will begin his career with Texaco Research at the Port Arthur Research Labs in Port Arthur, Texas.

I certify that I have read this study and that in my opinion it conforms to acceptable standards of scholarly presentation and is fully adequate, in scope and quality, as a dissertation for the degree of Doctor of Philosophy.

Russell S. Drago, Chair
Graduate Research Professor
of Chemistry

I certify that I have read this study and that in my opinion it conforms to acceptable standards of scholarly presentation and is fully adequate, in scope and quality, as a dissertation for the degree of Doctor of Philosophy.

Robert C. Stoufer
Associate Professor
of Chemistry

I certify that I have read this study and that in my opinion it conforms to acceptable standards of scholarly presentation and is fully adequate, in scope and quality, as a dissertation for the degree of Doctor of Philosophy.

James Boncella
Assistant Professor
of Chemistry

I certify that I have read this study and that in my opinion it conforms to acceptable standards of scholarly presentation and is fully adequate, in scope and quality, as a dissertation for the degree of Doctor of Philosophy.

James A. Deyrup
Professor of Chemistry

I certify that I have read this study and that in my opinion it conforms to acceptable standards of scholarly presentation and is fully adequate, in scope and quality, as a dissertation for the degree of Doctor of Philosophy.

Paul H. Holloway
Professor of Material Science
and Engineering

This dissertation was submitted to the Graduate Faculty of the Department of Chemistry in the College of Liberal Arts and Sciences and to the Graduate School and was accepted as partial fulfillment of the requirements for the degree of Doctor of Philosophy.

December 1989

Dean, Graduate School